Spring 1993

Effects of Radiative Interactions in Molecular Gases Under Local and Nonlocal Thermodynamic Equilibrium Conditions

Manoj Kumar Jha
Old Dominion University

EFFECTS OF RADIATIVE INTERACTIONS IN MOLECULAR GASES UNDER LOCAL AND NONLOCAL THERMODYNAMIC EQUILIBRIUM CONDITIONS

by

Manoj Kumar Jha

B.E. June 1991, Regional Engineering College, Durgapur, India

A Thesis Submitted to the Faculty of Old Dominion University in Partial Fulfillment of the Requirements for the Degree of

MASTER OF SCIENCE

MECHANICAL ENGINEERING

OLD DOMINION UNIVERSITY

May, 1993

Approved by :

Dr. Surendra N. Tiwari (Director)

Dr. Sushil K. Chaturvedi

Dr. Arthur C. Taylor

ABSTRACT

EFFECTS OF RADIATIVE INTERACTIONS IN MOLECULAR GASES UNDER LOCAL AND NONLOCAL THERMODYNAMIC EQUILIBRIUM CONDITIONS

Manoj K. Jha

Old Dominion University, 1993

Director: Dr. Surendra N. Tiwari

Basic formulations, analyses, and numerical procedures are presented to investigate radiative heat interactions in diatomic and polyatomic gases under local and nonlocal thermodynamic equilibrium conditions. Essential governing equations are presented for both gray and nongray gases. Information is provided on absorption models, relaxation times, and transfer equations. Radiative flux equations are developed which are applicable under local and nonlocal thermodynamic equilibrium conditions.

The problem is solved for fully developed laminar incompressible flows between two parallel plates under the boundary condition of a uniform surface heat flux. For specific applications, three diatomic and three polyatomic gases are considered. The results are obtained numerically by employing the method of variation of parameters. The results are compared under local and nonlocal thermodynamic equilibrium conditions at different temperature and pressure conditions. Both gray and nongray studies are conducted extensively for all molecular gases considered. The particular gases selected for this investigation are,

CO, NO, OH, CO_2, H_2O, and CH_4. The temperature and pressure range considered are 300–2000 K and 0.1–10 atmosphere, respectively. In general, results demonstrate that the gray gas approximation overestimates the effect of radiative interaction for all conditions. The conditions of NLTE, however, result in underestimation of radiative interactions. The method developed for this study can be extended to solve complex problems of radiative heat transfer involving nonequilibrium phenomena.

ACKNOWLEDGEMENTS

I would like to take this opportunity to express my appreciation to my advisor Dr. Surendra N. Tiwari of Old Dominion University for his valuable guidance and support. I also would like to thank my thesis committee members Dr. S. K. Chaturvedi and Dr. A. C. Taylor for their kind cooperation.

This work, in part, was supported by the NASA Langley Research Center through Grant NAG–1–423 and Cooperative Agreement NCC1–68.

TABLE OF CONTENTS

LIST OF FIGURES

LIST OF SYMBOLS

Latin Symbols

A, A_i	Total band absorptance, cm^{-1}
A_{0i}	Correlation quantity, cm^{-1}
$\overline{A}$, $\overline{A}_i$	Dimensionless band absorptance
B^2, B_i^2	Correlation quantity
B_e, B_{ei}	Rotational constant, cm^{-1}
B_ν	Black body intensity of frequency ν and at local temperature
$B_\omega(T_1)$, $B_\omega(T_w)$	Spectral surface radiosity, $(watts/cm^2)cm^{-1}$
c	Speed of light
C_0^2, C_{0i}^2	Correlation quantity
$E_n(t)$	Exponential integral
E_r	Rotational Energy
E_v	Vibrational energy
E_v^*	Equilibrium vibrational energy
e	Total black body emissive power
e_ω	Planck's function, $(watts/cm^2)/cm^{-1}$
$e_{1\omega}$, $e_{1\omega i}$	Planck's function evaluated at temperature T_1
h	Planck's constant
I_ν	Intensity of a beam of radiation of frequency ν
J_ν, $J_{\nu c}$	Radiative source function
k	Boltzmann constant

P	Gas pressure, atm
q_w	Wall heat flux, watts/cm^2
q_R	Total radiative heat flux, watts/cm^2
q_{Ri}	Radiation heat flux for ith band, watts/cm^2
$q_{R\omega}$, $q_{R\omega i}$	Spectral radiative flux, (watts/cm^2)/cm^{-1}
$S(T)$	Total band intensity, atm^{-1} cm^{-2}
S_ν	Nonequilibrium source function
S_ν^*	Equilibrium source function
T	Temperature, K
T_0	Reference temperature (equilibrium)
T_1, T_2, T_w	Wall temperature
T_b	Bulk temperature, K
u, u_i	Dimensionless coordinate, C_0^2Py
u_0, u_{0i}	Dimensionless path length, C_0^2PL
v_x	Velocity, cm/sec
v_m	Mean velocity, cm/sec
y	Physical coordinate, cm
Greek Symbols	
α	Thermal diffusivity, cm^2/sec
β, β_i	Line structure parameter, B^2Pe
γ_1	Nondimensional quantity, $3\,\tau_0^2/\overline{N}$
ε, ε_i	Surface emittance
η_c	Vibrational relaxation time, sec
η_r	Radiative life time of vibrational state, sec
θ_p	Dimensionless temperature, $(T-T_1)/(q_wL/\kappa)$
θ_{bp}	Dimensionless bulk temperature, $(T_b-T_1)/(q_wL/\kappa)$

κ, $\varkappa$	Thermal conductivity, watts/cm^2/K
κ_ν	Absorption coefficient of frequency ν
κ_ν^*	Equilibrium absorption coefficient at frequency ν
κ_ω	Equilibrium spectral absorption coefficient, cm^{-1}
κ_m	Modified Planck mean coefficient, cm^{-1}
κ_p	Planck mean coefficient, cm^{-1}
ν	Frequency
ν_c, ν_0, ν_i	Frequency corresponding to band center
ξ	Dimensionless coordinate, y/L
ρ, ϱ	Density
σ	Stefan–Boltzmann constant
Ω	Solid angle
ω	Wave number, cm^{-1}
ω_c, ω_i	Band center, cm^{-1}

Chapter 1

INTRODUCTION

Radiation is an important mode of energy transfer in systems involving high temperature variations. In past several years, radiative energy transfer has been the subject of research in many heat transfer problems. This is because of the specific applicability of radiative heat transfer analyses in certain important areas. Some of the popular areas of application are, remote sensing, earth's radiation budget studies and climate modelling, fire and combustion research, entry and reentry phenomena, hypersonic propulsion, and defense oriented research. Until the sixties and early seventies, attentions were directed mainly on one dimensional treatment of radiative transfer problems. Multidimensional analyses became popular only in the mid–to–late seventies. Today, there are several books [1–11]*, review articles, and research papers available which deal with radiative heat transfer analyses in a variety of systems.

To understand the radiative energy transfer, it is important to understand the basic transfer processes (mass, momentum, and energy) in various systems. Essential formulations for such processes are available in standard references [12–19]. It is necessary to assume a suitable model for vibration–rotation bands, and to obtain relevant spectroscopic information

* Numbers in brackets represent references

for the gases under consideration. One should be thoroughly conversant with different numerical and computational procedures.

There are a number of analyses involving duct flows of absorbing–emitting gases in literature. Usiskin and Sparrow [20] studied thermal radiation between parallel plates separated by an absorbing–emitting, nonisothermal gas. Viskanta and Grosh [21] studied heat transfer in an absorbing and scattering medium. Lick [22] studied the effect of energy transfer by combined radiation and conduction. Viskanta [23] studied the interaction of conduction, laminar convection, and radiation in a plane layer of radiating fluid. Cess and Tiwari [24] investigated heat transfer to laminar flow of an absorbing–emitting gas between parallel plates. Tiwari [25] studied radiative interaction in transient energy transfer in gaseous systems. Tiwari and Singh [26] extended Tiwari's work to fully developed laminar flows. The studies involving nonlocal thermodynamic equilibrium (NLTE) phenomena are discussed in [27–31]. The studies presented in [32–35] have reviewed other available literature on gray as well as nongray radiative transfer between planar geometries.

Most of the radiative heat transfer treatment have been done under local thermodynamic equilibrium (LTE) conditions. The goal of this research is to treat the radiative heat transfer problems under NLTE conditions. The gases under consideration are, CO, NO, OH, CO_2, H_2O, and CH_4. Both gray and nongray analyses have been conducted for these gases. The analyses have been presented for laminar flow between black parallel plates. However, the same analyses can be extended to circular, triangular, or other complex geometries with proper modifications. The LTE and NLTE results are compared at different pressures and temperatures. The range of pressure, temperature, and plate spacing is chosen in such a way that maximum radiative effect is observed. The pressure ranges from 0.1 to 10 atmosphere,

and the temperature ranges from 300 to 2000 K. The spacing between the plates is taken from 0.1 to 100 centimeters.

The basic theoretical formulation is provided in Chap. 2. Chapter 3 presents radiative transfer models which include absorption models, rate equations and equations for relaxation times, the equation of radiative transfer, and radiative flux equations. Chapter 4 deals with gray gas analyses under LTE and NLTE conditions. Chapter 5 provides nongray radiative transfer formulations under LTE and NLTE conditions. Results and discussion for all the cases are presented in Chap. 6.

Chapter 2

BASIC THEORETICAL FORMULATION

As stated in the introduction, the basic governing equations for fluid mechanics and heat transfer are available in standard references [12–19]. These equations are used in different forms depending upon the nature of the problem being solved. These are presented here without providing detailed derivations.

The equation for conservation of mass which is known as continuity equation, is given as

$$\frac{\partial \varrho}{\partial t} + \nabla . (\varrho\, u) = 0 \qquad (2.1a)$$

For an incompressible fluid, this reduces to

$$\nabla . u = 0 \qquad (2.1b)$$

The equation for conservation of momentum, in most general form, is given as

$$\varrho \frac{Du}{Dt} = \varrho\, f - \nabla P + \frac{\partial}{\partial x_j} \left[u \left(\frac{\partial u_i}{\partial x_j} + \frac{\partial u_j}{\partial x_i} \right) - \frac{2}{3}\, \delta_{ij}\, \mu \frac{\partial u_k}{\partial x_k} \right] \qquad (2.2a)$$

where δ_{ij} is known as the Kronecker delta and i,j,k = 1,2,3. In deriving Eq. (2.2a), the coefficient of bulk viscosity is assumed to be zero. Assuming incompressible fluid and viscosity μ to be constant, Eq. (2.2a) reduces to

$$\frac{Du}{Dt} = f - \frac{\nabla P}{\varrho} + \nu \nabla^2 u \qquad (2.2b)$$

The energy equation is expressed in several forms which are available in [12,15,16]. The proper form which is convenient for this study is given as

$$\varrho C_p \left(\frac{DT}{Dt} \right) = \frac{\partial Q}{\partial t} + \nabla . (\varkappa \nabla T) - \nabla . q_R + \beta T \left(\frac{Dp}{Dt} \right) + \phi \qquad (2.3)$$

where

$$\phi = \mu \left[2 \left(\frac{\partial u}{\partial x} \right)^2 + 2 \left(\frac{\partial v}{\partial y} \right)^2 + 2 \left(\frac{\partial w}{\partial z} \right)^2 + \left(\frac{\partial v}{\partial x} + \frac{\partial u}{\partial y} \right)^2 + \left(\frac{\partial w}{\partial y} + \frac{\partial v}{\partial z} \right)^2 \right.$$

$$\left. + \left(\frac{\partial u}{\partial z} + \frac{\partial w}{\partial x} \right)^2 - \frac{2}{3} \left(\frac{\partial u}{\partial x} + \frac{\partial v}{\partial y} + \frac{\partial w}{\partial z} \right)^2 \right]$$

In Eq. (2.3), the quantity Q represents the heat generated (or lost) by external agencies, and β is the coefficient of thermal expansion of the fluid. Other quantites are defined in cited references.

Equations (2.1)–(2.3), in general, are called Navier–Stokes equations. For computational conveniences, these equations are expressed in a compact vector form as [19]

$$\frac{\partial U}{\partial t} + \frac{\partial E}{\partial x} + \frac{\partial F}{\partial y} + \frac{\partial G}{\partial z} = 0 \qquad (2.4)$$

where it is assumed that there is no external heat addition and no body forces. The quantities U, E, F,and G are vectors and are defined as

$$U = \begin{bmatrix} \varrho \\ \varrho u \\ \varrho v \\ \varrho w \\ Et \end{bmatrix}$$

$$E = \begin{bmatrix} \rho u \\ \rho u^2 + P - \tau_{xx} \\ \rho uv - \tau_{xy} \\ \rho uw - \tau_{xz} \\ (E_t + P) u - u\tau_{xx} - v\tau_{xy} - w\tau_{xz} + q_{cx} + q_{Rx} \end{bmatrix}$$

$$F = \begin{bmatrix} \rho v \\ \rho uv - \tau_{xy} \\ \rho v^2 + P - \tau_{yy} \\ \rho vw - \tau_{yz} \\ (E_t + P) v - u\tau_{xy} - v\tau_{yy} - w\tau_{yz} + q_{cy} + q_{Ry} \end{bmatrix}$$

$$G = \begin{bmatrix} \rho w \\ \rho uw - \tau_{xx} \\ \rho vw - \tau_{yz} \\ \rho w^2 + P - \tau_{zz} \\ (E_t + P) w - u\tau_{xz} - v\tau_{yz} - w\tau_{zz} + q_{cz} + q_{Rz} \end{bmatrix}$$

where

$$E_t = \rho \left(e + \frac{V^2}{2} \right) ; \quad V^2 = u^2 + v^2 + w^2$$

$$\tau_{xx} = \frac{2}{3}\mu \left(2\frac{\partial u}{\partial x} - \frac{\partial v}{\partial y} - \frac{\partial w}{\partial z} \right)$$

$$\tau_{yy} = \frac{2}{3}\mu \left(2\frac{\partial v}{\partial y} - \frac{\partial u}{\partial x} - \frac{\partial w}{\partial z} \right)$$

$$\tau_{zz} = \frac{2}{3}\mu \left(2\frac{\partial w}{\partial z} - \frac{\partial u}{\partial x} - \frac{\partial v}{\partial y} \right)$$

$$\tau_{xy} = \mu \left(\frac{\partial u}{\partial y} + \frac{\partial \mathrm{v}}{\partial x} \right) = \tau_{yx}$$

$$\tau_{xz} = \mu \left(\frac{\partial w}{\partial x} + \frac{\partial u}{\partial z} \right) = \tau_{zx}$$

$$\tau_{yz} = \mu \left(\frac{\partial \mathrm{v}}{\partial z} + \frac{\partial w}{\partial y} \right) = \tau_{zy}$$

In Eq. (2.4), first row represents the continuity equation, second, third, and fourth rows represent the three momentum equations, and the last row represents the energy equation.

For two–dimensional laminar flow in channels, the energy equation given by Eq. (2.3) reduces to [6]

$$\varrho C_p \left(\frac{\partial T}{\partial t} + u\frac{\partial T}{\partial x} + \mathrm{v}\frac{\partial T}{\partial y} \right) = \frac{\partial}{\partial y}\left(\varkappa \frac{\partial T}{\partial y} \right) + \beta\, T\, u\, \frac{dP}{dx} + \mu \left(\frac{\partial u}{\partial y} \right)^2 - div\ q_R \qquad (2.5)$$

The energy equation given in this form can be applied to radiatively induced nonequilibrium flows by replacing the divergence of the radiative flux by its nonequilibrium counterpart.

In deriving Eq. (2.5), it has been assumed that the conduction heat transfer in the x–direction is negligible compared to that in the y–direction. This represents the physical condition of a large value of the Peclet number. Similar reasoning can be applied to show that the radiative heat transfer in the x–direction is negligible in comparison to that in the y–direction.

Within the confines of the foregoing assumptions, for small values of the Eckert number, Eq. (2.5) reduces to

$$\frac{\partial T}{\partial t} + u\frac{\partial T}{\partial x} + \mathrm{v}\frac{\partial T}{\partial y} = \alpha \frac{\partial^2 T}{\partial y^2} - \frac{1}{\varrho C_p}\frac{\partial q_R}{\partial y} \qquad (2.6)$$

where $\alpha=\kappa/\rho C_p$ is the thermal diffusivity of the fluid and fluid properties has been assumed to be constant locally.

In order to apply energy equation to problems involving radiation participating medium, it is necessary to have an appropriate formulation for the radiative flux, q_R. As stated earlier, in dealing with problems involving nonequilibrium phenomena, one should use the nonequilibrium counterpart of the radiative flux equation. Different forms of radiative flux equation as well as other relevant topics are covered in the next chapter.

Chapter 3

RADIATIVE TRANSPORT MODELS

As stated in Chap. 2, one should consider an appropriate radiative transport model while applying the energy equation to problems involving radiation participating medium. This section presents discussion on absorption models, rate equations and relaxation times, transfer equations, and radiative flux equations.

3.1 Absorption Models

To study the radiative effects in nonhomogeneous medium, it is essential to know the absorption, emission, and scattering characteristics of the gases under consideration. An accurate model for the spectral absorption coefficient is required to formulate radiative flux equations. In addition, one needs to identify the major bands of the gas under consideration, and to evaluate the line parameters (line intensity, line half–width, and line spacing) of these bands. The line parameters depend on temperature, pressure, and concentration of the absorbing molecules. Considerable efforts have been made to obtain the line parameters and absorption coefficient of some important atomic and molecular species.

The quantity of primary interest which is applied with respect to the band approximation, is the integrated band intensity, S. This is also called integrated band absorption or band intensity, and is defined as

$$S(T) = \int_{\Delta\omega} \frac{\varkappa_\omega}{P} d\omega \tag{3.1}$$

where κ_ω represents the spectral absorption coefficient. This quantity is independent of pressure because the total area of the individual rotational line is independent of pressure.

The temperature variation of the integrated band intensity is given by [33–35]

$$T\ S(T) = T_0\ S(T_0)\ F(T) \tag{3.2}$$

where T_0 is the reference temperature (usually 300 K) and F(T)=1for fundamental and pure rotation bands, but it differs from unity for overtone and combination bands. For combination and overtone bands of important molecules, relations for F(T) exists in literature [35]. Band intensities for some important gases are presented in Appendix A.

For gray gas analyses, the total band absorption coefficient is expressed in terms of either the Planck mean absorption coefficient κ_p or the modified Planck mean absorption coefficient κ_m. For a single–band gas, these are defined as [6]

$$\varkappa_p(T) = \frac{\int_{\Delta\omega} \varkappa_\omega(T)\ e_\omega(T)\ d\omega}{e(T)} \tag{3.3}$$

$$\varkappa_m(T, T_1) = \int_{\Delta\omega} \frac{\varkappa_\omega(T)\ e_\omega(T_1)\ d\omega}{\sigma\ T_1^4} \tag{3.4}$$

where e_ω is Planck function. Assuming the Planck function $e_\omega(T)$ to be independent of the wave number within the band, and using Eqs. (3.1) and (3.2), Eqs. (3.3) and (3.4) can be written as

$$\frac{\kappa_p(T)}{P} = \frac{e_{\omega c}(T)}{\sigma T^4} S(T) \tag{3.5}$$

$$\frac{\kappa_m(T, T_1)}{P} = \frac{e_{\omega c}(T_1)}{\sigma T_1^4} S(T) = \frac{\kappa_p(T_1)}{P} \frac{T_1}{T} \tag{3.6}$$

The definition of κ_p and κ_m can be extended to multiband gases, and by combining Eqs. (3.2), (3.3), and (3.4), a general expression can be obtained as

$$\frac{T\,\kappa_m\,(T, T_1)}{T_1 \kappa_p\,(T_1)} = \frac{\sum_{i=1}^{n} e_{\omega i}\,(T_1)\; S_i\,(T_0)\; F_i\,(T)}{\sum_{i=1}^{n} e_{\omega i}\,(T_1)\; S_i\,(T_0)\; F_i\,(T_1)} \tag{3.7}$$

where n is the number of bands. By including the contributions from overtone and combination bands, calculations performed for CO, CO_2, and H_2O [31] show that the right hand side of Eq. (3.7) is approximately equal to unity, and therefore Eq. (3.6) is an excellent approximation for Eq. (3.7).

In a similar manner, the general expression for Eq. (3.5) for multiband gases can be given as

$$\kappa_p(\,T\,) = \frac{P \sum_{i=1}^{n} [\; e_b(\,\omega_{ci}, T\,)\; S_i\,(\,T\,)\;]}{\sigma\, T^4} \tag{3.8}$$

For a mixture of gases, Eq. (3.8) can be written as

$$\kappa_p(T) = \frac{\sum_j P_j \{ \sum_{i=1}^{n} [\, e_b(\, \omega_{ci}, T\,)\, S_i\, (\, T\,)\,] \}}{\sigma\, T^4} \tag{3.9}$$

where j is the number of species and P_j is the partial pressure of the j th species.

For an accurate evaluation of the absorptance of a molecular band, a convenient line model is used to represent the variation of the spectral absorption coefficient. The commonly used line models are Lorentz, Doppler, and Voigt line models. A detailed discussion of these line models is presented in [31]. In a particular band consisting of many lines, the absorption coefficient varies very rapidly with frequency. Thus, it is very difficult to evaluate the total band absorptance over the actual band contour by employing the line model. To overcome this difficulty, several band models (narrow as well as wide) have been proposed which represent absorption from an actual band with reasonable accuracy [33–35]. There are several continuous correlations for the total band absorptance which are available in literature. The detailed discussion of the various band models are given in cited references.

3.2 Rate Equations and Relaxation Times

In this section, discussion on rate equations and equations for relaxation times are presented briefly. For any radiative heat exchange process, it is important to know the rate of change of vibrational energy [31]. The rate of change of vibrational energy of a system of oscillator can be given as

$$\frac{dE_v}{dt} = \left(\frac{dE_v}{dt}\right)_{coll} + \left(\frac{dE_v}{dt}\right)_{rad} \tag{3.10}$$

where first and second terms on the right hand side represent vibrational energy due to collisional and radiative processes respectively. The radiative field exchanges energy with rotational as well as vibrational degree of freedom. The relation for radiative flux in terms of rate of change of vibrational as well as rotational energy is given by

$$-\ div\ q_R = -\left(\frac{dE_v}{dt}\right)_{rad} + \left(\frac{dE_r}{dt}\right)_{rad} \tag{3.11}$$

where E_v and E_r are vibrational and rotational energy per unit volume. The second term on the right of Eq. (3.11) can be neglected because of small separation of rotational levels.

The divergence of radiative flux is related to specific intensity I_ν, and for one–dimensional case, it is given as

$$div\ q_R = \frac{dq_R}{dy} = \int_0^\infty \frac{dq_{R\nu}}{dy} d\nu = \int_0^\infty \int_0^{4\pi} \frac{dI_\nu}{ds} d\Omega d\nu \tag{3.12}$$

Combining Eqs. (3.10) – (3.12), one obtains

$$\frac{dE_v}{dt} = \left(\frac{dE_v}{dt}\right)_{coll} - \int_0^\infty \int_0^{4\pi} \frac{dI_\nu}{ds} d\Omega d\nu \tag{3.13}$$

The first part of Eq. (3.13), i.e. the rate of change of vibrational energy of a system undergoing a collisional relaxation process is given by the Bethe–Teller relation [31]

$$\frac{dE_v}{dt} = \frac{E_v^* - E_v}{\eta_c} \qquad (3.14)$$

where E_v^* is the equilibrium value of the vibrational energy and η_c is vibrational relaxation time. The relaxation time is defined as the average time required to transfer energy from one mode to another by collision. Therefore, it is also termed as collisional relaxation time.

By assuming E_{v0} to be the initial amount of vibrational energy, integration of Eq. (3.14) yields

$$E_v - E_v^* = (E_{v0} - E_v^*) \exp\left(-\frac{t}{\eta_c}\right) \qquad (3.15)$$

In order to use Eq. (3.15), an explicit relation for $\eta_c = \eta_c$ (T,P) is required. There are several expressions available in literature to calculate η_c. Some of them are briefly discussed here. An explicit relation for η_c is given by the Landau–Teller relation [31]

$$\eta_c = K_1 P^{-1} \exp\left(K_2 T^{-1/3}\right) \qquad (3.16)$$

where K_1 and K_2 are positive constants and depend on the physical properties of the molecule. For diatomic gases, an empirical relation for η_c is given by [36, 37]

$$P\,\eta_c = \exp\left[A\left(T^{-1/3} - 0.015\,\mu^{1/4}\right) - 18.42\right] \qquad (3.17)$$

where A is a constant and is related to the molecular constants of the colliding species and μ is the reduced mass of the colliding pairs. Values of A and μ for some gases are available in the references. For CO_2, the relation for η_c is given by [31]

$$\eta_c = \frac{1}{P}\left[\exp\left(AT^{-1/3} - B\right) \times 10^{-6}\right] \qquad (3.18)$$

For CH_4, η_c is given by [31]

$$\eta_c = \frac{1}{P}[\ -5.4 + 40\ T^{-1/3}\ ] \times 10^{-6} \qquad (3.19)$$

For cases where specific relation for η_c do not exist, one can use the general expression given by Millikan and White [36, 37]

$$P\ \eta_c = \exp\ [\ (\ 1.16 \times 10^{-3}\ )\ \mu^{1/2}\ \theta^{4/3}\ (\ T^{-1/2} - 0.15\mu^{1/4}\ ) - 18.42\ ] \qquad (3.20)$$

where θ is the characteristic temperature (K) and is given as $\theta = hc/k\lambda$, and h is the Planck's constant, c is the speed of light, k is the Boltzmann constant, and λ is the wavelength.

In all the expressions for η_c, P is the total pressure in atmosphere, η_c is in seconds, and T is the temperature in degrees Kelvin. Although these relations show a strong dependency of η_c on pressure, in reality it has a larger temperature variation. This is because collisional frequencies are higher at higher temperatures and consequently it takes relatively less time to deactivate the excited states. Further discussions on collisional relaxation time are provided by Tiwari and Manian [30].

3.3 Transfer Equations

By transfer equations, we mean equations for radiative energy transfer over a specifically defined volume. These equations are usually represented in terms of intensity of radiation I_ν. In this section, we will derive several forms of radiative transfer equations and discuss their physical meaning. The transfer equations are derived for a simple harmonic oscillator based on the assumption that the rotational and vibrational levels are populated according

to the Boltzmann distribution. The rotational energy is characterized by equilibrium temperature T whereas the vibrational energy is characterized by the the nonequilibrium temperature T_v. Two level transitions between the vibrational states are considered in such a way that a single independent vibration–rotation band is obtained corresponding to the fundamental frequency of vibration. Therefore, the nonequilibrium transfer equation which is described next, is applicable to only fundamental bands of diatomic and polyatomic gases.

For a two level system, let n(v–1) and n(v) represent the number density of molecules in the lower and upper vibrational levels respectively. In each vibrational level, molecules are assumed to be distributed over rotational levels according to Boltzmann distribution function f(j) such that Σ f(j) =1. The quantity v is called the vibrational quantum number and j is a set of rotational quantum numbers corresponding to the lower vibrational level. Thus, number density in the state (v–1,j) is given as n(v–1) f(j). Number of molecules that actually make a transition from state (v–1,j) to (v.j′) are governed by the Einstein coefficients such that number of molecules undergoing spontaneous emission, induced or stimulated emission, and absorption are given by a(j′,j) A(v,v–1), b(j′,j) B(v,v–1), and b(j,j′) B(v–1,v) respectively. If rotational and vibrational wave functions are assumed to be separable, j coefficients can be assumed such that the following relation is satisfied

$$\sum_j a(j',j) = \sum_j b(j,j') = \sum_j b(j,j') = 1$$

Based on the above assumption for a two level transition of molecules contained in a volume dS (cross section is assumed to be unity), the change in radiative energy within the solid angle dΩ, can be written as

$$\frac{dI_\nu}{ds} d\Omega = n(\mathrm{v}) f(j') a(j',j) A(\mathrm{v}, \mathrm{v}-1)\left(\frac{d\Omega}{4\pi}\right)$$

$$- [n(\mathrm{v}-1)f(j)b(j,j')B(\mathrm{v}-1,\mathrm{v}) - n(\mathrm{v})f$$

$$- n(\mathrm{v})f(j')b(j',j)B(\mathrm{v},\mathrm{v}-1)]\frac{I_\nu}{c}d\Omega \qquad (3.21)$$

where first, second, and third terms on the right represent contribution due to spontaneous emission, absorption, and induced emission respectively, and c is the speed of light.

If one applies the principle of detailed balance, following relations are obtained

$$a(j',j)\ A(\mathrm{v},\mathrm{v}-1) = \delta_\nu\ b(j',j)\ B(\mathrm{v},\mathrm{v}-1) \qquad (3.22a)$$

$$b(j',j)\ B(\mathrm{v},\mathrm{v}-1) = \frac{g(j)}{g(j')}b(j,j')\ B(\mathrm{v}-1,\mathrm{v}) \qquad (3.22b)$$

where $\delta_\nu = 8\pi\,\nu^2/c^3$ and g(j) is the statistical weight of j th rotational level. The following relation is obtained for a simple harmonic oscillator from quantum mechanics

$$B\ (\mathrm{v},\mathrm{v}-1) = \mathrm{v}\ B(0,1) \qquad (3.23)$$

Since each pair of vibrational levels of a simple harmonic oscillator absorb and emit equal quanta, a summation over all the vibrational level is possible. As a result, the following relation can be obtained

$$E_\mathrm{v} = \sum_{\mathrm{v}=1}^{\infty} \mathrm{v}\ n(\mathrm{v}) \qquad (3.24)$$

where E_v is written in the normalized form, and

$$E_\mathrm{v}{}^* = n\ [\exp(\frac{h\nu_0}{\varkappa T} - 1]^{-1} \qquad (3.25a)$$

such that [31]

$$\frac{E_\mathrm{v}}{E_\mathrm{v}{}^*} = \frac{[\ \exp(\frac{h\nu_0}{\varkappa T}\ ) - 1\ ]}{[\ \exp(\frac{h\nu_0}{\varkappa T_\mathrm{v}}\ ) - 1\ ]} \qquad (3.25b)$$

where T_v is the nonequilibrium temperature.

By using Eqs. (3.22) through (3.25) in Eq. (3.21), the transfer equation can be written in the form

$$\frac{dI_\nu}{ds} = \frac{n\ B(0,1)\ b(j,j')\ f(j)}{c[1 - \exp(-\frac{h\nu_0}{\varkappa T_v})\ ]}$$

$$\left\{\frac{2h\nu^3}{c^2}\exp[-\frac{h}{\varkappa}(\frac{\nu_0}{T_v} + \frac{\nu - \nu_0}{T})\ ] - I_\nu + I_\nu \exp[-\frac{h}{\varkappa}(\frac{\nu_0}{T_v} + \frac{\nu - \nu_0}{T})]\right\} \quad (3.26)$$

where n is the total number of molecules.

Equation (3.26) is written in an alternative form as

$$\frac{dI_\nu}{ds} = \varkappa_\nu\ (\ S_\nu - I_\nu\ ) \quad (3.27)$$

where κ_ν and S_ν are net absorption coefficient and source function respectively, and are given as

$$\varkappa_\nu\ (n, T, T_v) = \frac{n\ B(0,1)\ b(j,j')\ f(j)}{c\ [\ 1 - \exp\ (\frac{-h\nu_0}{\varkappa T_v})\ ]}\left\{\ 1 - \exp\ [-\frac{h}{\varkappa}(\frac{\nu_0}{T_v} + \frac{\nu - \nu_0}{T})\ ]\right\} \quad (3.27a)$$

$$S_\nu\ (T, T_v) = (\frac{2h\nu^3}{c^2})\left\{\exp\ [\frac{h}{\varkappa}\ (\frac{\nu_0}{T_v} + \frac{\nu - \nu_0}{T})\ ] - 1\right\} \quad (3.27b)$$

For the case of LTE, $T_v = T$ and Eqs. (3.27a) and (3.27b) can be written as

$$\varkappa_\nu^*\ (n, T) = \frac{n\ B(0,1)}{c}\ b(j,j')\ f(j)\left\{\frac{1 - \exp\ (\frac{-h\nu}{\varkappa T})}{1 - \exp\ (\frac{-h\nu_0}{\varkappa T})}\right\} \quad (3.28a)$$

$$S_\nu^* = B_\nu\ (T) = \frac{(\frac{2h\nu^3}{c^2})}{[\ \exp\ (\frac{h\nu}{\varkappa T}) - 1\ ]} \quad (3.28b)$$

where B_ν is black body intensity of frequency ν at local temperature.

Using Eqs. (3.25) through (3.28), radiation transfer equation can be given as

$$\frac{dI_\nu}{ds} = \varkappa_\nu \left(\frac{\varkappa_\nu^*}{\varkappa_\nu} B_\nu \frac{E_\nu}{E_\nu^*} - I_\nu \right) = \varkappa_\nu^* \left(B_\nu \frac{E_\nu}{E_\nu^*} - \frac{\varkappa_\nu}{\varkappa_\nu^*} I_\nu \right) \qquad (3.29)$$

Comparing Eq. (3.29) with Eq. (3.27), it is seen that the quantity $\frac{\kappa_\nu^*}{\kappa_\nu} B_\nu \frac{E_\nu}{E_\nu^*}$ is the source function $S(T,T_\nu)$. Equation (3.29) can be regarded as the nonequilibrium radiative transfer equation and is identical to that obtained by Goody [4].

Under steady state conditions, for each fundamental band, a combination of Eqs. (3.13), (3.14), and (3.29) results in

$$\left(\frac{E_\nu}{E_\nu^*} \right) \left[\left(\frac{E_\nu^*}{\eta_c} \right) + \int d\Omega \int \varkappa_\nu B_\nu d\nu \right] = \left(\frac{E_\nu^*}{\eta_c} \right) + \int d\Omega \int \varkappa_\nu I_\nu d\nu \qquad (3.30)$$

where integration is taken over the frequency range of an individual band and over the solid angle from 0 to 4π. If one introduces a time constant η_r as

$$\eta_r = \frac{E_\nu^*}{\int d\Omega \int \varkappa_\nu B_\nu d\nu} \qquad (3.31)$$

then combining Eqs. (3.29) and (3.30), one can write the radiative transfer equation as

$$\frac{dI_\nu}{ds} = \varkappa_\nu (J_\nu - I_\nu) \qquad (3.32a)$$

where

$$J_\nu = B_\nu \frac{(\eta_r + \eta_c X)}{(\eta_r + \eta_c)} \qquad (3.32b)$$

and

$$X = \frac{\int d\Omega \int \varkappa_\nu I_\nu \, d\nu}{\int d\Omega \int \varkappa_\nu B_\nu \, d\nu} \qquad (3.32c)$$

The quantity η_r is called the radiative life time of vibrational states. It can be shown that [33] $\eta_r = 1/A(1,0)$, where A(1,0) is the Einstein coefficient for spontaneous emission from the first vibrational level.

A combination of Eqs. (3.12) and (3.32) yields an alternative expression for J_ν

$$J_\nu = \frac{B_\nu}{\eta_r + \eta_c} \frac{\{\eta_r + \eta_c [\, (\, \bar{h} + \int d\Omega \int \varkappa_\nu J_\nu \, d\nu \,) \,]\}}{\int d\Omega \int \varkappa_\nu \, B_\nu \, d\nu} \qquad (3.33a)$$

where

$$\bar{h} = - \int \frac{dq_{R\nu}}{dy} \, d\nu \qquad (3.33b)$$

By noting that B_ν and J_ν are isotropic, J_ν can be expressed as

$$J_{\nu c} = B_{\nu c} + \frac{1}{2} \left(\frac{\eta_c}{\eta_r} \right) \bar{H} \qquad (3.34a)$$

where

$$\bar{H} = \frac{\bar{h}}{2\pi \int \varkappa_\nu \, d\nu} \qquad (3.34b)$$

and $J_{\nu c}$ and $B_{\nu c}$ are the values evaluated at the band center. This is because J_ν and B_ν are slowly varying functions of ν and for narrow bands, they can be assumed to be independent of ν. In Eqs. (3.32) and (3.33), B_ν is called blackbody intensity of radiation and is related to the Planck function of radiation $e_{b\nu}$ by $e_{b\nu} = \pi B_\nu$. This relation is true for isotropic radiation.

For very low pressures, the collisional relaxation time η_c is large compared to η_r [31]. Therefore, the right hand side of Eq. (3.32b) reduces to B_ν X. On the other hand, for high pressures, η_c approaches zero and the right hand side of Eq. (3.32b) becomes B_ν which is equivalent to the Planck function. This is the situation of LTE usually assumed in most radiation transfer analyses.

The NLTE effect is characterized by the nonequilibrium parameter η which is expressed as $\eta = \eta_c / \eta_r$. When η is unity or greater than unity, NLTE effect usually prevails; whereas for η being less than unity, LTE effect usually prevails.

A combination of Eqs. (3.25a), (3.28b), and (3.31) results in an expression for η_r [31]

$$\eta_r^{-1} = 8\pi \left(\frac{\nu_0}{c} \right)^2 \int \left(\frac{\kappa_\nu}{n} \right) d\nu = 8\,\pi\, c\, \omega_c^2 \left(\frac{P}{n} \right) \int \left(\frac{\kappa_\omega}{P} \right) d\omega \qquad (3.35)$$

where n is the number density of the molecules, and $\omega_c = (\nu_0 / c)$ is the wave number corresponding to ν_0. In the derivation of Eq. (3.35), it has been assumed that B_ν is independent of frequency. An alternative form of Eq. (3.35) is given as

$$\eta_r^{-1} = \left(8\,\pi\,\omega_c^2 \right) \left(4.08 \times 10^{-12} \right) T_0 S(T_0) \qquad (3.36)$$

where S is the integrated band intensity as defined in the earlier section and T_0 is the reference temperature. The radiative life time η_r has the units of seconds, and for fundamental bands of some important molecules values of η_r are tabulated in Appendix A.

3.4 Radiative Flux Equations

For this study, the physical model consists of an absorbing–emitting gas bounded by two infinite parallel plates (Fig. 3.1). The plate surfaces are assumed to emit and reflect in a diffused manner. For the physical model considered, the integration of the transfer equation, Eq. (3.32a), gives

$$q_{R\omega} = 2\,B_{1\omega}\,E_3(\tau_\omega) - 2\,B_{2\omega}E_3\,(\tau_{0\omega} - \tau_\omega) + 2\pi\,\Big[\int_0^{\tau_\omega} J_\omega(t)\,E_2(\tau_\omega - t)\,dt - \int_{\tau_\omega}^{\tau_{0\omega}} J_\omega(t)\,E_2(t - \tau_\omega)\,dt\,\Big] \qquad (3.37)$$

where

$$\tau_\omega = \varkappa_\omega y,\ \tau_{0\omega} = \varkappa_\omega L \qquad (3.38a)$$

$$J_\omega(t) = \frac{e_\omega(t)}{\pi} + \frac{1}{2}\eta\,\overline{H}(t),\ \eta = \frac{\eta_c}{\eta_r} \qquad (3.38b)$$

$$\overline{H}(y) = \frac{-\,\mathrm{div}\,q_R\,(y)}{2\,\pi\,P\,S(T)} = \frac{-\int_0^{\infty}\left(\frac{dq_{R\omega}}{dy}\right)d\omega}{2\,\pi\,P\,S(T)} \qquad (3.38c)$$

In Eq. (3.37), $\tau_{0\omega}$ is the optical path length and t is a dummy variable for τ_ω. The quantities $B_{1\omega}$ and $B_{2\omega}$ are surface radiosities, and $E_n(t)$ are exponential integral functions. It has been assumed that the spectral absorption coefficient κ_ω is independent of temperature. The detailed explanation of the derivation of Eq. (3.37) is given in [31]. The expressions for surface radiosity can be given as [6]

$$B_{1\omega} = \varepsilon_{1\omega} e_{1\omega} + 2\,(1 - \varepsilon_{1\omega})\,[\, B_{2\omega} E_3(\tau_{0\omega}) + \pi \int_0^{\tau_{0\omega}} J_\omega(t)\, E_2(t)\, dt\,] \qquad (3.39a)$$

$$B_{2\omega} = \varepsilon_{2\omega} e_{2\omega} + 2\,(1 - \varepsilon_{2\omega})\,[\, B_{1\omega} E_3(\tau_{0\omega}) + \pi \int_0^{\tau_{0\omega}} J_\omega(t)\, E_2(\tau_{0\omega} - t)\, dt\,] \qquad (3.39b)$$

For black surfaces, $B_{1\omega} = e_{1\omega}$ and $B_{2\omega} = e_{2\omega}$. This is obvious from Eq. (3.39) because in that case $\varepsilon_{1\omega} = \varepsilon_{2\omega} = 1$. Under the assumptions of LTE,

$$J_\omega(t) = \frac{e_\omega(t)}{\pi}$$

The total radiative flux is given by

$$q_R = \int_0^\infty q_{R\omega}\, d\omega \qquad (3.40)$$

Under LTE assumptions, Eq. (3.37) may be expressed for black bounding surfaces as

$$q_{R\omega}(\tau_\omega) = e_{1\omega} - e_{2\omega} + 2\,[\int_0^{\tau_\omega} F_{1\omega}(t)\, E_2(\tau_\omega - t)\, dt - \int_{\tau_\omega}^{\tau_{0\omega}} F_2(t)\, E_2(t - \tau_\omega)\, dt\,] \qquad (3.41)$$

where

$$F_{1\omega}(t) = e_{\omega}(t) - e_{1\omega} \; ; \; F_{2\omega}(t) = e_{\omega}(t) - e_{2\omega}$$

A direct differentiation of Eq. (3.41) gives

$$-\frac{dq_{R\omega}}{d\tau_{\omega}} = -2\,[\,F_{1\omega}(\tau_{\omega}) + F_{2\omega}(\tau_{\omega})] + 2\,[\int_{0}^{\tau_{\omega}} F_{1\omega}(t)\,E_1(\tau_{\omega} - t)\,dt$$

$$+ \int_{\tau_{\omega}}^{\tau_{0\omega}} F_{2\omega}(t)\,E_1(t - \tau_{\omega})\,dt\,] \qquad (3.42)$$

Equations (3.41) and (3.42) are the LTE radiative flux equations for the physical model described in Figs. (3.1) and (3.2).

Equation (3.37) can be written in a different form by replacing the exponential integral E_n (t) by an exponential function. The exponential integrals E_2 (t) and E_3 (t) in Eq. (3.37) are approximated as follows

$$E_2(t) \simeq \frac{3}{4}\exp\left(-\frac{3}{2}t\right) \; ; \; E_3(t) = -\int E_2(t)\,dt \simeq \frac{1}{2}\exp\left(-\frac{3}{2}t\right) \qquad (3.43)$$

The detailed discussion of this approximation is available in [6]. Substituting Eq. (3.43) in Eq. (3.37), one obtains

$$q_{R\omega} = B_{1\omega}\exp\left[-\frac{3}{2}\kappa_{\omega}y\right] - B_{2\omega}\exp\left[-\frac{3}{2}\kappa_{\omega}(L - y)\right]$$

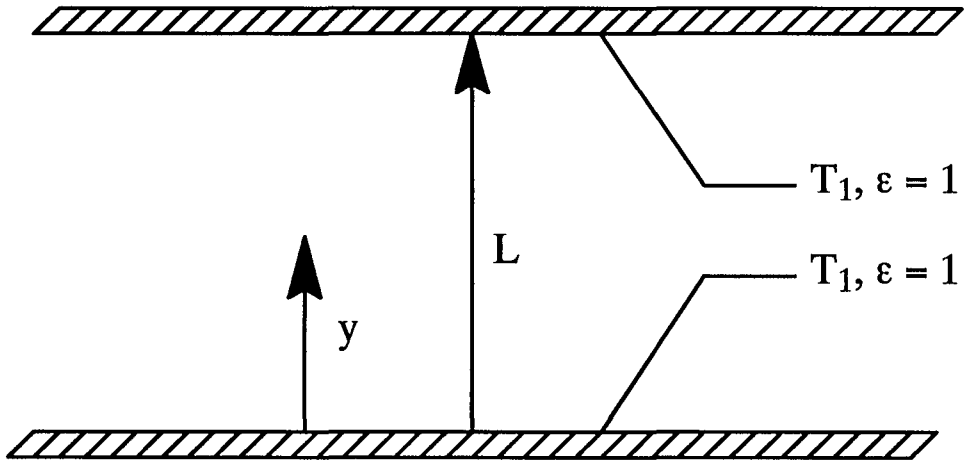

Fig. 3.1 Physical model for radiative interaction

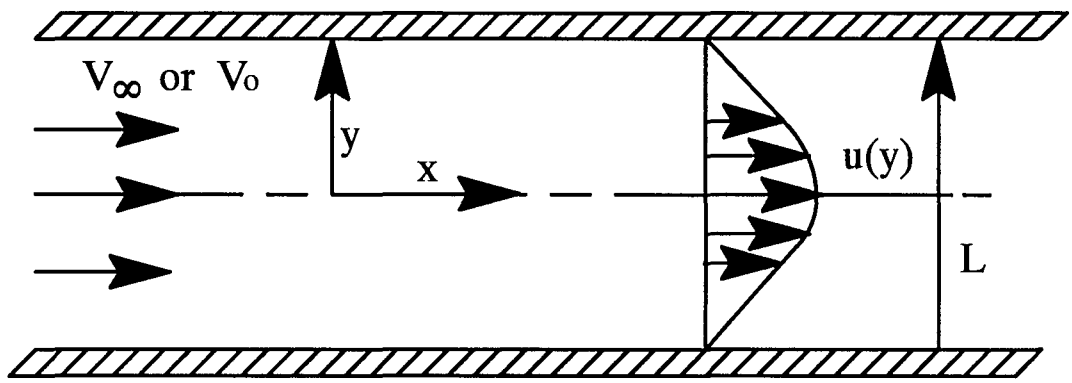

Fig. 3.2 Incompressible laminar flow between two parallel plates

$$+\frac{3\pi}{2}\left\{\int_0^y J_\omega(z)\ \kappa_\omega \exp[-\frac{3}{2}\ \kappa_\omega(y-z)]\ dz - \int_y^L J_\omega(z)\ \kappa_\omega \exp[-\frac{3}{2}\ \kappa_\omega\ (z-y)]\ dz\right\} \tag{3.44}$$

For black bounding surfaces, the radiosities appearing in Eq. (3.44) should be replaced by appropriate expressions of the Planck function.

3.4.1 Nongray Formulation

A combination of Eqs. (3.40) and (3.44) gives the following expression for radiative flux for nongray gases

$$q_R = e_1 - e_2 + \frac{3}{2}\int_0^y [\ \pi\ J_{\omega c}(z) - e_{1\omega c}\ ] \int_{\Delta\omega} \kappa_\omega \exp[-\frac{3}{2}\kappa_\omega(y-z)\ ]\ d\omega dz$$

$$-\frac{3}{2}\int_y^L [\ \pi\ J_{\omega c}(z) - e_{2\omega c}\ ] \int_{\Delta\omega} \kappa_\omega \exp[-\frac{3}{2}\kappa_\omega(z-y)\ ]\ d\omega dz \tag{3.45}$$

Equation (3.45) is valid for black bounding surfaces and it has been assumed that $J_\omega(y)$ is independent of wave number within the band.

By defining the following nondimensional independent variables

$$\xi = \frac{y}{L} = \frac{\tau_\omega}{\tau_{0\omega}} = \frac{u}{u_0}\ ;\ \xi' = \frac{u'}{u_0} = \frac{z}{L} \tag{3.46}$$

where u is the dimensionless path length and u_0 = (S/A_0) PL, the radiative flux equation is expressed in it's final form as

$$q_R(\xi) = e_1 - e_2$$

$$+ \frac{3}{2}A_0u_0\left\{\int_0^{\xi} F_{1\omega c}\overline{A}'[\frac{3}{2}u_0(\xi - \xi')d\xi'] - \int_{\xi}^{1} F_{2\omega c}\overline{A}_i'[\frac{3}{2}u_0(\xi' - \xi)]d\xi'\right\}$$

$$- \frac{3}{8}\eta\left\{\int_0^{\xi} (\frac{dq_R}{d\xi'})\overline{A}'[\frac{3}{2}u_0(\xi - \xi')]d\xi' - \int_{\xi}^{1} (\frac{dq_R}{d\xi'})\overline{A}'[\frac{3}{2}u_0(\xi' - \xi)d\xi'\right\} \qquad (3.47)$$

where $\overline{A}'$ (u) is the derivative of the dimensionless band absorptance $\overline{A}$ (u) with respect to u. The detailed derivation of Eq. (3.47) is provided in [31].

Equation (3.47) is applicable to gases which have only one fundamental band contributing to the radiative process. For a multiband system, Eq. (3.47) can be written in the form

$$q_R(\xi) = e_1 - e_2$$

$$+ \frac{3}{2}\sum_{i=1}^{n} A_{0i}u_{0i}\left\{\int_0^{\xi} F_{1\omega i}\overline{A}_i'[\frac{3}{2}u_{0i}(\xi - \xi')d\xi'] - \int_{\xi}^{1} F_{2\omega i}\overline{A}_i'[\frac{3}{2}u_{0i}(\xi' - \xi)]d\xi'\right\}$$

$$- \frac{3}{8}\sum_{i=1}^{n} \eta_i\left\{\int_0^{\xi} (\frac{dq_R}{d\xi'})\overline{A}_i'[\frac{3}{2}u_{0i}(\xi - \xi')]d\xi' - \int_{\xi}^{1} (\frac{dq_R}{d\xi'})\overline{A}_i'[\frac{3}{2}u_{0i}(\xi' - \xi)d\xi'\right\} \qquad (3.48)$$

where n denotes the number of bands.

Equation (3.48) can be regarded as a general expression for radiative flux equation. For LTE case, the last two terms, i.e., the terms involving η, vanish, and for NLTE case, Eq. (3.48) could be regarded as the radiative flux equation in nongray gases.

3.4.2 Gray Consideration under LTE Assumption

Under LTE assumption, a combination of Eq. (3.40) and (3.44) results in the following radiative flux equation

$$q_{RL}(\tau) = F(\tau) + \Gamma\left\{\int_0^{\tau} T^4(t)\exp[-b(\tau - t)]dt - \int_{\tau}^{\tau_0} T^4(t)\exp[-b(t - \tau)]dt\right\} \tag{3.49a}$$

where

$$F(\tau) = \sigma T_1^4 \exp(-b\tau) - \sigma T_2^4 \exp[-b(\tau_0 - \tau)] \tag{3.49b}$$

$$b = \frac{3}{2}; \quad \Gamma = b\sigma \tag{3.49c}$$

Differentiating Eq. (3.49a) twice by using the Leibnitz formula, one obtains

$$\frac{d^2 q_{RL}}{d\tau^2} = \frac{d^2 F}{d\tau^2} + 2\Gamma\frac{dT^4}{d\tau} +$$

$$\Gamma b^2\left\{\int_0^{\tau} T^4(t)\exp[-b(\tau - t)]dt - \int_{\tau}^{\tau_0} T^4(t)\exp[-b(t - \tau)]dt\right\} \tag{3.50}$$

Elimination of integrals between Eqs. (3.49a) and (3.50) results in

$$\frac{d^2 q_{RL}}{d\tau^2} - b^2 q_R(\tau) = 2\Gamma\frac{dT^4}{d\tau} + \frac{d^2 F}{d\tau^2} - b^2 F(\tau) \tag{3.51}$$

Equation (3.51) is the general differential equation for radiative flux for gray gases under LTE assumption. For the specific relation of F (τ) as defined in Eq. (3.49b), there is obtained

$$\frac{d^2F}{d\tau^2} - b^2F(\tau) = 0$$

Consequently, Eq. (3.51) reduces to

$$\frac{d^2q_{RL}}{d\tau^2} - \frac{9}{4}q_R = 3\sigma\frac{dT^4}{d\tau} \qquad (3.52)$$

This is the appropriate relation for radiative flux for gray gas analyses under LTE assumption of the present physical problem.

3.4.3 Gray Consideration under NLTE Assumption

The radiative flux equation for gray gas analyses under NLTE assumption can be obtained by adding the NLTE part of the radiative flux equation in Eq. (3.50). The NLTE part of the radiative flux equation can be given by

$$q_{RN} = -KS\left\{\int_0^{\tau}\frac{dq_R}{dt}\exp[-b(\tau - t)]dt - \int_{\tau}^{\tau_0}\frac{dq_R}{dt}\exp[-b(t - \tau)]dt\right\} \qquad (3.53a)$$

where

$$KS = \frac{3}{8}\frac{\eta}{PS(T)} \qquad (3.53b)$$

Differentiating Eq. (3.53a) twice by using Leibnitz formula, one obtains

$$\frac{d^2q_{RN}}{d\tau^2} = -2KS\frac{d^2q_R}{d\tau^2} - KSb^2\left\{\int_0^{\tau}\frac{dq_R}{dt}\exp[-b(\tau - t)]dt - \int_{\tau}^{\tau_0}\frac{dq_R}{dt}\exp[-b(t - \tau)]dt\right\} \tag{3.54}$$

Equation (3.50) is the radiative flux equation under LTE assumption. The flux equation under NLTE assumption is given by combining Eqs. (3.50) and (3.54).

$$M_2\frac{d^2q_R}{d\tau^2} - \frac{9}{4}q_R = 3\sigma\frac{dT^4}{d\tau} \tag{3.55a}$$

where

$$M_2 = (1 + 2KS) \tag{3.55b}$$

Equation (3.55a) can be regarded as the radiative flux equation for gray gas analyses under NLTE assumption. The complete derivation of Eq. (3.55a) is provided in Appendix B.

Chapter 4

GRAY RADIATIVE TRANSFER IN LAMINAR FLOW

Gray medium assumption is probably the greatest approximation for the real gases. This assumption replaces the wave number dependent absorption coefficient by a wave number averaged quantity. The following sections deal with the general formulation and the resulting equations under LTE and NLTE conditions for gray gas assumption.

4.1 General Formulation

The physical model considered is assumed to be the same as discussed in the previous chapter (Figs. 3.1 and 3.2). The boundary condition along each of the plate surfaces is taken to be that of a uniform heat flux, and thus the temperature of the plates T varies in the axial direction only. Only fully developed flow and heat transfer are considered. Attention is additionally restricted to small temperature differences, such that constant properties and linearized radiation may be assumed.

Since the wall temperature varies in the axial direction, there will exist radiative transfer between wall elements located at different axial positions, and in general this would preclude the possibility of achieving fully developed heat transfer. For linearized radiation, however,

it is easily shown that fully developed heat transfer can be obtained with the subsequent result that there will be no net radiative transfer between the wall elements.

Within the confines of the foregoing assumptions, the energy equation for the present problem can be obtained from Eq. (2.6) as

$$v_x \frac{\partial T}{\partial x} = \alpha \frac{\partial^2 T}{\partial y^2} - \frac{1}{\varrho C_p} \frac{\partial q_R}{\partial y} \tag{4.1}$$

where the parabolic velocity profile is given by

$$v_x = 6v_m[\frac{y}{L} - (\frac{y}{L})^2] \tag{4.2a}$$

The mean velocity is given by the expression

$$v_m = \frac{1}{A_c} \int_{A_c} v_x dA_c \tag{4.2b}$$

where A_c represents the cross sectional area normal to the direction of flow. For uniform wall heat flux and fully developed heat transfer, $\partial T/\partial x$ is a constant and is given by the expression

$$\frac{\partial T}{\partial x} = \frac{2\alpha q_w}{v_m L \varkappa} \tag{4.2c}$$

Employing these quantities, Eq. (4.1) can be written in dimensionless form as

$$12(\xi - \xi^2) = \frac{d^2\theta_p}{d\xi^2} - \frac{1}{q_w} \frac{dq_R}{d\xi} \tag{4.3a}$$

where

$$\xi = \frac{y}{L} \; ; \quad \theta_p = \frac{(T - T_1)}{(\frac{q_w L}{\varkappa})} \tag{4.3b}$$

Upon integrating this equation once, and by noting that $d\theta_p/d\xi = 0$ and $q_R = 0$ at $\xi = 1/2$, one finds

$$\frac{d\theta_p}{d\xi} - 2(3\xi^2 - 2\xi^3) + 1 = \frac{q_R}{q_w} \tag{4.4}$$

Equation (4.4) can be treated as the general governing equation for both gray and nongray analyses. The only difference will be shown by the radiative flux equation on the right hand side of Eq. (4.4). Proper form of the radiative flux equation should be used in Eq. (4.4) to get the final solution for the dimensionless temperature, θ_p.

4.2 LTE Assumption

As mentioned earlier, gray medium approximation replaces the wave number dependent absorption coefficient by a wave number averaged quantity. For lack of more rational choice, this average coefficient will be taken to be $\kappa_p(T_1)$. For convenience, attention will be directed only to black bounding surfaces. Replacing κ_ω by κ_p in Eq. (3.44), integrating over the wave number, and utilizing the linearized expression $T^4 - T_1^4 = 4T^3(T - T_1)$, following expression is obtained for the present problem

$$q_R =$$

$$6\sigma\kappa_p T_1^3 \left\{ \int_0^y [T(z) - T_1] \exp[-\tfrac{3}{2}\kappa_p(y - z)]dz - \int_y^L [T(z) - T_1] \exp[-\tfrac{3}{2}\kappa_p(z - y)]dz \right\} \tag{4.5}$$

Upon differentiating this equation twice, the integrals repeat themselves and may be eliminated, and the resulting equation can be expressed as

$$\frac{d^2q_R}{d\xi^2} - \frac{9}{4}\tau^2 q_R = \gamma_1 q_w \frac{d\theta_p}{d\xi} \qquad (4.6a)$$

where

$$\gamma_1 = \frac{3\tau_0^2}{\overline{N}} \; ; \; \overline{N} = \frac{\kappa\kappa_p}{4\sigma T_1^3} \; ; \; \tau_0 = \kappa_p L \qquad (4.6b)$$

The boundary conditions for this equation are

$$q_R(\tfrac{1}{2}) = 0 \; ; \; \frac{3}{2}q_R(0) = \frac{1}{\tau_0}(\frac{dq_R}{d\xi})_{\xi=0} \qquad (4.6c)$$

Note that Eq. (4.6a) is analogous to Eq. (3.52) which was the radiative flux equation for gray gases under LTE assumption. The simultaneous solution of Eqs. (4.4) and (4.6) is straightforward and the final expression for the dimensionless bulk temperature, θ_{bp}, is expressed as [31]

$$\theta_{bp} = C_1[24 - 12M_1 + M_1^3 + (M_1^3 - 12M_1 - 24)\exp(-M_1)] - \frac{12}{5}\frac{\gamma_1}{M_1^4} + \frac{17}{70}\frac{\gamma_1}{M_1^2} - \frac{17}{70} \qquad (4.7a)$$

where

$$C_1 = \frac{\gamma_1}{M_1^8}\left[\frac{48 - 3\tau_0 M_1^2 + 36\tau_0}{3\tau_0(1 - e^{-M_1}) + 2M_1(1 + e^{-M_1})}\right] \qquad (4.7b)$$

$$M_1^2 = 3\,\tau_0^2(\frac{3}{4} + \frac{1}{\overline{N}}) \qquad (4.7c)$$

The governing parameters for this equation are $\overline{N}$ and τ_0. Note that $\overline{N}$ characterizes the relative importance of radiation versus conduction for gray gases.

4.3 NLTE Consideration

Under NLTE consideration, a combination of Eqs. (3.55) and (4.4) gives

$$\frac{d^2 q_R}{d\xi^2} - \overline{M_1}^{\,2} q_R = \overline{\gamma_1}\, q_w\, (6\xi^2 - 4\xi^4 + 1) \qquad (4.8a)$$

where

$$\overline{M_1} = \frac{M_1}{\sqrt{M_2}}\ ;\ \overline{\gamma_1} = \frac{\gamma_1}{M_2};\ M_2 = 1 + \frac{3}{4}\frac{\eta}{PS(T)} \qquad (4.8b)$$

The quantities M_1 and γ_1 are defined in the same way as discussed in the preceding section.

The solution of Eq. (4.8) is given as

$$\theta_{bp} = C_1[24 - 12\overline{M_1} + \overline{M_1}^{\,3} + (\overline{M_1}^{\,3} - 12\overline{M_1} - 24)e^{-\overline{M_1}}] - \frac{12}{5}\frac{\overline{\gamma_1}}{\overline{M_1}^{\,4}} + \frac{17}{70}\frac{\overline{\gamma_1}}{\overline{M_1}^{\,2}} - \frac{17}{70} \qquad (4.9a)$$

where

$$C_1 = \frac{\overline{\gamma_1}}{\overline{M_1}^{\,8}}\ [\ \frac{48 - 3\tau_0\overline{M_1}^{\,2} + 36\tau_0}{3\tau_0(1 - e^{-\overline{M_1}}) + 2\overline{M_1}(1 + e^{-\overline{M_1}})}\ ] \qquad (4.9b)$$

Thus it is obvious that η is the driving force for NLTE. For $\eta = 0$, $M_2 = 1$, and the solution for θ_{bp} reduces to that under LTE.

Chapter 5

NONGRAY RADIATIVE TRANSFER IN LAMINAR FLOW

In this chapter, the radiative heat transfer is discussed for nongray gases. General formulation of the problem is the same as discussed in the previous chapter. The solutions under LTE and NLTE conditions are presented in next sections.

5.1 LTE Assumption

The nongray radiative flux equation under LTE assumption is given by dropping the NLTE part of Eq. (3.48)

$$q_R(\xi) = e_1 - e_2$$

$$+ \frac{3}{2}\sum_{i=1}^{n} A_{0i}U_{0i}\left\{\int_0^{\xi} F_{1\omega i}\overline{A_i}'[\frac{3}{2}u_{0i}(\xi - \xi')d\xi'] - \int_{\xi}^{0} F_{2\omega i}\overline{A_i}'[\frac{3}{2}u_{0i}(\xi' - \xi)]d\xi'\right\} \tag{5.1}$$

Using the following relations

$$F_{1\omega i} = e_{\omega i}(\xi') - e_{1\omega i} = \left(\frac{de_{\omega i}}{dT} \right)_{T_1} (T - T_1) \tag{5.2a}$$

$$F_{2\omega i} = e_{\omega i}(\xi') - e_{2\omega i} = \left(\frac{de_{\omega i}}{dT} \right)_{T_2} (T - T_2) \tag{5.2b}$$

$$H_{1i} = A_{0i}(T) \left(\frac{de_{\omega i}}{dT} \right)_{T_1} \tag{5.2c}$$

$$H_{2i} = A_{0i}(T) \left(\frac{de_{\omega i}}{dT} \right)_{T_2} \tag{5.2d}$$

$$\theta_{1p}(\xi) = \frac{(T - T_1)}{\left(\frac{q_w L}{\kappa}\right)} \tag{5.2e}$$

$$\theta_{2p}(\xi) = \frac{(T - T_2)}{\left(\frac{q_w L}{\kappa}\right)} \tag{5.2f}$$

Equation (5.1) can be expressed in an alternative form as

$$\frac{q_R(\xi)}{q_\omega} = e_1 - e_2 + \frac{3}{2}\frac{L}{\kappa} \sum_{i=1}^{n} u_{0i} \left\{ H_{1i} \int_0^{\xi} \theta_{1p}(\xi')\bar{A}'(I)d\xi' - H_{2i} \int_{\xi}^{1} \theta_{2p}(\xi')\bar{A}'(II)d\xi' \right\} \tag{5.3a}$$

where

$$\bar{A}'(I) = \bar{A}'\left[\frac{3}{2}u_{0i} (\xi - \xi') \right] \; ; \; \bar{A}'(II) = \bar{A}'\left[\frac{3}{2}u_{0i}(\xi' - \xi) \right] \tag{5.3b}$$

If, at any x–location, the two plates have the same temperature, then $T_1 = T_2$ and $e_1 = e_2$, and Eq. (5.3a) becomes

$$\frac{q_R(\xi)}{q_\omega} = \frac{3}{2}\frac{L}{\kappa} \sum_{i=1}^{n} H_i u_{0i} \left\{ \int_0^{\xi} \theta_p(\xi')\bar{A}'(I)d\xi' - \int_{\xi}^{1} \theta_p(\xi')\bar{A}'(II)d\xi' \right\} \tag{5.4}$$

Combining Eqs. (4.4) and (5.4), one obtains

$$\frac{d\theta_p}{d\xi} - 2(3\xi^2 - 2\xi^3) + 1 =$$

$$\frac{q_R(\xi)}{q_\omega} = \frac{3}{2}\frac{L}{\varkappa}\sum_{i=1}^{n} H_i u_{0i}\left\{\int_0^{\xi} \theta_p(\xi')\bar{A}'(I)d\xi' - \int_{\xi}^{1} \theta_p(\xi')\bar{A}'(II)d\xi'\right\} \qquad (5.5)$$

The temperature profile within the gas, $\theta_p(\xi)$, is thus described by Eq. (5.5). The boundary condition for this equation follows to be $\theta_p(0) = 0$.

For flow problems, the quantity of primary interest is the bulk temperature of the gas, which is the mean temperature at any location x in the flow direction. It is the temperature which fluid would assume if it was instantaneously and adiabatically mixed after leaving the cross section under consideration. Mathematically, the bulk temperature is defined as

$$T_b = \frac{1}{u_m A_c}\int_{A_c} u\ T\ dA \qquad (5.6)$$

The bulk temperature can be expressed in dimensionless form as

$$\theta_{bp} = \frac{T_b - T_1}{\left(\frac{q_w L}{\varkappa}\right)} = 6\int_0^1 \theta_p(\xi)\ (\xi - \xi^2)\ d\xi \qquad (5.7)$$

The heat transfer q_w is given by the expression $q_w = h_c(T_1 - T_b)$, where h_c is the equivalent heat transfer coefficient in Watts / m^2–K. The heat transfer results are expressed usually in terms of the Nusselt number, N_u, defined in terms of the hydraulic diameter D_h. For the present geometry, $D_h = 2L$. Eliminating the effective heat transfer coefficient h_c from the expression for q_w and N_u, a relation between the Nusselt number and the bulk temperature is obtained as

$$N_u = \frac{2L\ q_w}{\varkappa(T_1 - T_b)} = \frac{-2}{\theta_{bp}} \qquad (5.8)$$

The numerical solution of Eq. (5.5) is obtained by employing the method of undetermined parameters. For this case, a polynomial solution for $\theta_p(\xi)$ is assumed as

$$\theta_p(\xi) = a_0 + a_1\xi + a_2\xi^2 + a_3\xi^3 + a_4\xi^4 \qquad (5.9)$$

After employing the conditions $\theta_p(0) = 0$, $\theta_p'(1/2) = 0$, and $\theta_p'(0) = -\theta_p'(1)$, Eq. (5.9) becomes

$$\theta_p(\xi) = a_1(\xi - 2\xi^3 + \xi^4) + a_2(\xi^2 - 2\xi^3 + \xi^4) \qquad (5.10)$$

The constants a_1 and a_2 are obtained by satisfying the governing integro–differential equation at two convenient locations $\xi = 0$, and $\xi = 1/4$. A combination of Eq. (5.7) and (5.10) results in

$$\theta_{bp} = \frac{1}{70}(17a_1 + 3a_2) \qquad (5.11)$$

Thus, with a_1 and a_2 known, the bulk temperature (or the Nusselt number) is obtained from Eq. (5.11). The procedure for evaluating the constants a_1 and a_2 is described in detail in [32].

5.2 NLTE Consideration

The radiative flux equation under NLTE consideration is given by Eq. (3.48). By employing definitions given in Eqs. (5.2) and (5.3b), Eq. (3.48) can be expressed in an alternative form as

$$q_R(\xi) = e_1 - e_2 + \frac{3}{2}\sum_{i=1}^{n}\left\{H_{1i}\int_0^{\xi}(T - T_1)\overline{A_i}'(I)d\xi' - H_{2i}\int_{\xi}^{1}(T - T_1)\overline{A_i}'(II)d\xi'\right\}$$

$$- \frac{3}{8}\sum_{i=1}^{n}\eta_i\left\{\int_0^{\xi}\frac{dq_R}{d\xi'}\overline{A_i}'(I)d\xi' - \int_{\xi}^{1}\frac{dq_R}{d\xi'}\overline{A_i}'(II)d\xi'\right\} \qquad (5.12)$$

For black plates with $T_1 = T_2$, $e_1 = e_2$, and Eq. (5.12) becomes

$$q_R(\xi) = \frac{3}{2}\sum_{i=1}^{n}u_{0i}H_i\left\{\int_0^{\xi}(T - T_1)\overline{A_i}'(I)d\xi' - \int_{\xi}^{1}(T - T_1)\overline{A_i}'(II)d\xi'\right\}$$

$$- \frac{3}{8}\sum_{i=1}^{n}\eta_i\left\{\int_0^{\xi}\frac{dq_R}{d\xi'}\overline{A_i}'(I)d\xi' - \int_{\xi}^{1}\frac{dq_R}{d\xi'}\overline{A_i}'(II)d\xi'\right\} \qquad (5.13)$$

The energy equation is given by Eq. (4.3a) which is rewritten as

$$\frac{dq_R}{d\xi} = q_w\left[\frac{d^2\theta_p}{d\xi^2} - 12(\xi - \xi^2)\right] \qquad (5.14)$$

Combining Eqs. (4.4), (5.7), (5.13), and (5.14), one obtains

$$\frac{d\theta_p}{d\xi} - 2(3\xi^2 - 2\xi^3) + 1 =$$

$$\frac{3}{2}\frac{L}{\varkappa}\sum_{i=1}^{n}H_iu_{0i}\left\{\int_0^{\xi}\theta(\xi')\overline{A_i}'(I)d\xi' - \int_{\xi}^{1}\theta(\xi')\overline{A_i}'(II)d\xi'\right\}$$

$$- \frac{3}{8}\sum_{i=1}^{n}\eta_i\left\{\int_0^{\xi}\left[\frac{d^2\theta}{d\xi'^2} - 12(\xi' - \xi'^2)\right]\overline{A_i}'(I)d\xi' - \int_{\xi}^{1}\left[\frac{d^2\theta}{d\xi'^2} - 12(\xi' - \xi'^2)\right]\overline{A_i}'(II)d\xi'\right\} \qquad (5.15)$$

The numerical solution of Eq. (5.15) is obtained by the same way as discussed in the previous section. Thus, θ_{bp} is given by Eq. (5.11). Note that the constants a_1 and a_2 in this case are different. The entire procedure of evaluating the constants a_1 and a_2 is described in Appendix C.

Chapter 6

RESULTS AND DISCUSSION

Extensive results were obtained after solving the equations described in earlier chapters. The results are presented in terms of bulk temperature as a function of temperature, pressure, and spacing between the plates. The results were obtained for six different gases. These are CO, NO, OH, CO_2, H_2O, and CH_4. LTE and NLTE results for these gases were compared at different temperature and pressure conditions. The results obtained for both gray and non-gray analyses are presented in the following sections.

6.1 Gray Results

In this section, results are presented for the six gases under consideration under gray gas assumption. Both LTE and NLTE results have been obtained for all the gases considered. The results are compared at pressures ranging from 0.1 to 10 atm. and at temperatures ranging from 300 K to 2000 K. The spacing between the plates is varied from 0.1 to 100 centimeters.

The LTE and NLTE results for CO are presented in Fig. 6.1. In Fig. 6.1(a), pressure is kept constant at one atmosphere and LTE results are compared at four different temperatures

(300 K, 500 K, 1000 K,and 2000 K). The results show that as one goes from higher temperature to lower temperature, the bulk temperature decreases for any particular plate spacing. At any given temperature, the bulk temperature is seen to vary significantly in the intermediate range of plate spacings. A lower value of bulk temperature means higher capacity of the gas to exchange radiation. For lower spacings, there is almost negligible radiative contribution. Radiative interaction increases with increasing plate spacing. Figure 6.1(b) illustrates the results at a fixed temperature of 500 K and for P = 0.1, 1, and 10 atm. The variation between the results at different pressures show that as we decrease the pressure, the radiative heat transfer effect decreases. Thus Figs. 6.1(a) and 6.1(b) show that under LTE assumption, the radiative heat exchange capacity of CO is higher at higher temperatures and pressures.

In Figs. 6.1(c) and 6.1(d), LTE and NLTE results are compared for CO. In Fig. 6.1(c), pressure is kept constant at one atmosphere and temperature is varied from 300 to 2000 K. The results show that the variation between LTE and NLTE results is maximum at lower temperatures. The LTE and NLTE results show maximum differences at moderate pressures (Fig. 6.1(d)). This implies that NLTE effect is pronounced at lower temperatures and moderate pressures. Thus NLTE effect must be considered when the temperature and pressures are relatively low. It should be noted that the effect of NLTE is to lower the ability of the gas for radiative interaction.

Figures 6.2 present results for NO. In Figs. 6.2(a) and 6.2(b), LTE results are compared at different temperatures and pressures, and in Figs. 6.2(c) and 6.2(d), LTE and NLTE results are compared at different temperatures and pressures. The result shows the same behavior as in the case of CO. In a similar manner, Figs. 6.3 show the results for OH. There appears to be no NLTE effect for OH. Figure 6.4 is a comparison of LTE and NLTE results for CO, NO, and OH at a temperature of 500 K and one atmospheric pressure. The results show that

OH has the lowest radiative ability while CO shows the highest radiative ability at the particular temperature and pressure considered. Further, The variation between the LTE and NLTE is maximum for CO and minimum for OH. This implies that CO has a higher tendency to show radiative effect as well as it is more sensitive to nonequilibrium phenomena.

The LTE and NLTE results for polyatomic gases are presented in Figs. 6.5 through 6.8. Figure 6.5 presents results for CO_2. The LTE results are compared for temperatures ranging from 300 K to 2000 K and one atmospheric pressure. The results illustrate that bulk temperature decreases with increasing temperature. In Fig. 5(b), LTE results are shown at different pressures between 0.1 and 10 atm. and at a temperature of 500 K. It is seen that bulk temperature decreases, in general, with increasing pressure. At higher pressures, bulk temperature decreases smoothly for low plate spacings, but at higher plate spacings, it becomes uniform. The reasons for this behavior of CO_2 are given in [31, 32]. Figure 6.5(c) is a comparison of LTE and NLTE results at various temperatures and 1 atmospheric pressure. It is seen that there is almost no difference between LTE and NLTE results at any temperature. In Fig. 6.5(d), LTE and NLTE results are compared at various pressures and a temperature of 500 K. At a pressure of 0.1 atm, there are some differences between LTE and NLTE results. The differences are negligible at higher pressures.

The results for H_2O are presented in Figs. 6.6. The trend of the results are more of less the same as observed in the case of CO_2. The LTE results are compared at different temperatures and one atmospheric pressure in Fig. 6.6(a). The results show that bulk temperature decreases with increasing temperature which implies higher capacity for radiative exchange. Figure 6.6(b) illustrates results at different pressures and 500 K temperature. In general,the bulk temperature is seen to decrease with pressure. It becomes uniform at higher pressures and at higher plate spacings. However, bulk temperature becomes uniform at higher plate

spacings compared to CO_2. Figures 6.6(c) and 6.6(d) show a comparison of LTE and NLTE results at different temperatures and pressures. There is almost no variation between LTE and NLTE results except at 500 K and 0.1 atm. The variation is more than that observed for CO_2.

The results for CH_4 are presented in Figs. 6.7. In Figs. 6.7(a) and 6.7(b), LTE results are presented at different pressures and temperatures. The trend of results is similar to that exhibited by CO_2 and H_2O. Figures 6.7(c) and 6.7(d) show comparison of LTE and NLTE results at different temperatures and pressures. There is absolutely no difference between LTE and NLTE results at any temperature and pressure. This implies that NLTE consideration is not important for CH_4.

Figure 6.8 shows a comparison of NLTE results for all the gases under consideration at 500 K and one atmospheric pressure. It is seen that bulk temperature is highest for OH and lowest for CO_2. This implies that OH is the least radiating gas whereas CO_2 has the highest ability for radiative exchange under the given conditions.

The overall conclusion is that the NLTE results for polyatomic gases do not show much variation from LTE results. On the other hand, the NLTE results for diatomic gases show significant variations from LTE results at lower temperatures and moderate pressures. This implies that NLTE has significant influence on diatomic gases at relatively low temperatures and pressures.

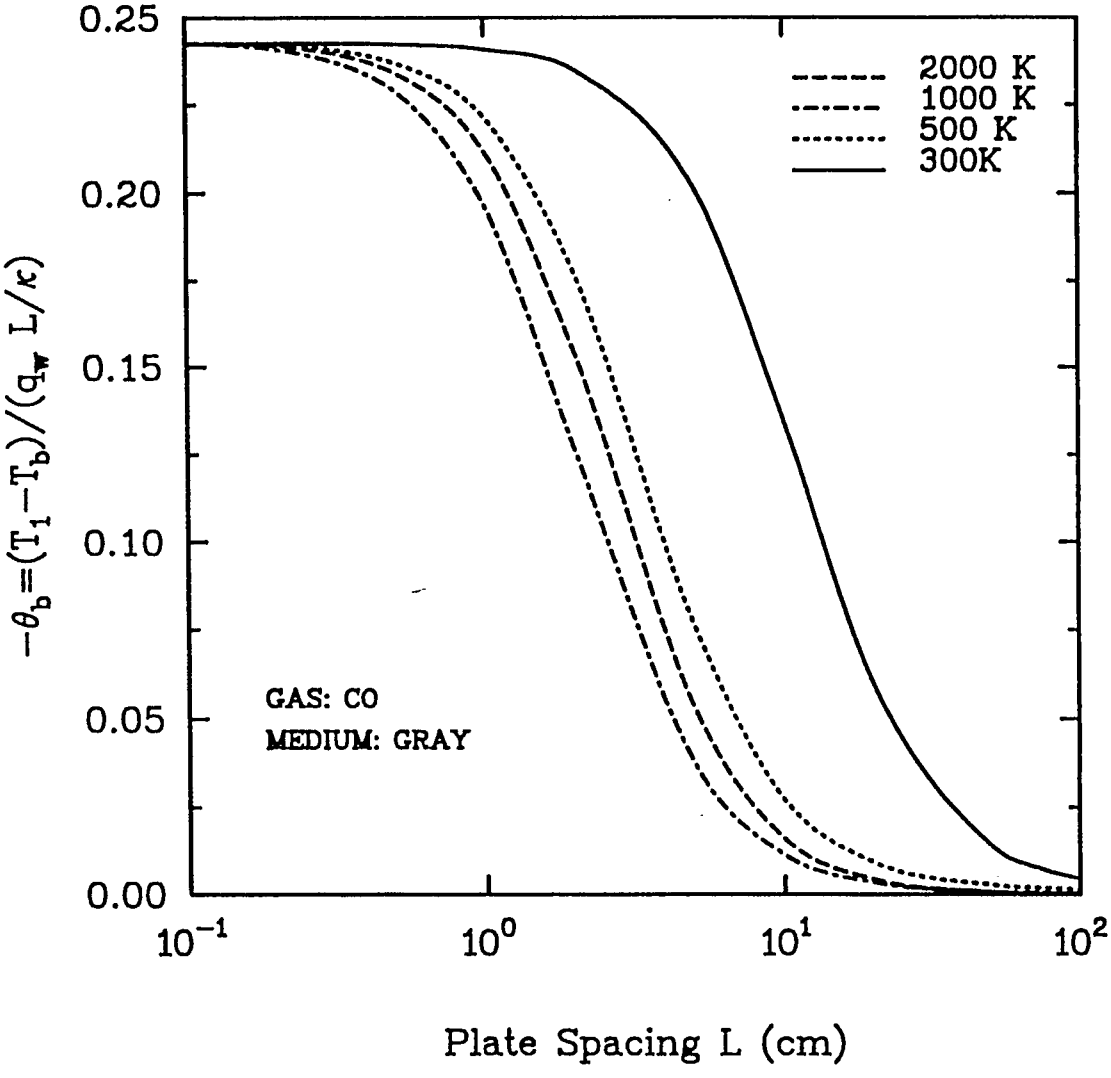

Fig. 6.1(a): LTE results for CO, P=1 atm, T_w=300–2000 K

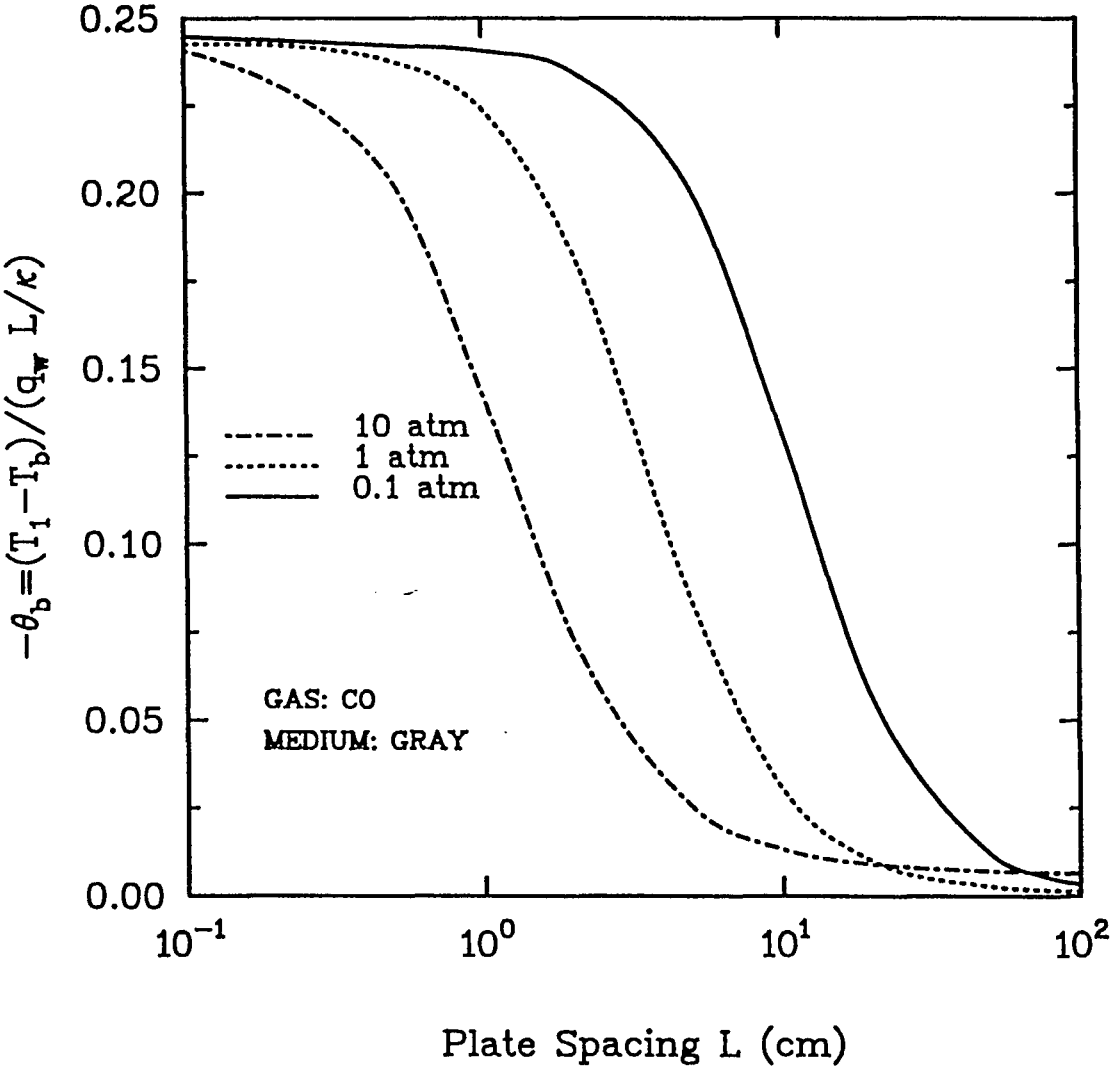

Fig. 6.1(b): LTE results for CO, T_w=500 K, P=0.1–10 atm

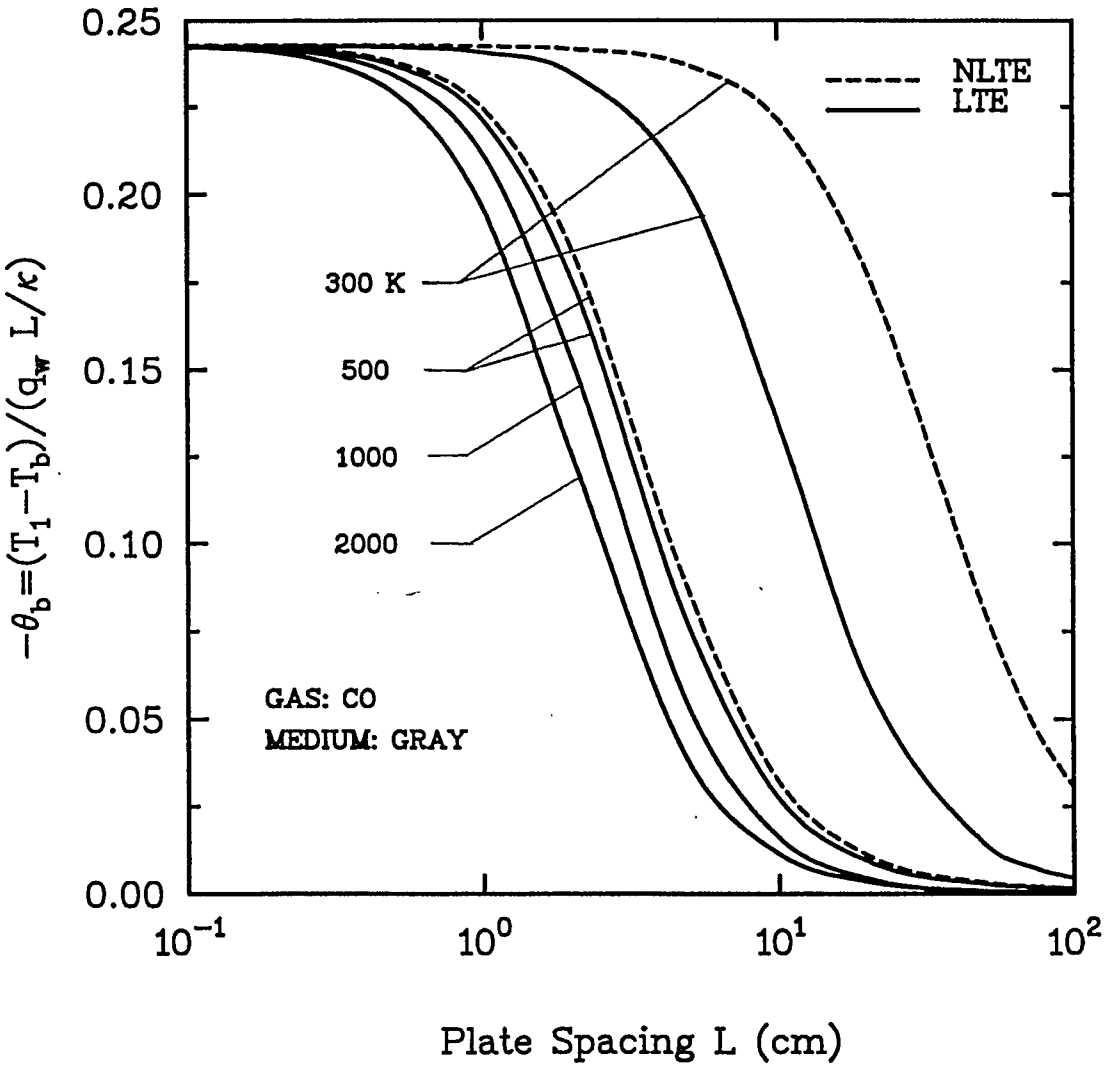

Fig. 6.1(c): LTE and NLTE results for CO, P=1 atm, T_w=300–2000 K

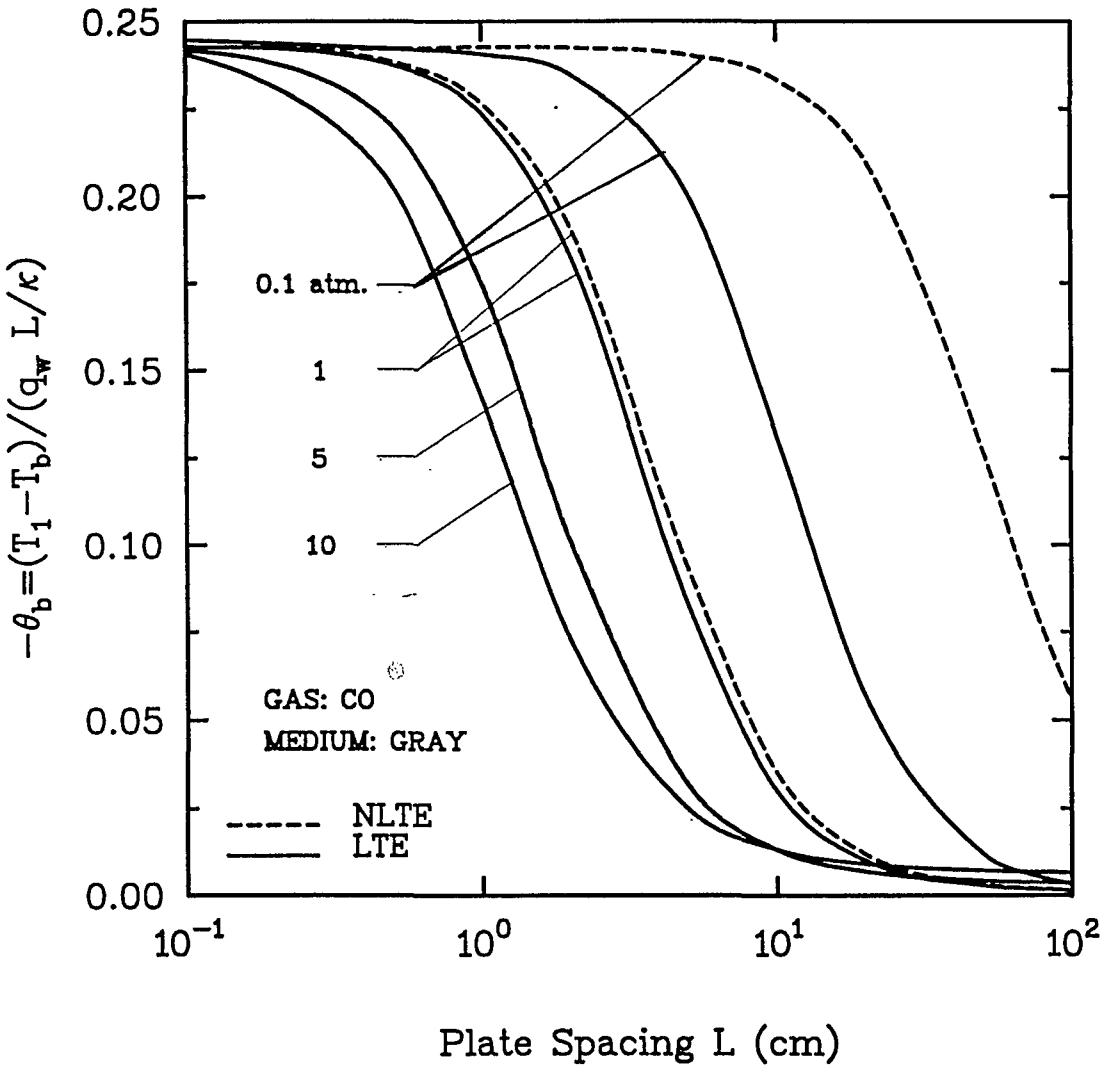

Fig. 6.1(d): LTE and NLTE results for CO, T_w=500 K, P=0.1–10 atm

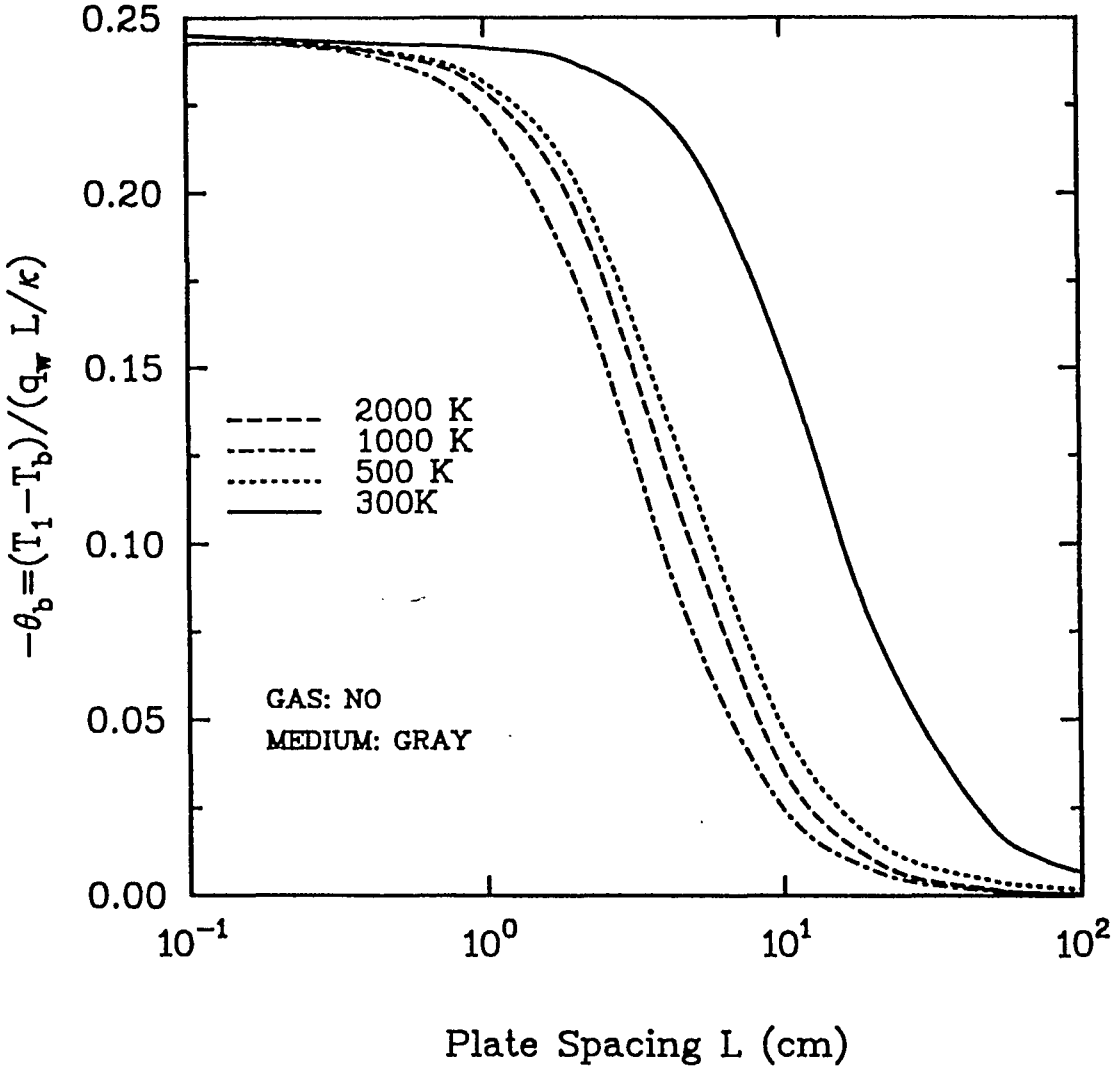

Fig. 6.2(a): LTE results for NO, P=1 atm, T_w=300–2000 K

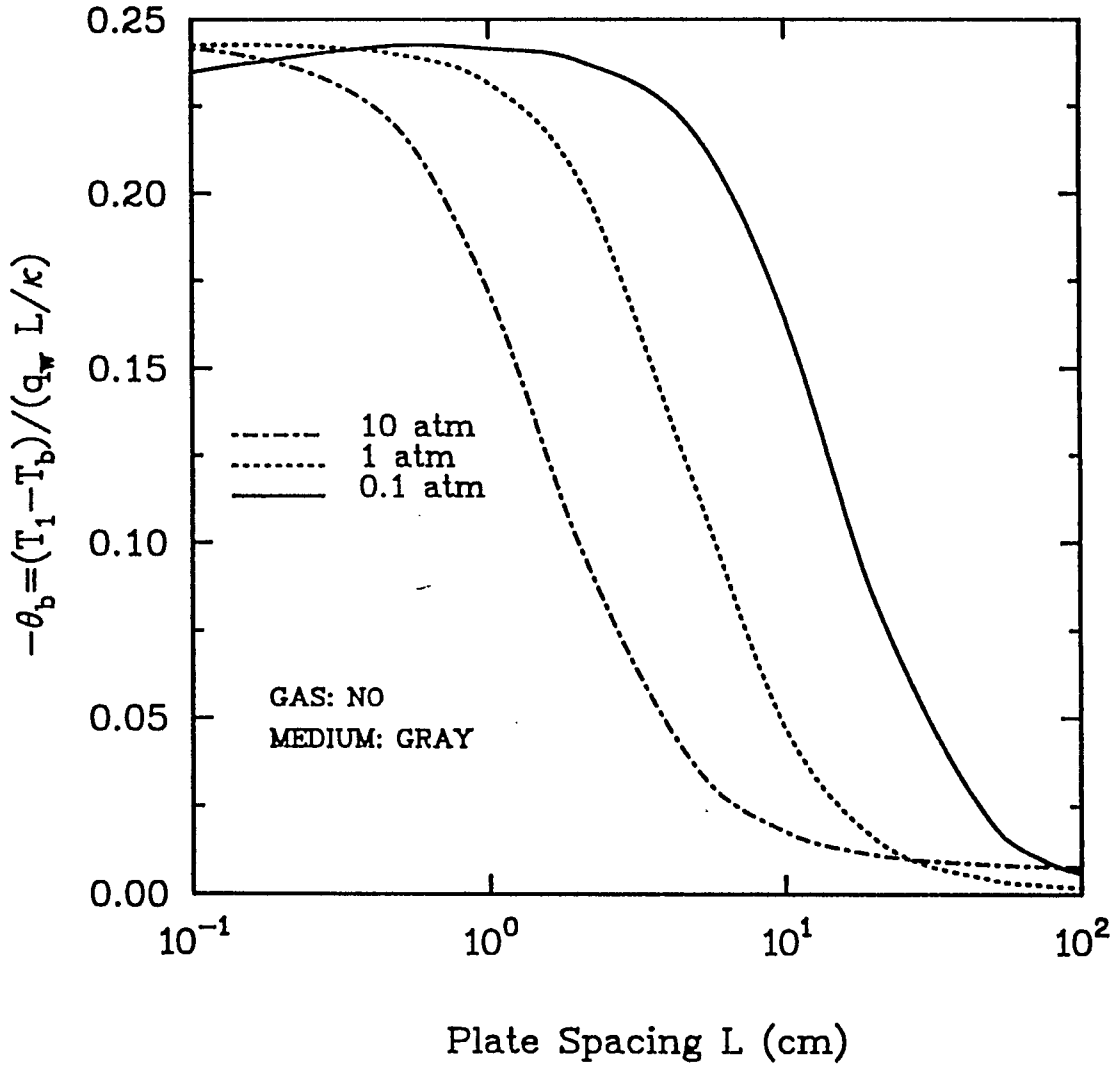

Fig. 6.2(b): LTE results for NO, T_w=500 K, P=0.1–10 atm

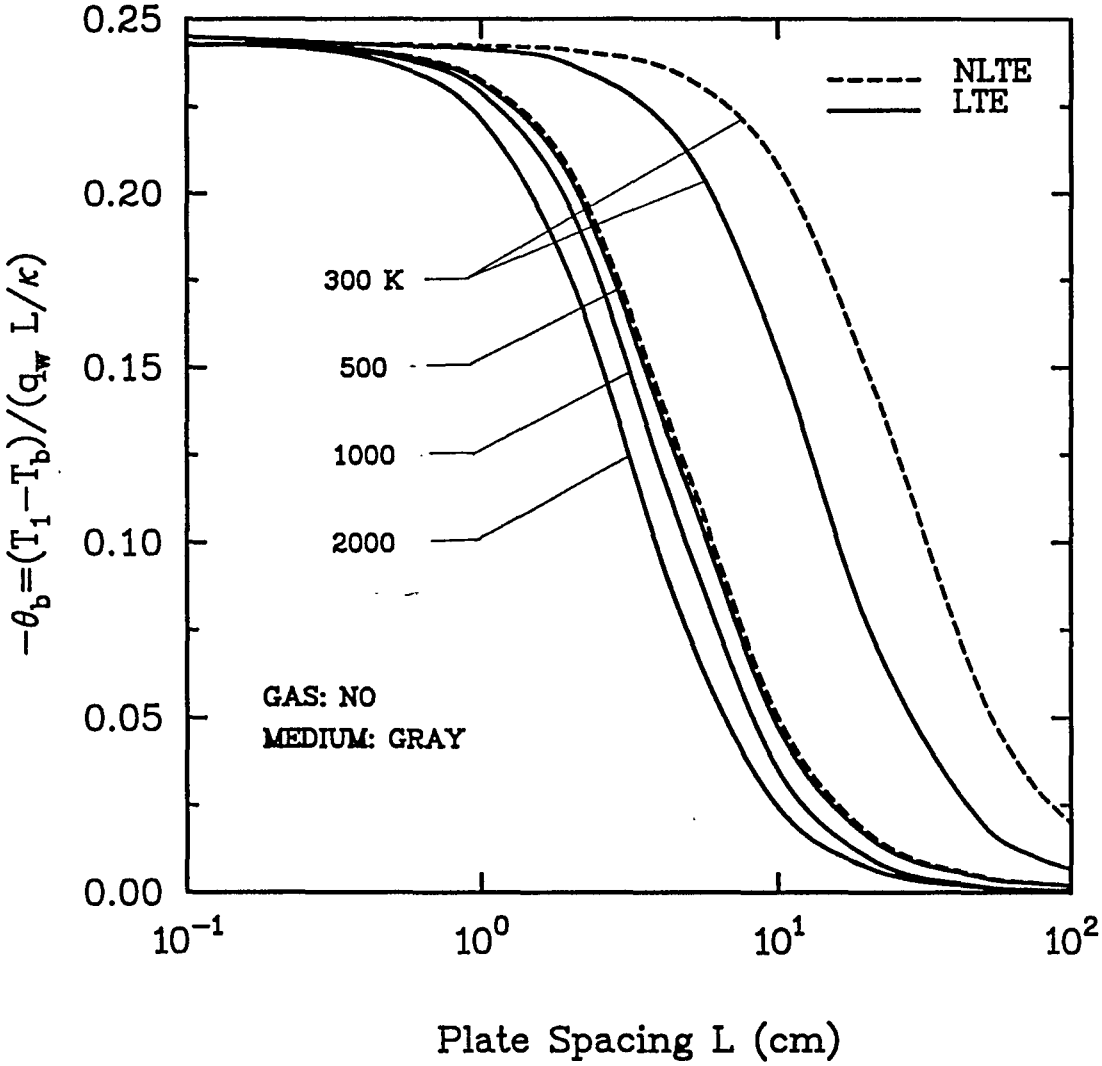

Fig. 6.2(c): LTE and NLTE results for NO, P=1 atm, T_w=300–2000 K

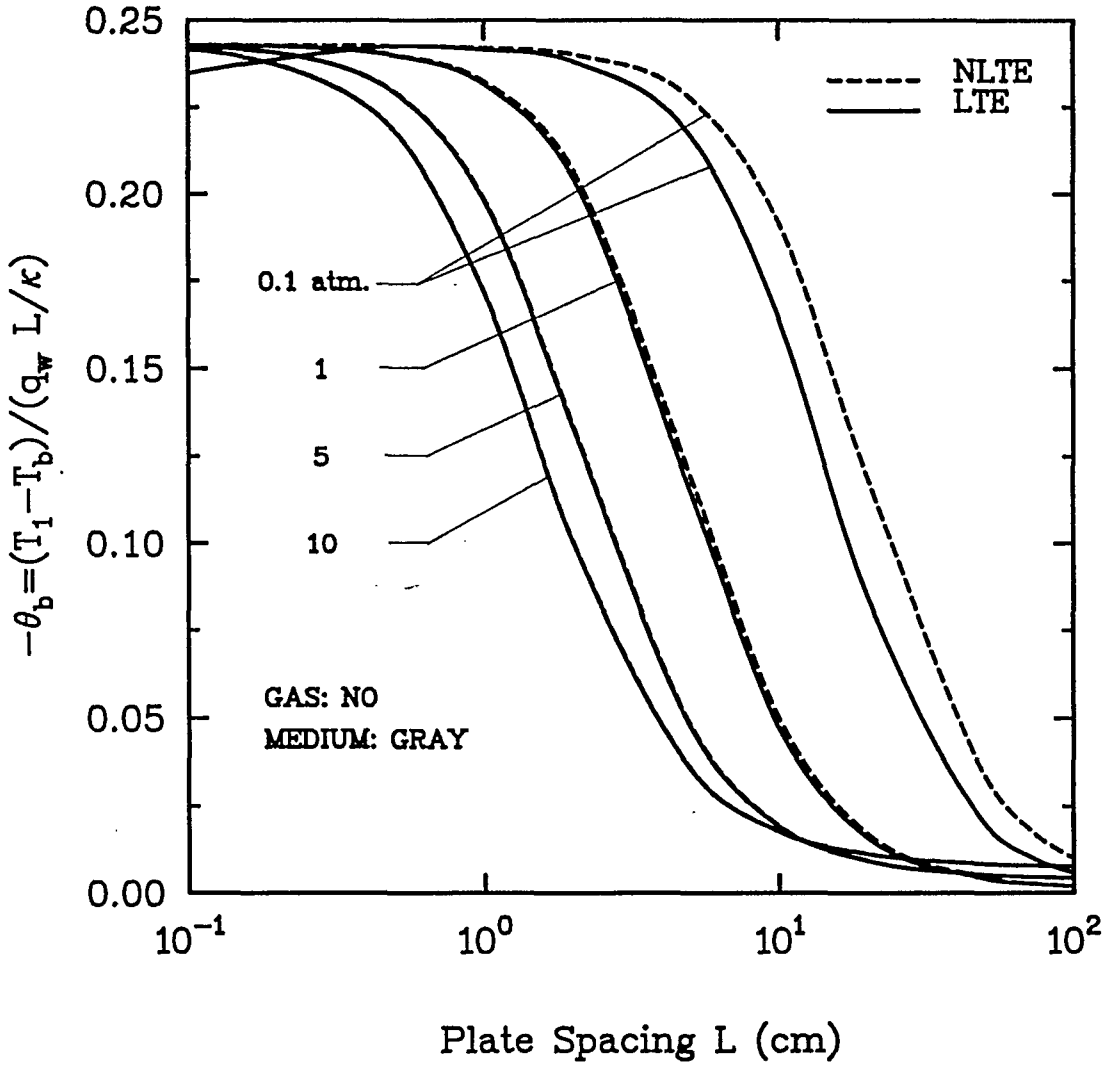

Fig. 6.2(d): LTE and NLTE results for NO, T_w=500 K, P=0.1–10 atm

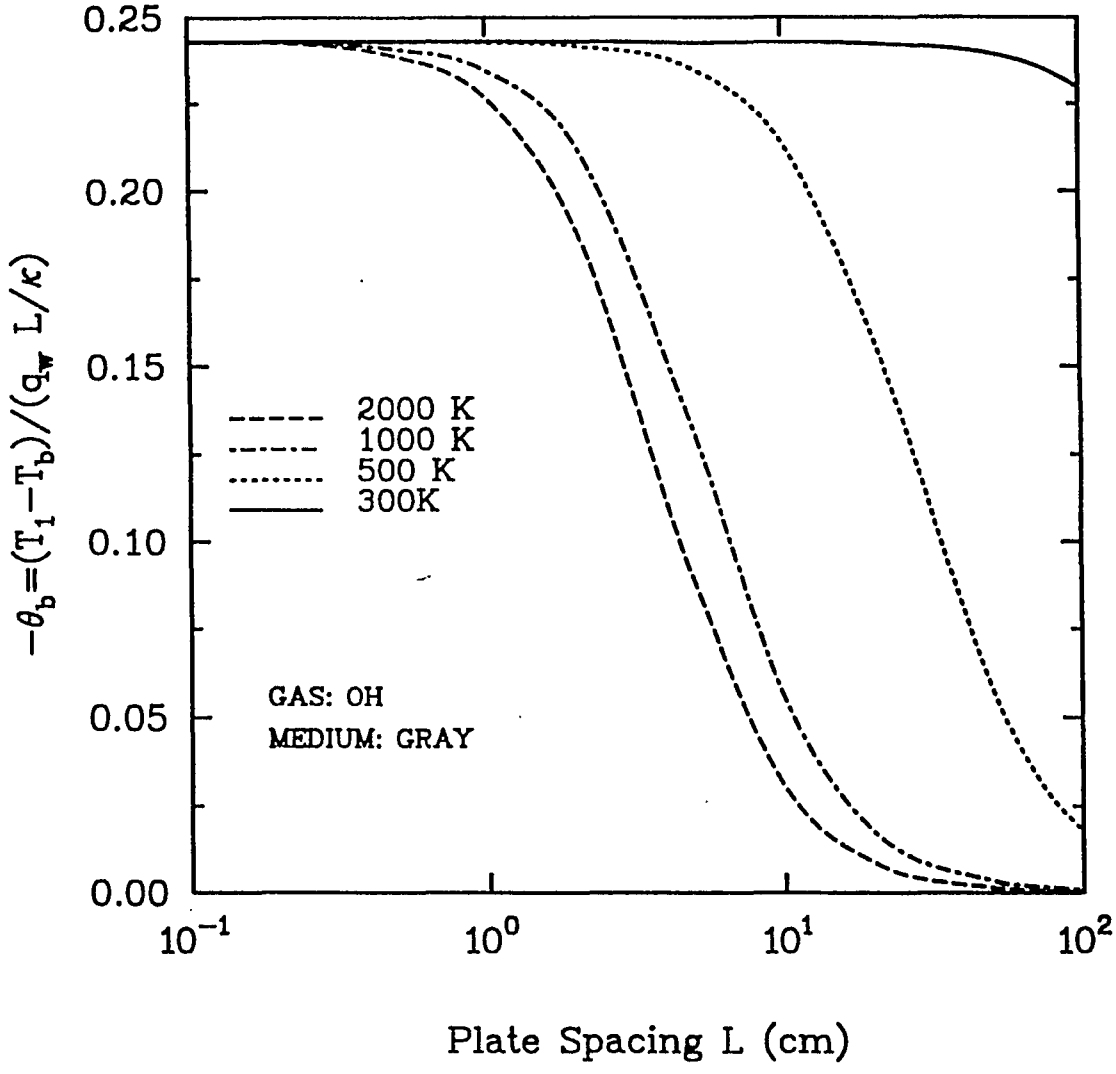

Fig. 6.3(a): LTE results for OH, P=1 atm, T_w=300–2000 K

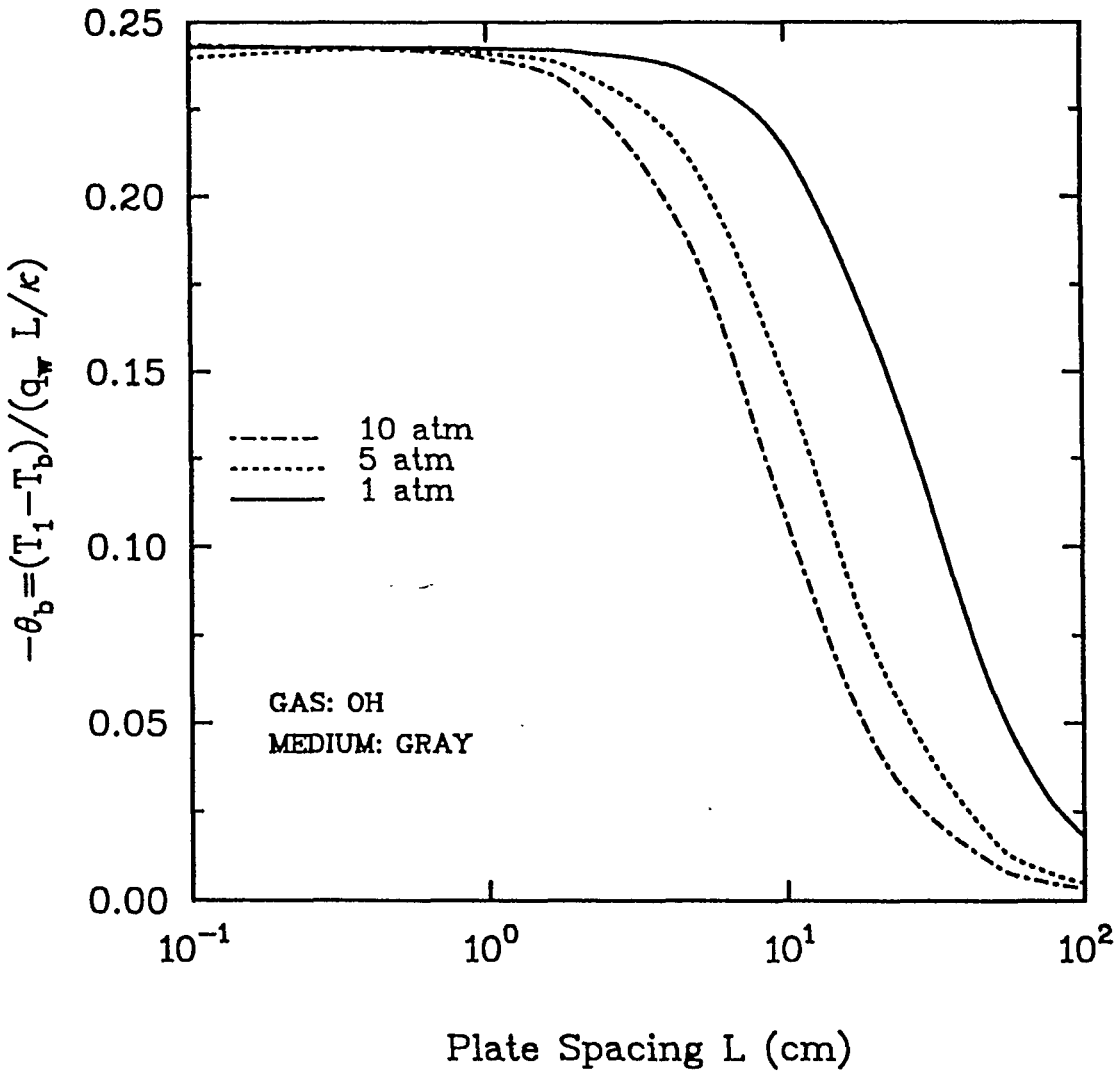

Fig. 6.3(b): LTE results for OH, T_w=500 K, P=1–10 atm

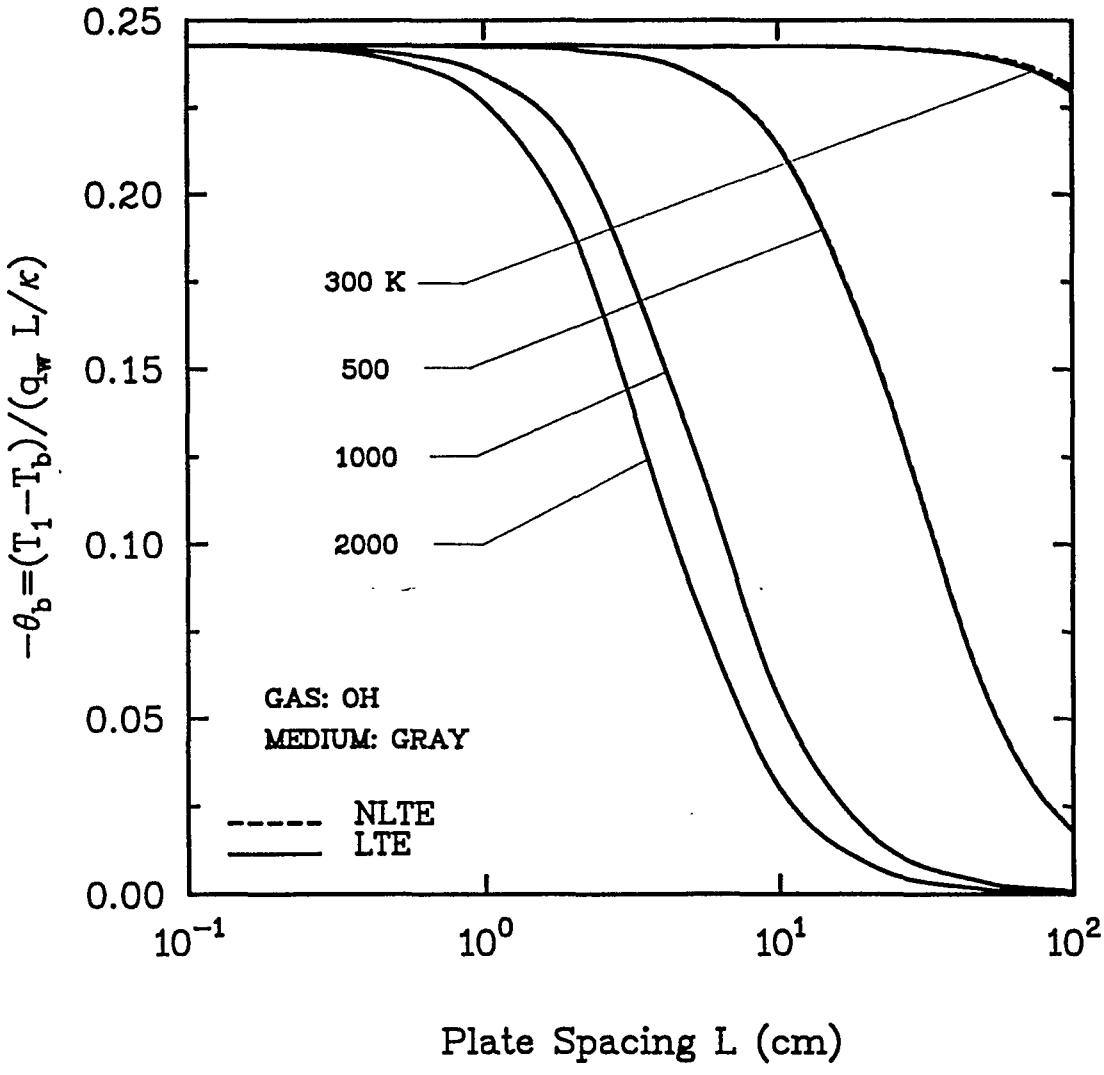

Fig. 6.3(c): LTE and NLTE results for OH, P=1 atm, T_w=300–2000 K

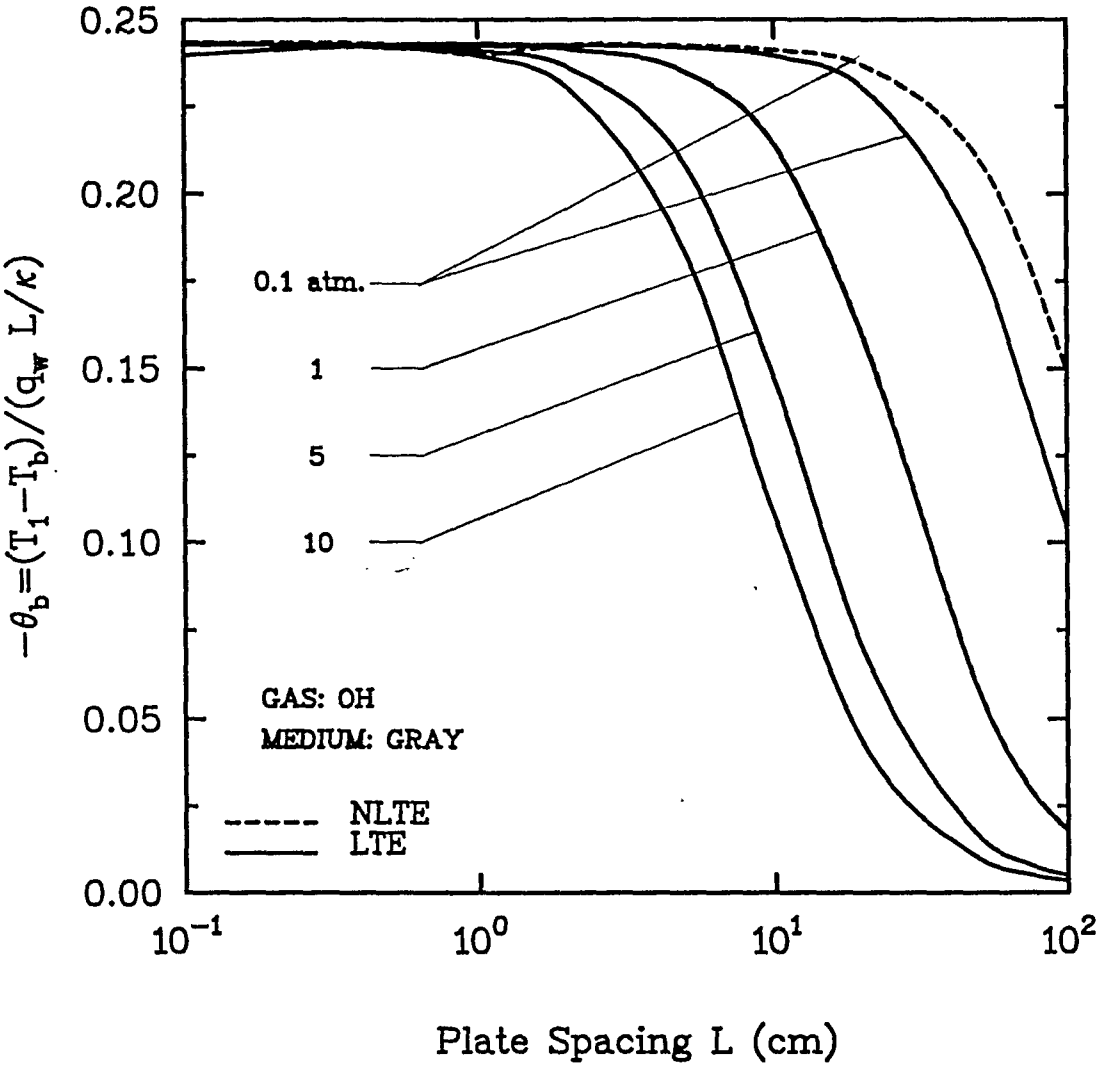

Fig. 6.3(d): LTE and NLTE results for OH, T_w=500 K, P=0.1–10 atm

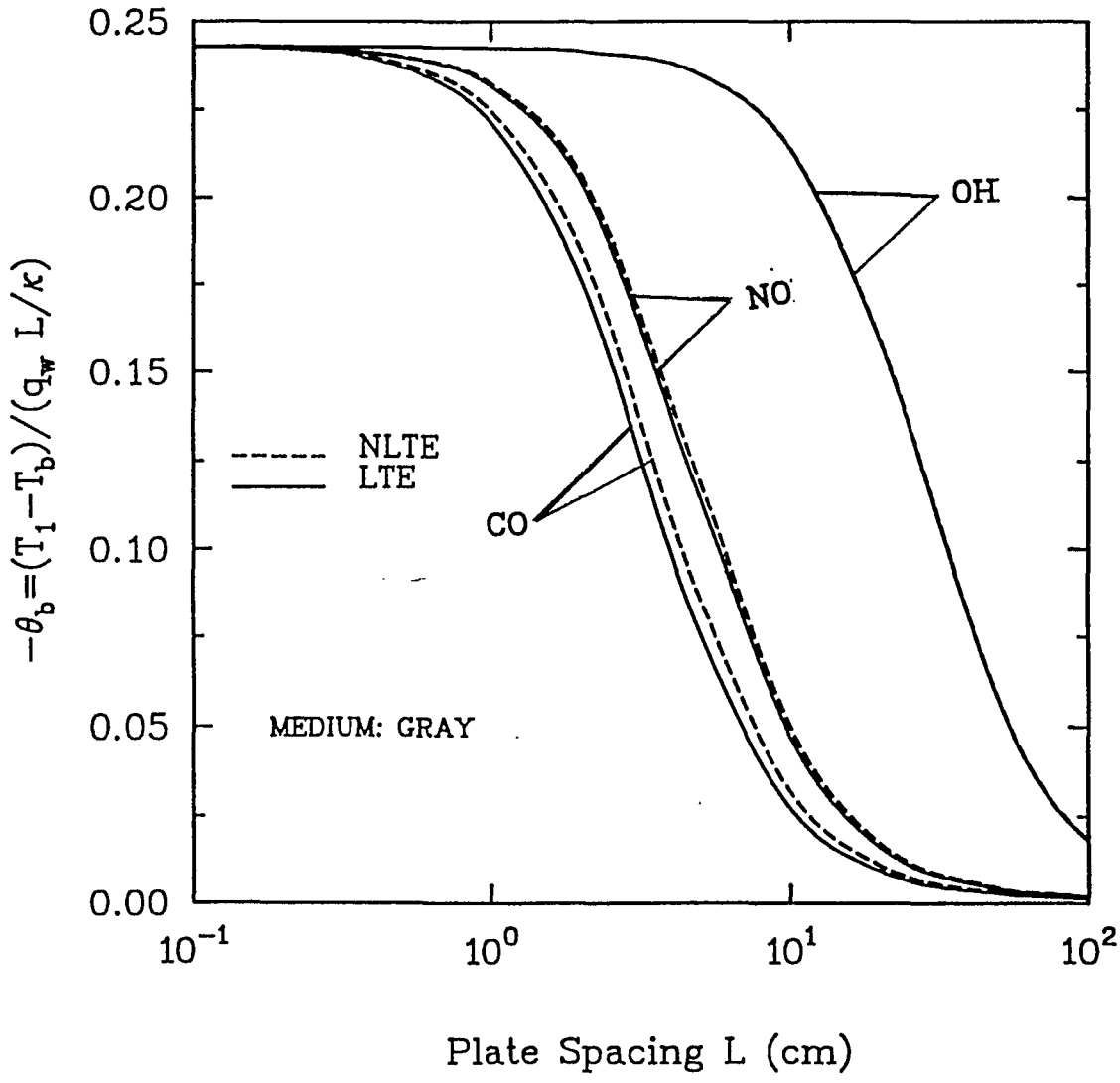

Fig. 6.4: Comparison of LTE and NLTE results for diatomic Gases at 500 K and 1 Atm.

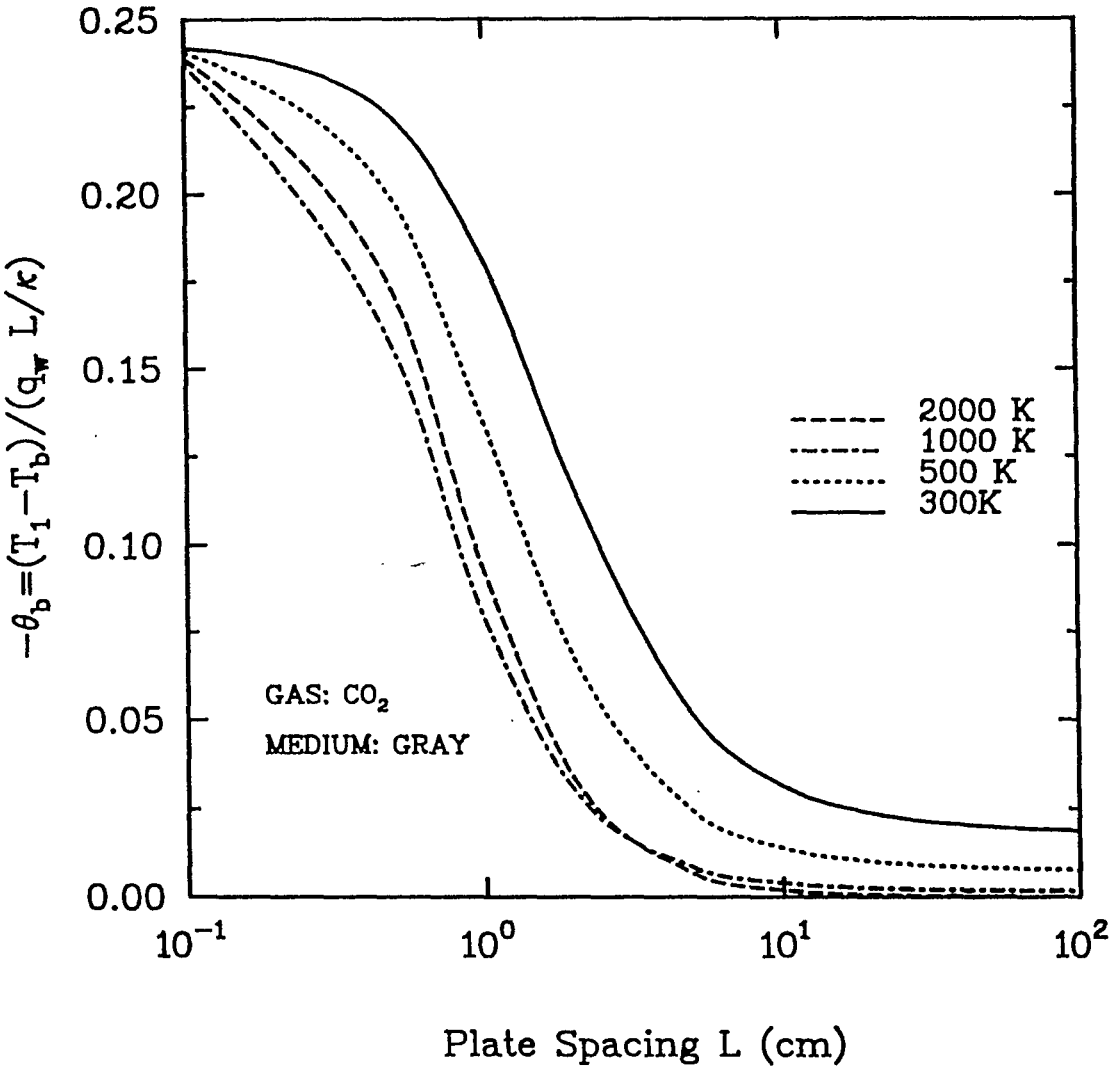

Fig. 6.5(a): LTE results for CO_2, P=1 atm, T_w=300–2000 K

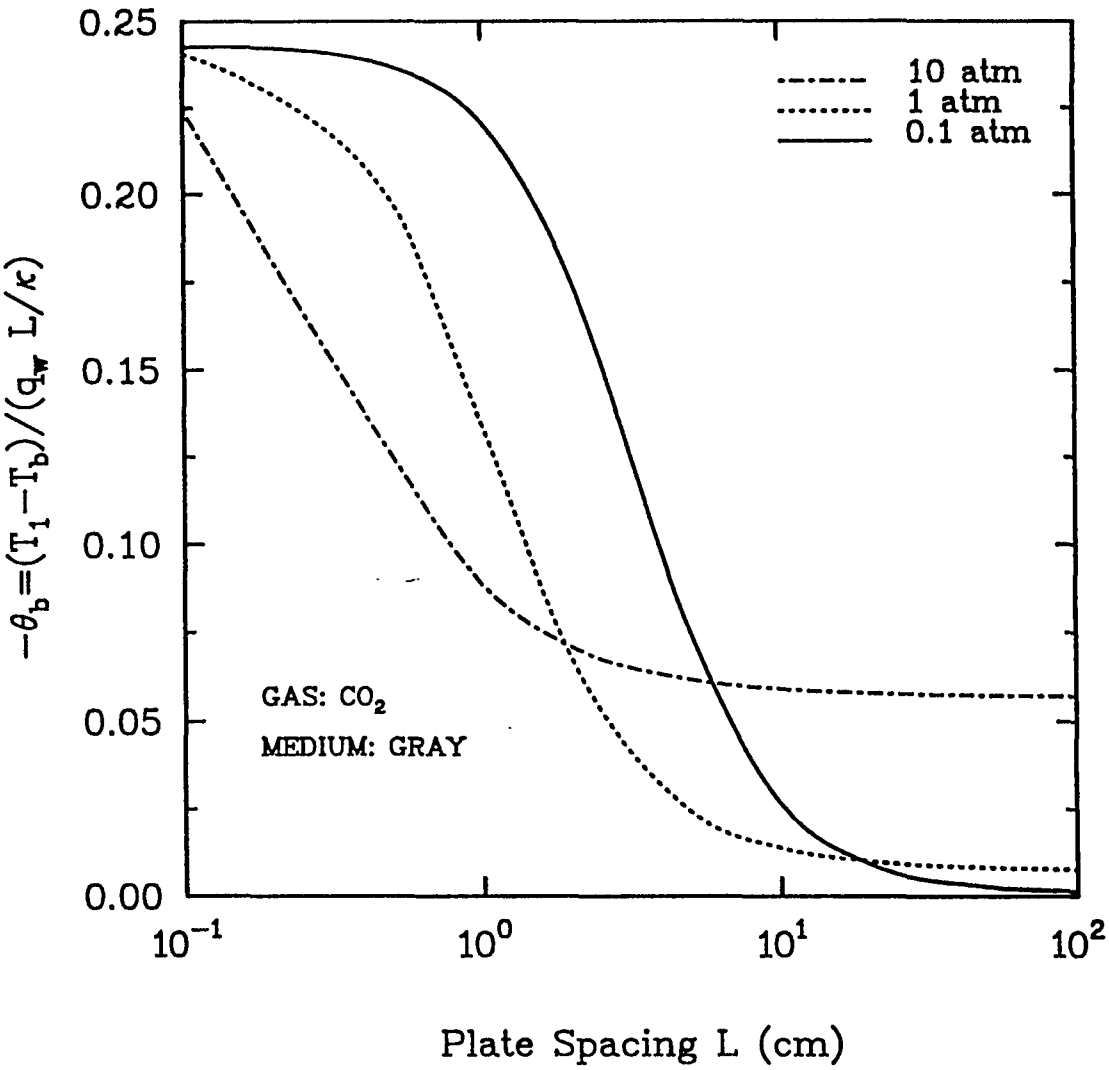

Fig. 6.5(b): LTE results for CO_2, T_w=500 K, P=0.1–10 atm

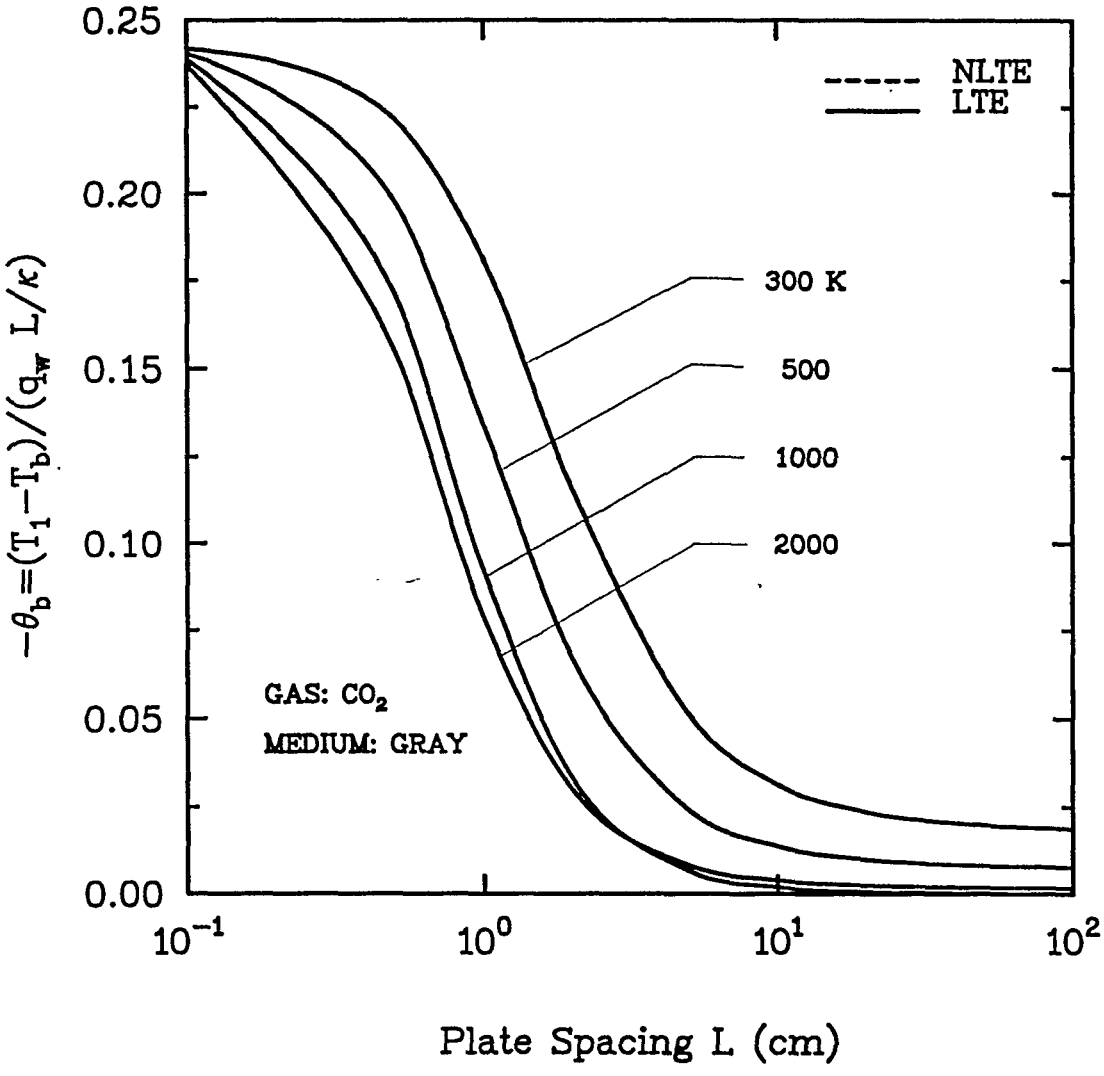

Fig. 6.5(c): LTE and NLTE results for CO_2, P=1 atm, T_w=300–2000 K

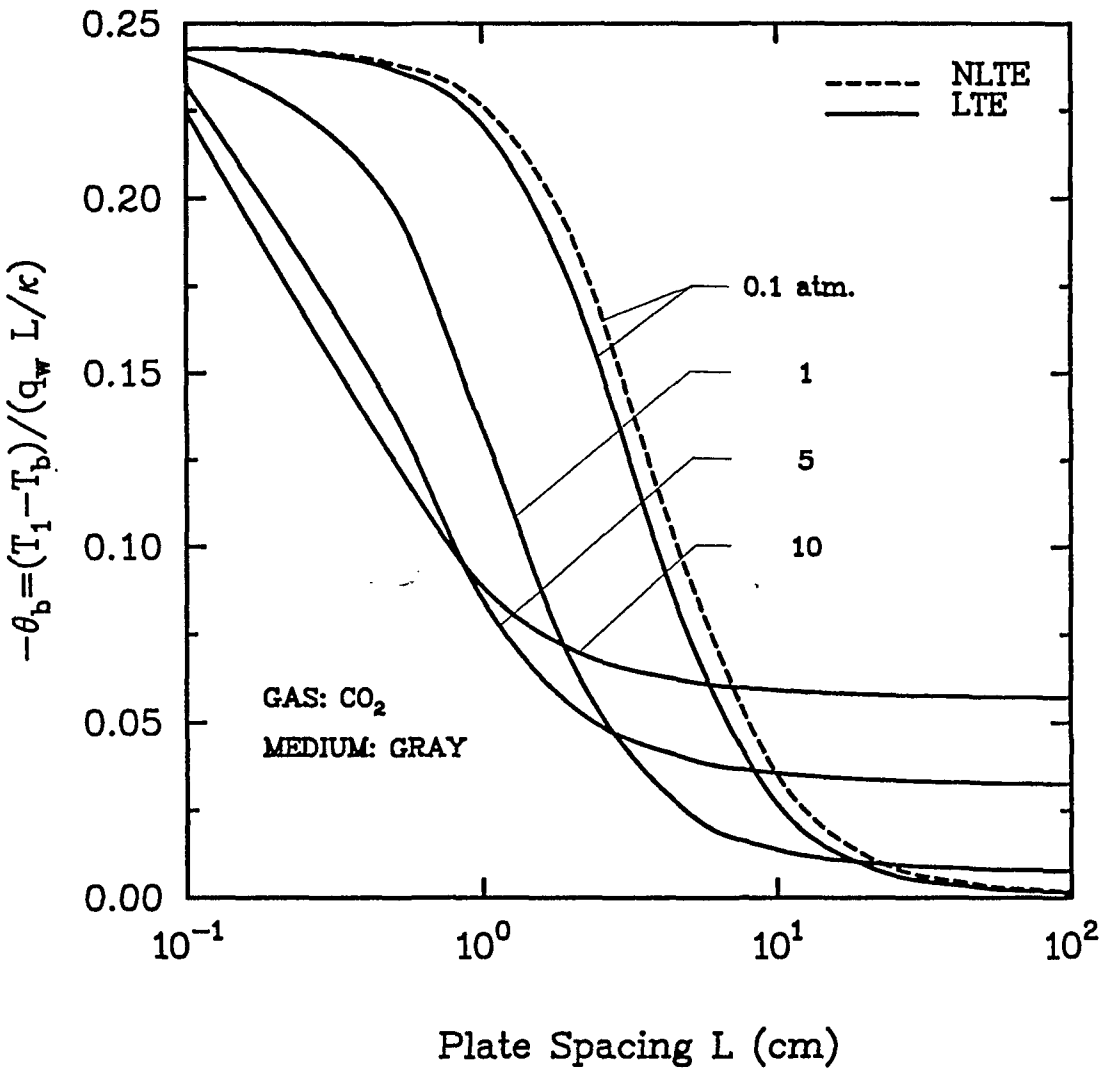

Fig. 6.5(d): LTE and NLTE results for CO_2, T_W=500 K, P=0.1–10 atm

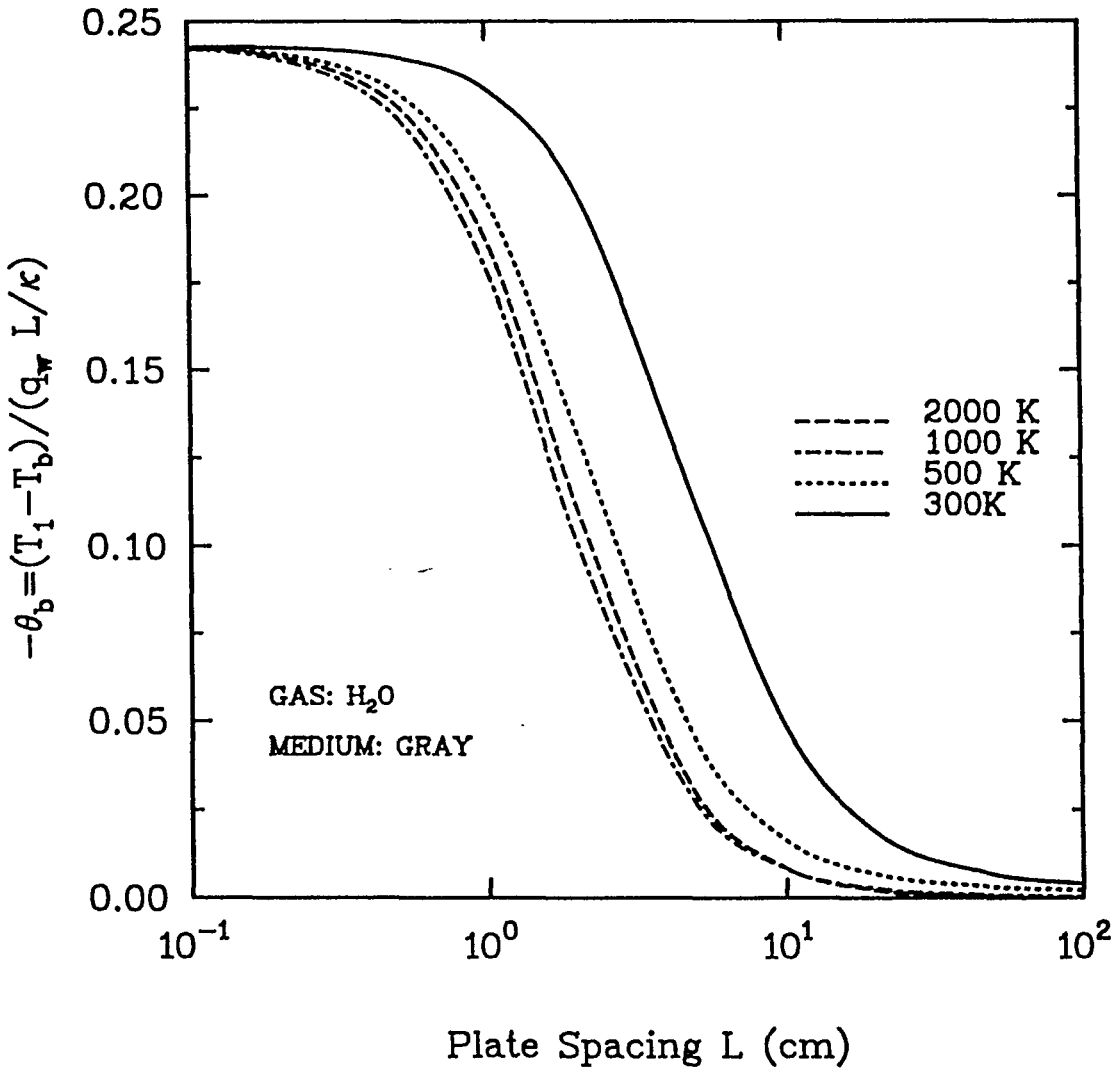

Fig. 6.6(a): LTE results for H_2O, P=1 atm, T_w=300–2000 K

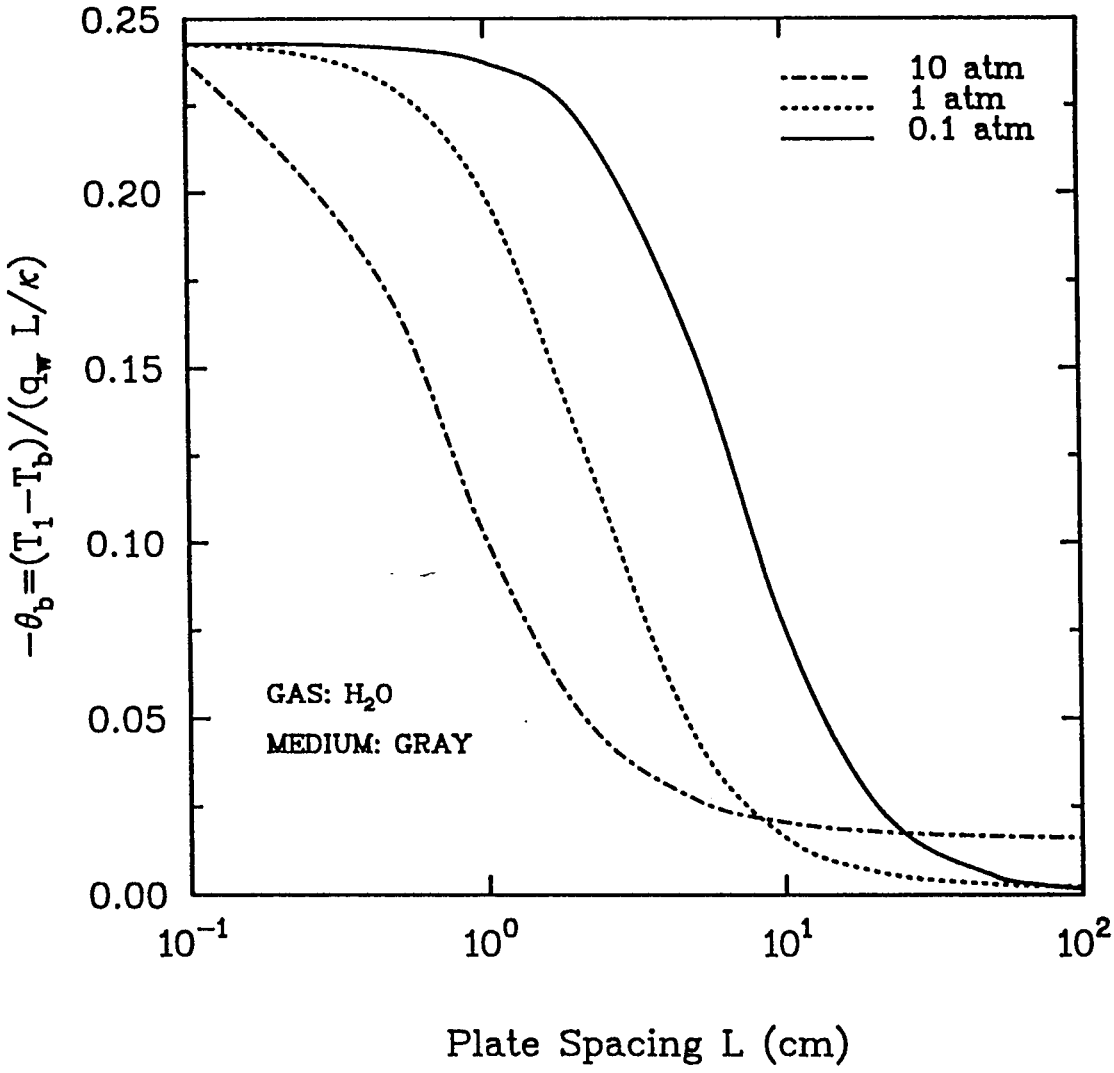

Fig. 6.6(b): LTE results for H_2O, T_w=500 K, P=0.1–10 atm

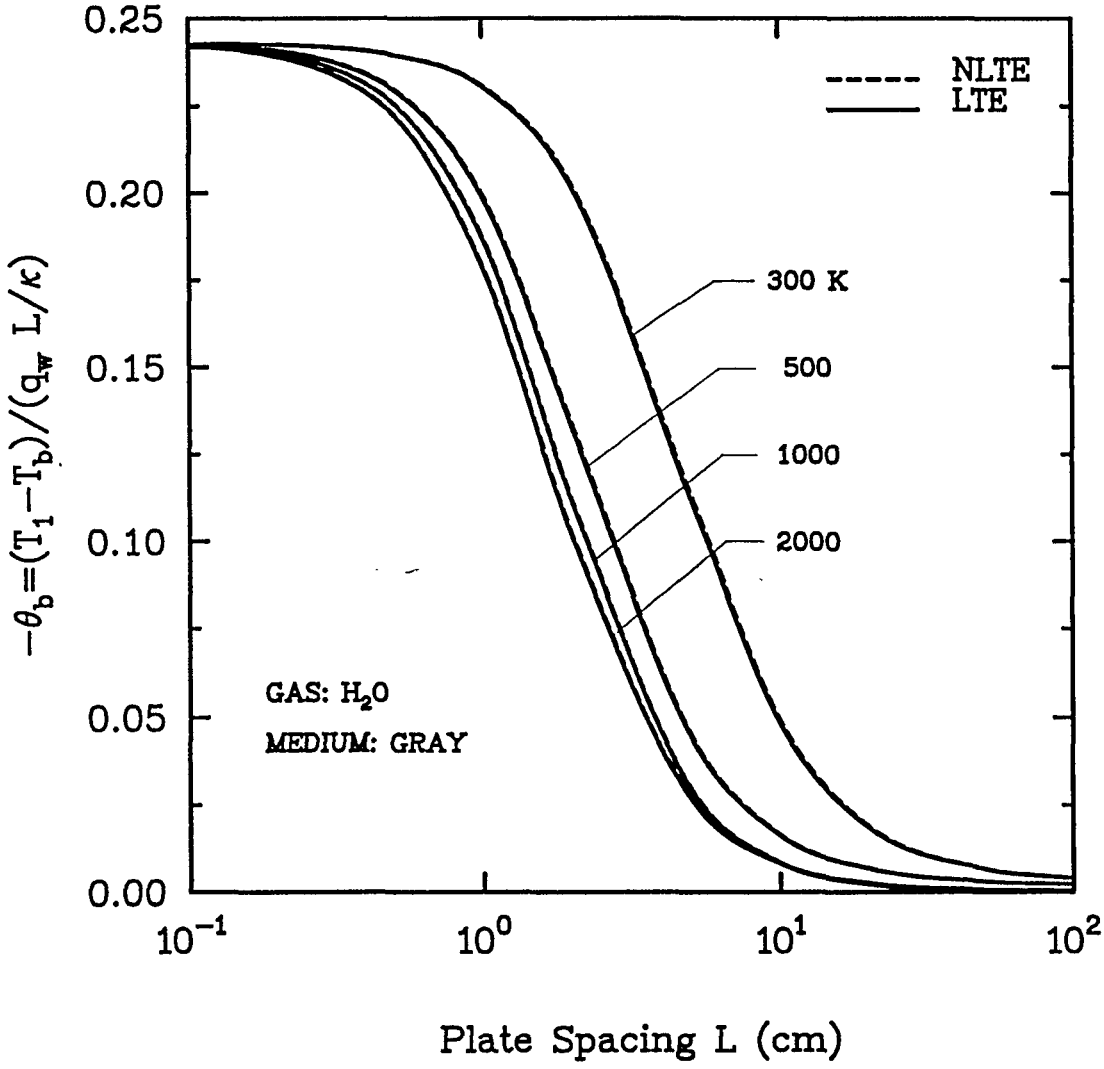

Fig. 6.6(c): LTE and NLTE results for H_2O, P=1 atm, T_W=300–2000 K

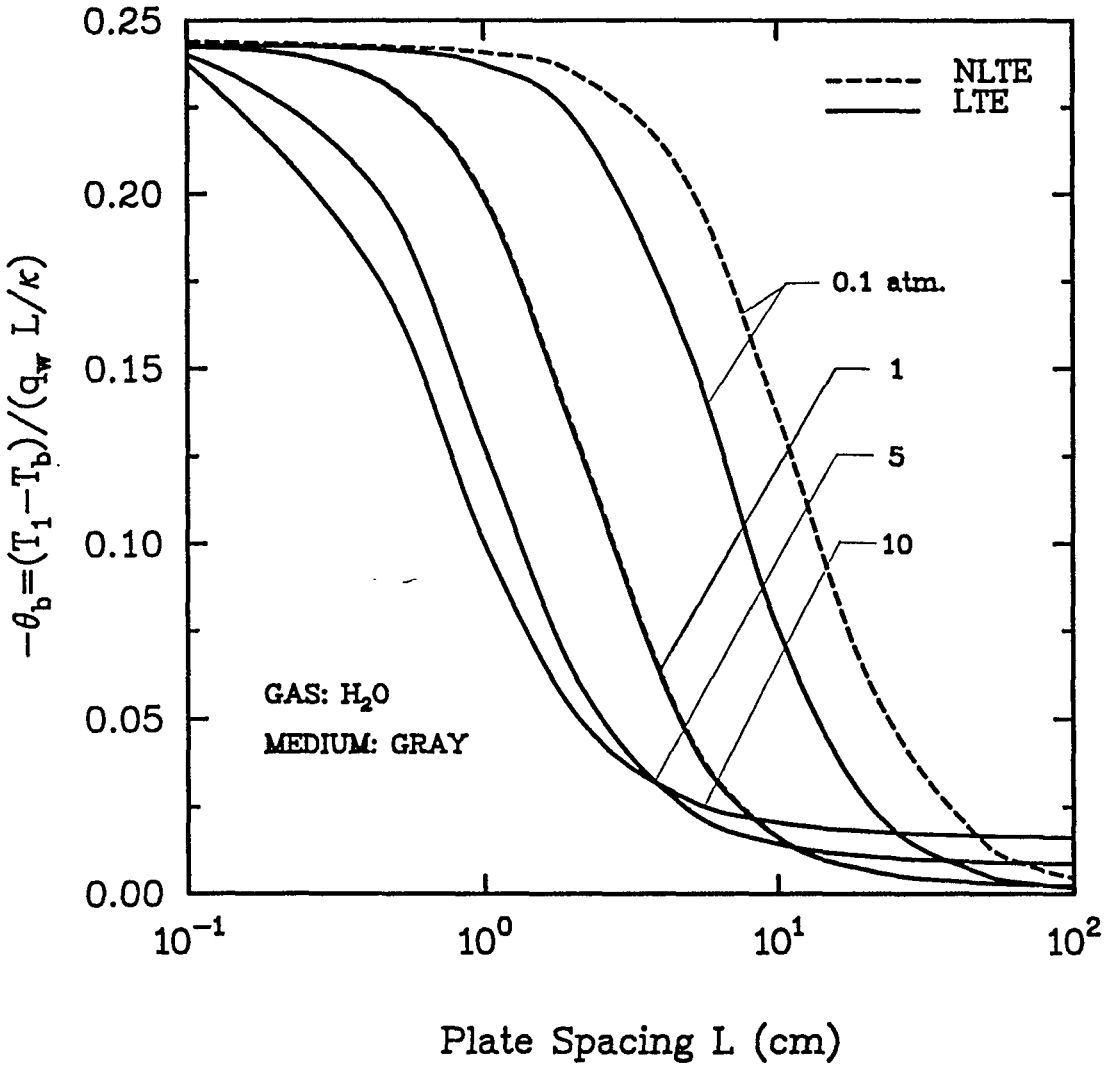

Fig. 6.6(d): LTE and NLTE results for H_2O, T_w=500 K, P=0.1–10 atm

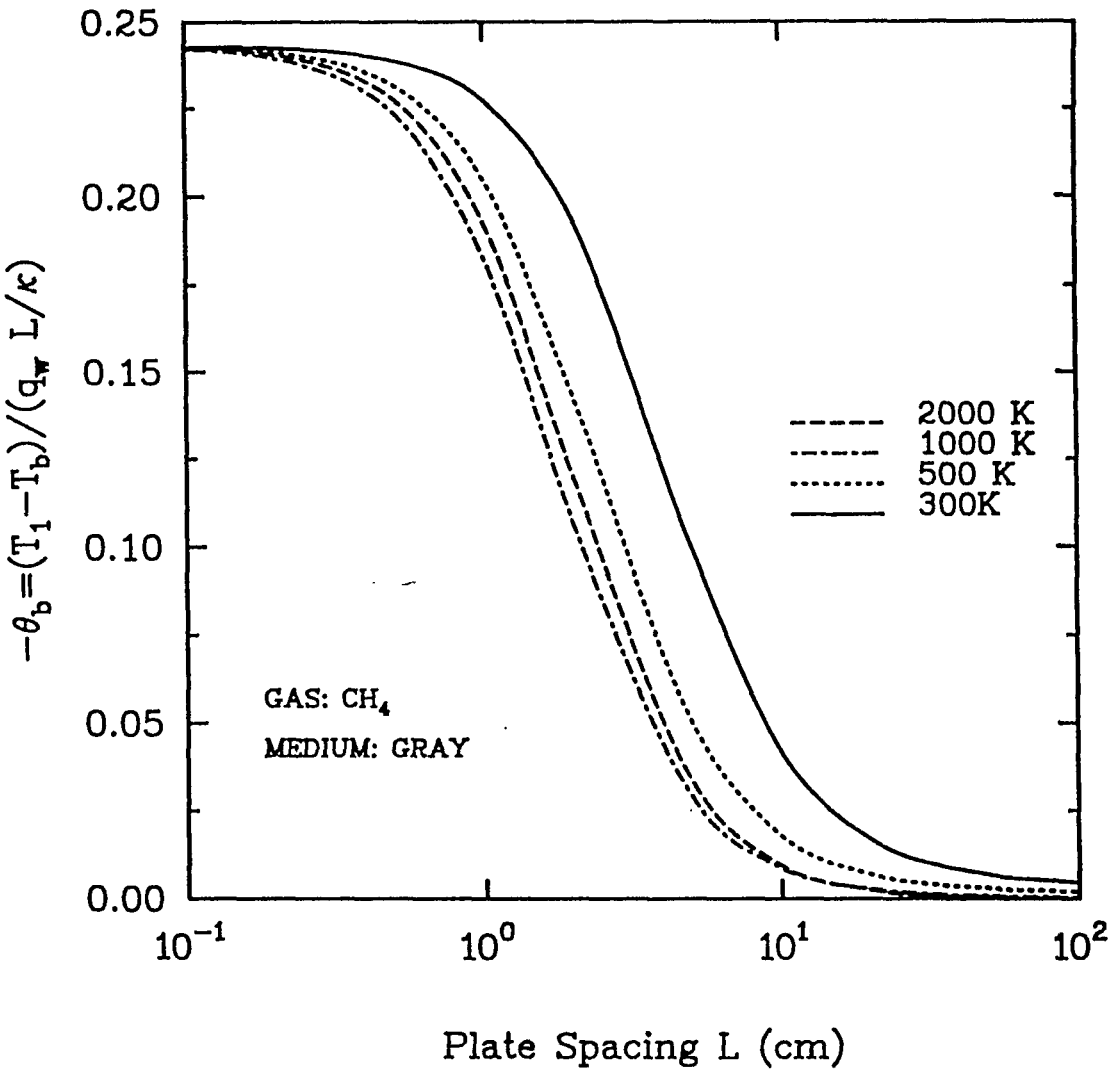

Fig. 6.7(a): LTE results for CH_4, P=1 atm, T_w=300–2000 K

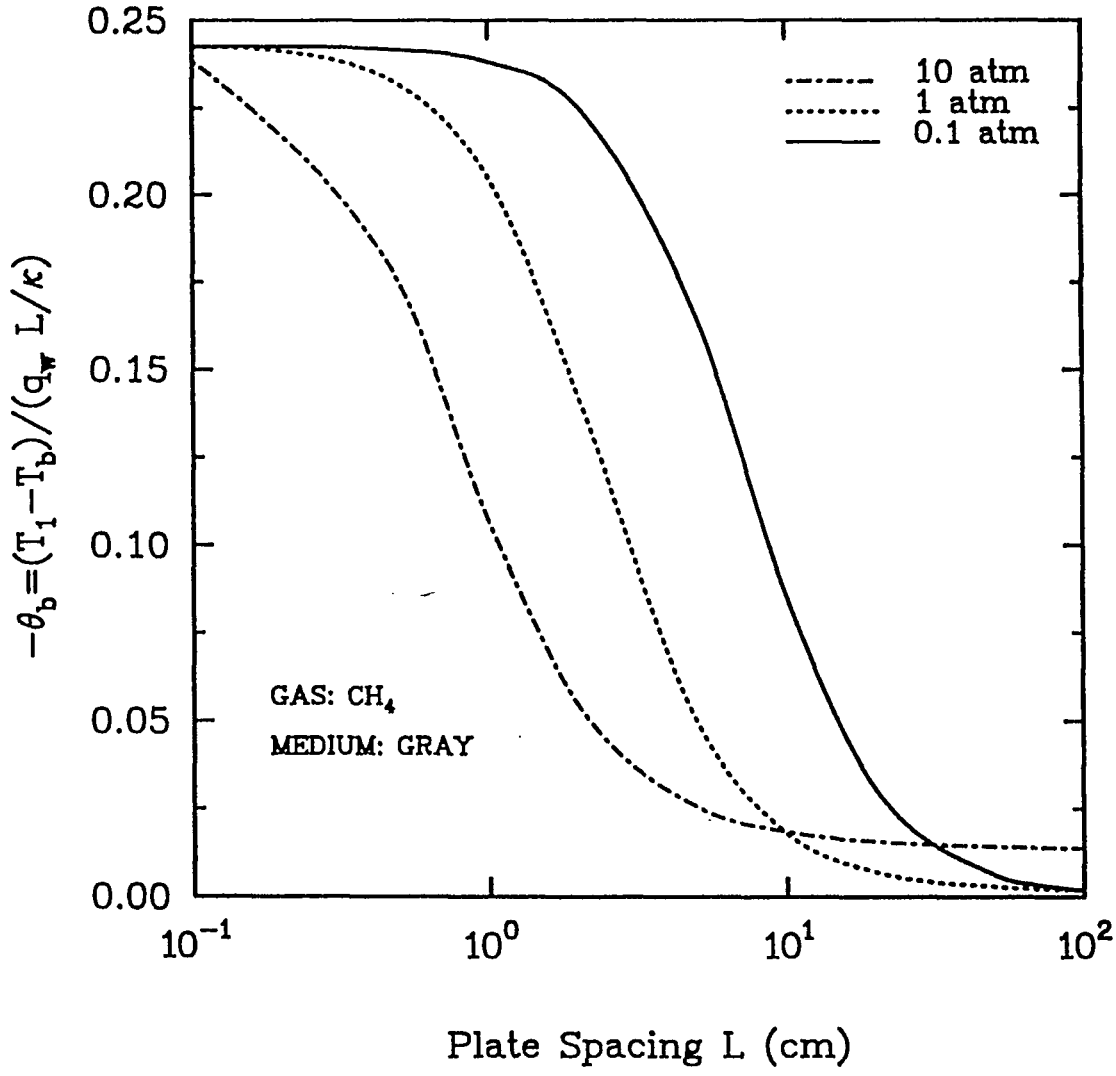

Fig. 6.7(b): LTE results for CH_4, T_w=500 K, P=0.1–10 atm

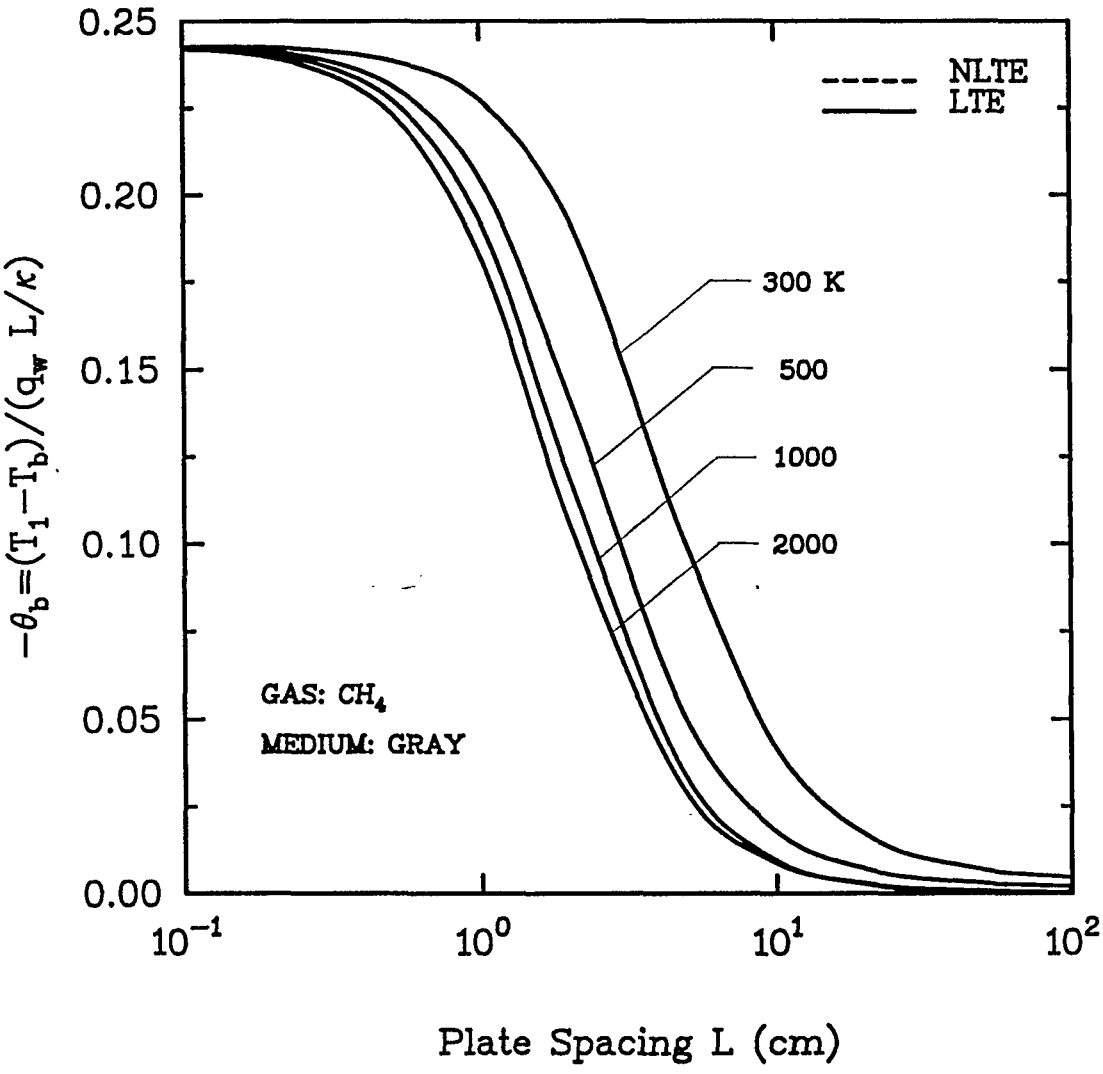

Fig. 6.7(c): LTE and NLTE results for CH_4, P=1 atm, T_w=300–2000 K

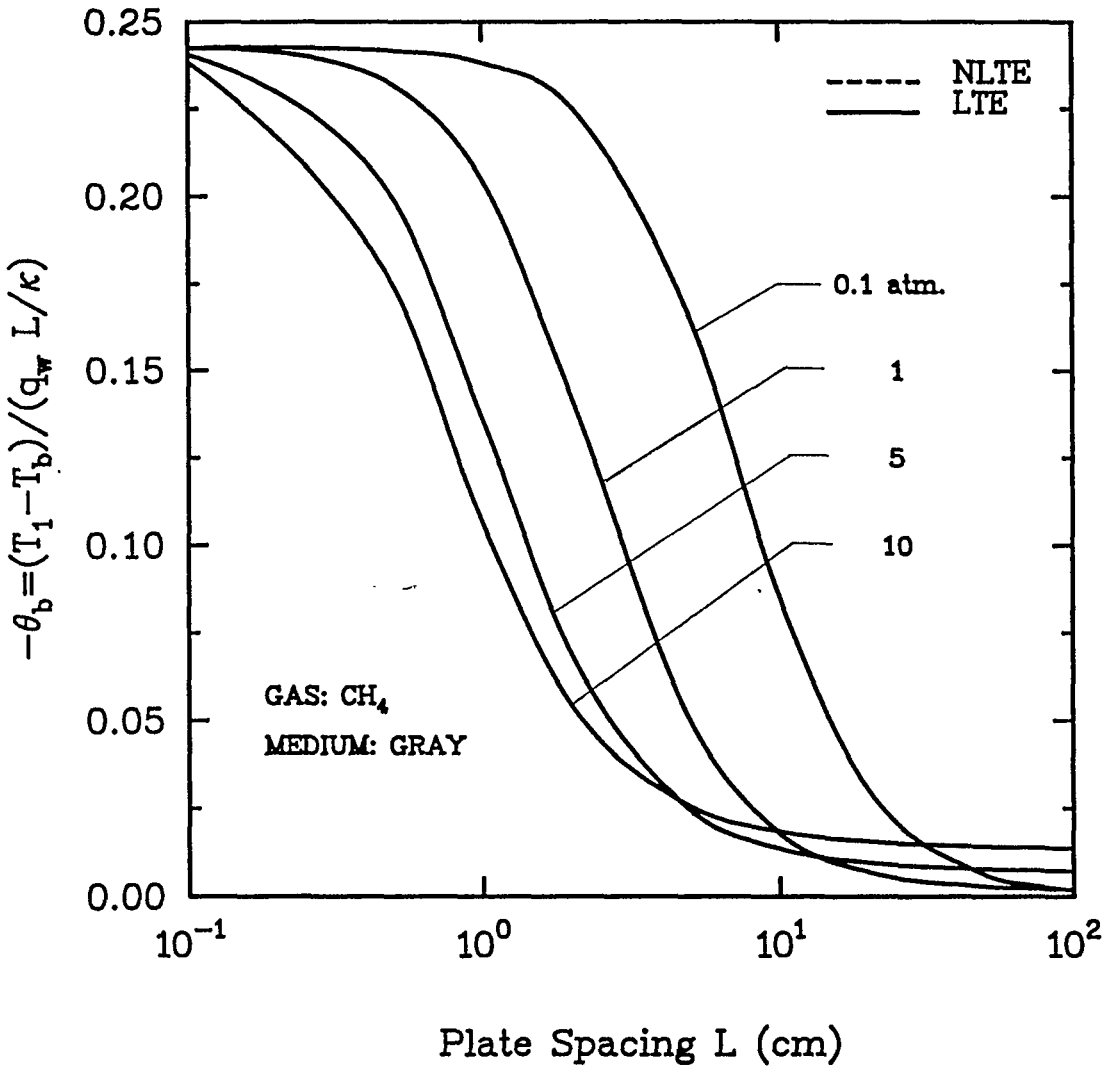

Fig. 6.7(d): LTE and NLTE results for CH_4, T_W=500 K, P=0.1–10 atm

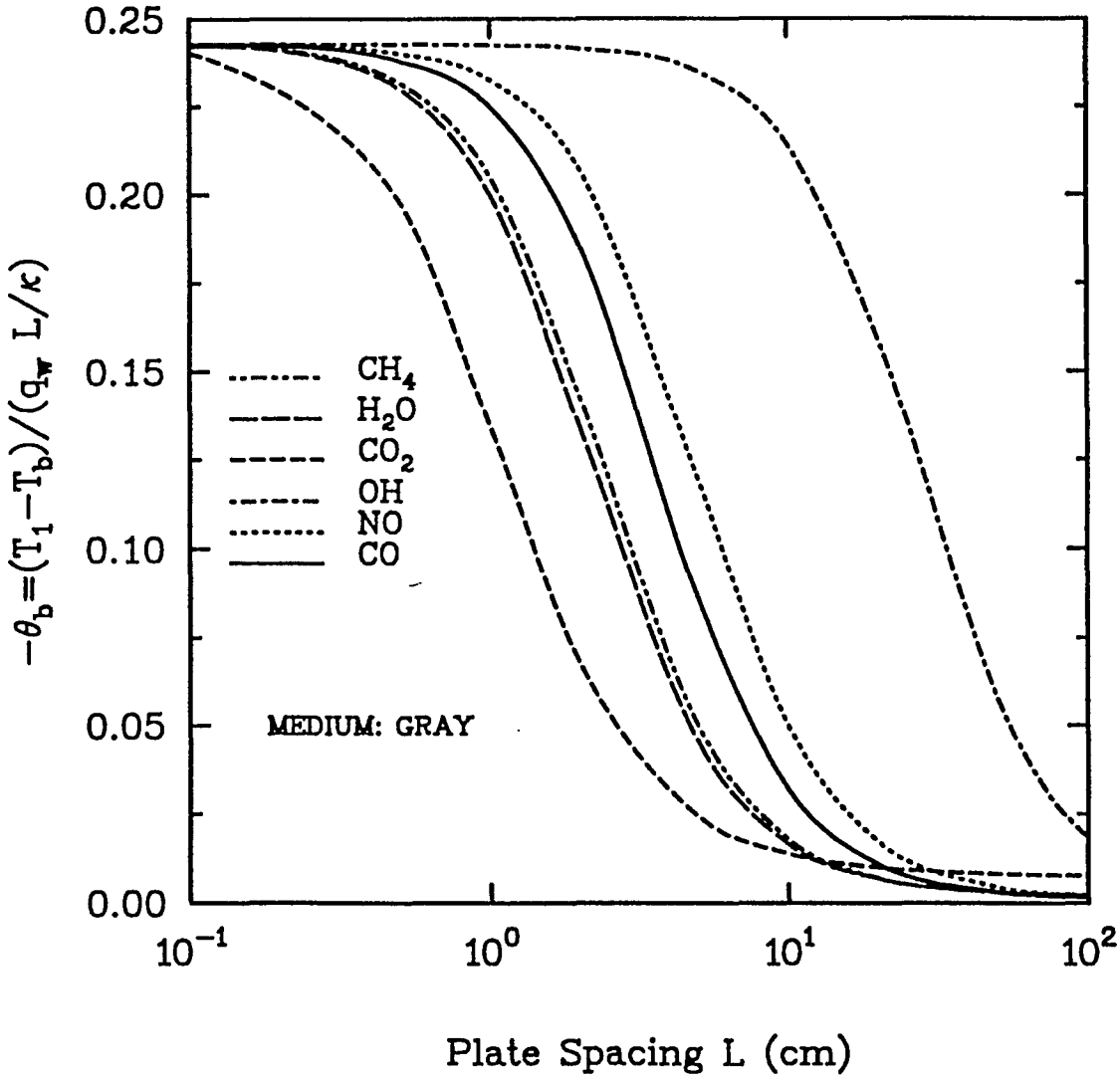

Fig. 6.8: Comparison of NLTE results for different Gases at 500 K and 1 Atm.

6.2 Nongray Results

In this section, nongray results are presented for different gases under LTE and NLTE conditions. The temperature and pressure ranges are same as for gray gas analyses. The plate spacing is kept between 0.01 to 100 centimeters. Figures 6.9 through 6.14 present results for CO,NO, OH, CO_2, H_2O, and CH_4, respectively.

Figure 6.9(a) presents LTE result for CO at temperatures ranging from 300 to 2000 K and for one atmospheric pressure. The results show that the bulk temperature decreases from lower to higher values of wall temperatures. In Fig. 6.9(b), temperature is kept fixed at 500 K and results are compared at 0.1, 1, 5, and 10 atm. It is seen that the bulk temperature decreases with increasing pressure. One interesting observation is that the variation is seen only at higher plate spacings. At lower plate spacings, the results are almost identical for any temperatures and pressures. This is due to optically thin radiative interaction in this region. Figure 6.9(c) is a comparison of LTE and NLTE results at one atmospheric pressure and temperatures in the range of 300 to 2000 K. The study reveals that LTE and NLTE results differ only at lower temperatures. Results presented in Fig. 6.9(d) demonstrate that NLTE effects are important only at low pressures.

Results for NO are presented in Fig. 6.10. Figures 6.10(a) and 6.10(b) are comparison of LTE results at different pressures and temperatures. The trend of the results are similar to that observed for CO. Figures 6.10(c) and 6.10(d) show LTE and NLTE comparisons at different pressures and temperatures. The results follow the same pattern as for CO. Figures 6.11 illustrate results for OH. A study of Fig. 6.11(a) shows that OH has very little radiative

interaction at a temperature of 300 K and one atmospheric pressure. However, it shows some effect at higher temperatures and pressures (Figs. 6.11(a) and 6.11(b)). In Figs. 6.11(c) and 6.11(d), LTE and NLTE results are compared. It is seen that there is no difference between LTE and NLTE results at any temperature and pressure. This implies that NLTE does not have significant effect on OH at any temperature and pressure. However, it does have some effect at low temperatures and pressures (Figs. 6.11(c) and 6.11(d)).

Figures 6.12 present results for CO_2. Figures 6.12(a) and 6.12(b) present LTE results at different temperatures and pressures, respectively. It is seen that bulk temperature decreases with increasing pressure and temperature. Figures 6.12(c) and 6.12(d) are comparison of LTE and NLTE results at different temperatures and pressures, respectively. There appears to be no difference between LTE and NLTE results at these conditions. Figure 6.12(d) suggests that there is little difference between LTE and NLTE results at 0.1 atm. and 500 K. Figures 6.13(a) and 6.13(b) are comparison of LTE results for H_2O at different pressures and temperatures. The trend is almost similar to that observed for CO_2. Figures 6.13(c) and 6.13(d) are comparisons of LTE and NLTE results. There is no difference between LTE and NLTE results except at low temperatures and pressures. The difference is quite significant at 0.1 atm. and 500 K. The difference in this case is more than that observed for CO_2. Figures 6.14(a) and 6.14(b) present LTE results for CH_4 at various temperatures and pressures, respectively. Again, the bulk temperature is seen to decrease with increasing temperature. Figures 6.14(c) and 6.14(d) are comparison of LTE and NLTE results for CH_4 at various temperatures and pressures, respectively. The results do not show any difference between LTE and NLTE at any temperature and pressure conditions. Thus, NLTE consideration is not important for CH_4. Figure 6.15 is a comparison of NLTE results for all the gases under consideration at 500 K and one atmospheric pressure. The results show that the gases in the descending order of bulk temperature are OH, CO, NO, CO_2, CH_4, and H_2O. This implies that among

the gases H_2O is highest radiating gas whereas OH is the least radiating gas.

By studying the results under nongray assumption, it becomes obvious that bulk temperature usually decreases with an increases in temperature and pressure. This implies that the radiating capacity of the gases increases with an increase in temperature and pressure. Second important observation is that polyatomic gases do not contribute significantly in NLTE process. However, OH being a diatomic radical, shows least variation from LTE conditions among the diatomic gases under consideration. Further, CH_4 shows absolutely no effect of NLTE at any temperature and pressure; whereas NLTE results for other polyatomic gases show little variation from LTE results at moderate pressures and temperatures.

6.3 Comparative Results for Gray and Nongray Analyses

In this section, gray and nongray results are compared at different temperatures and pressures. Figures 6.16 through 6.21 present these comparative results

Figure 6.16(a) presents gray and nongray NLTE results for CO at temperatures ranging from 300 to 2000 K and one atmospheric pressure. The results show that there is significant difference between gray and nongray results at lower temperatures. At higher temperatures, the difference is relatively lower. However, the rate of decrease of the difference between gray and nongray results is less as temperature is increased. Thus, even at 2000 K, significant difference between gray and nongray results is observed. Figure 6.16(b) is a comparison of gray and nongray results at 500 K and 0.1, 1, and 10 atm. The variation between gray and nongray results is quite significant and it increases with increasing pressure.

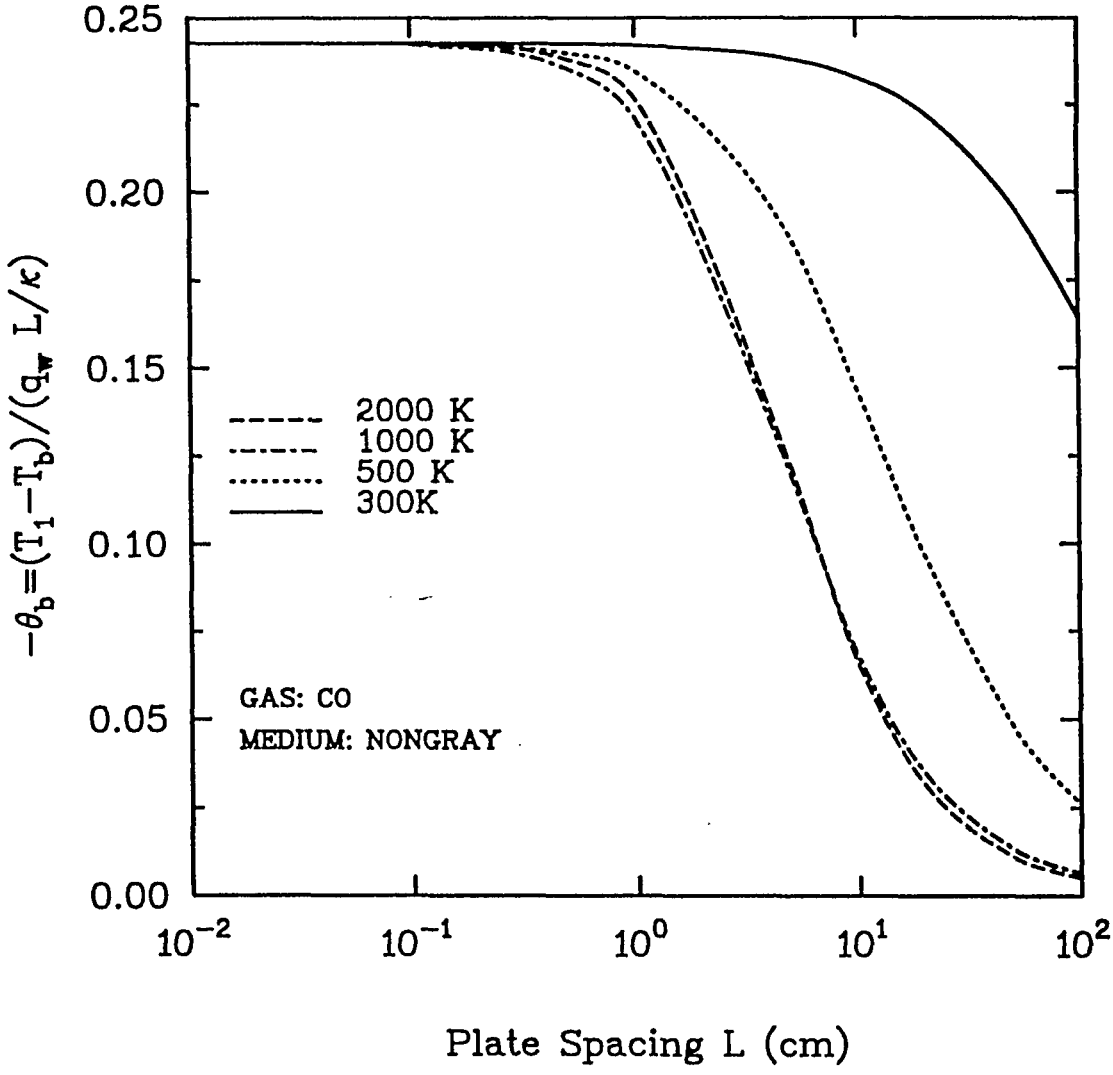

Fig. 6.9(a): LTE results for CO, P=1 atm, T_w=300–2000 K

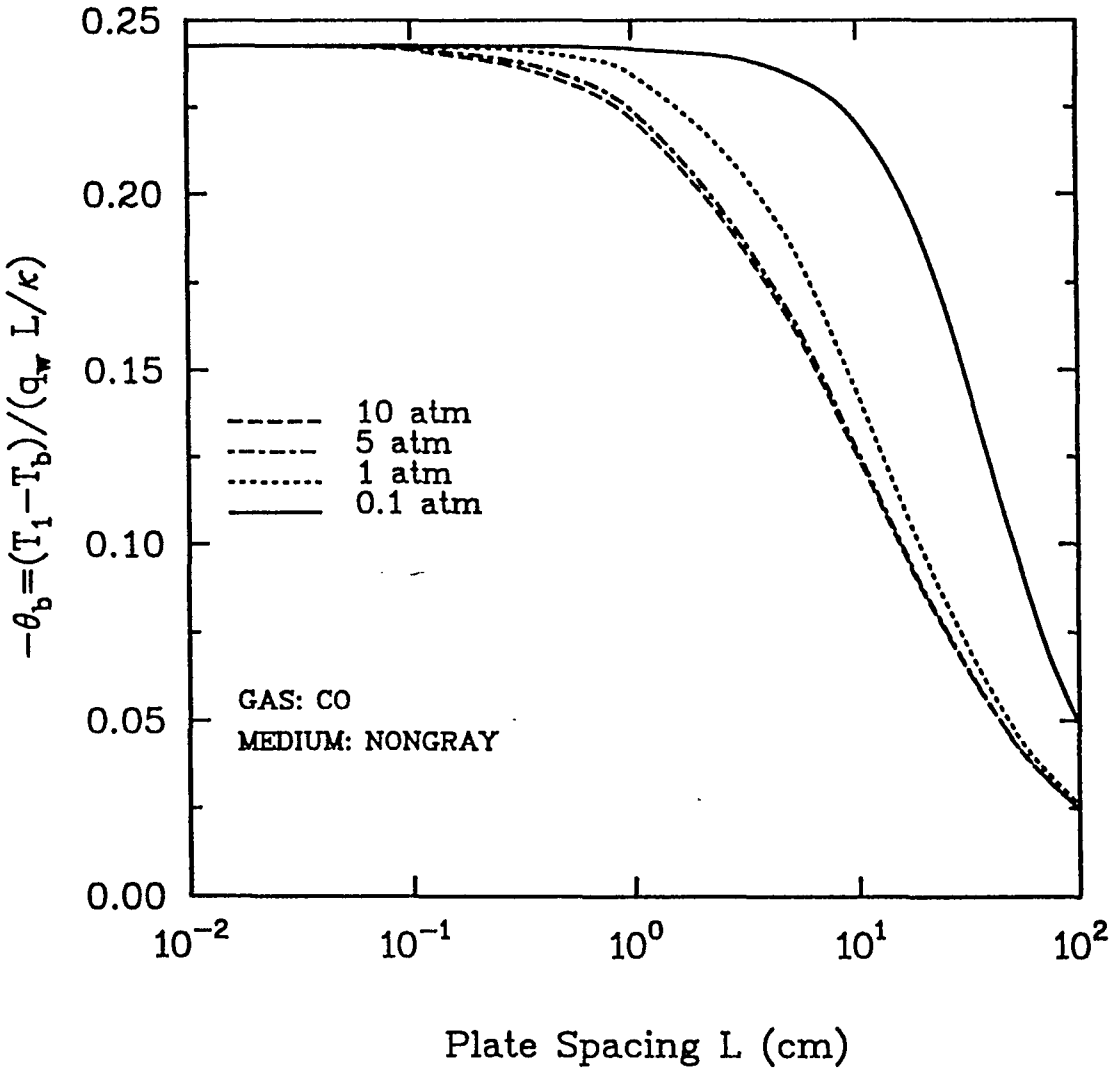

Fig. 6.9(b): LTE results for CO, T_w=500 K, P=0.1–10 atm

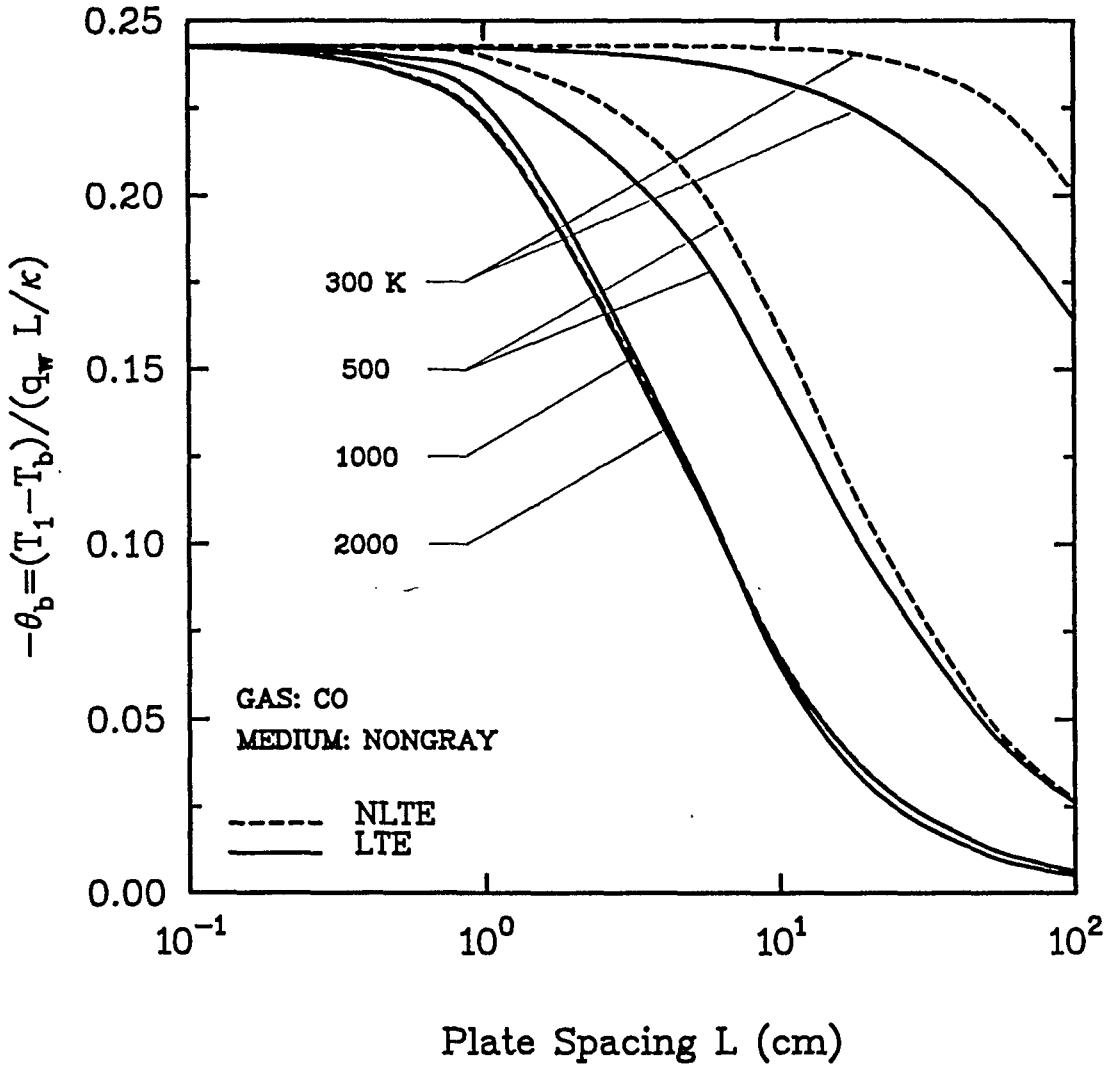

Fig. 6.9(c): LTE and NLTE results for CO, P=1 atm, T_w=300–2000 K

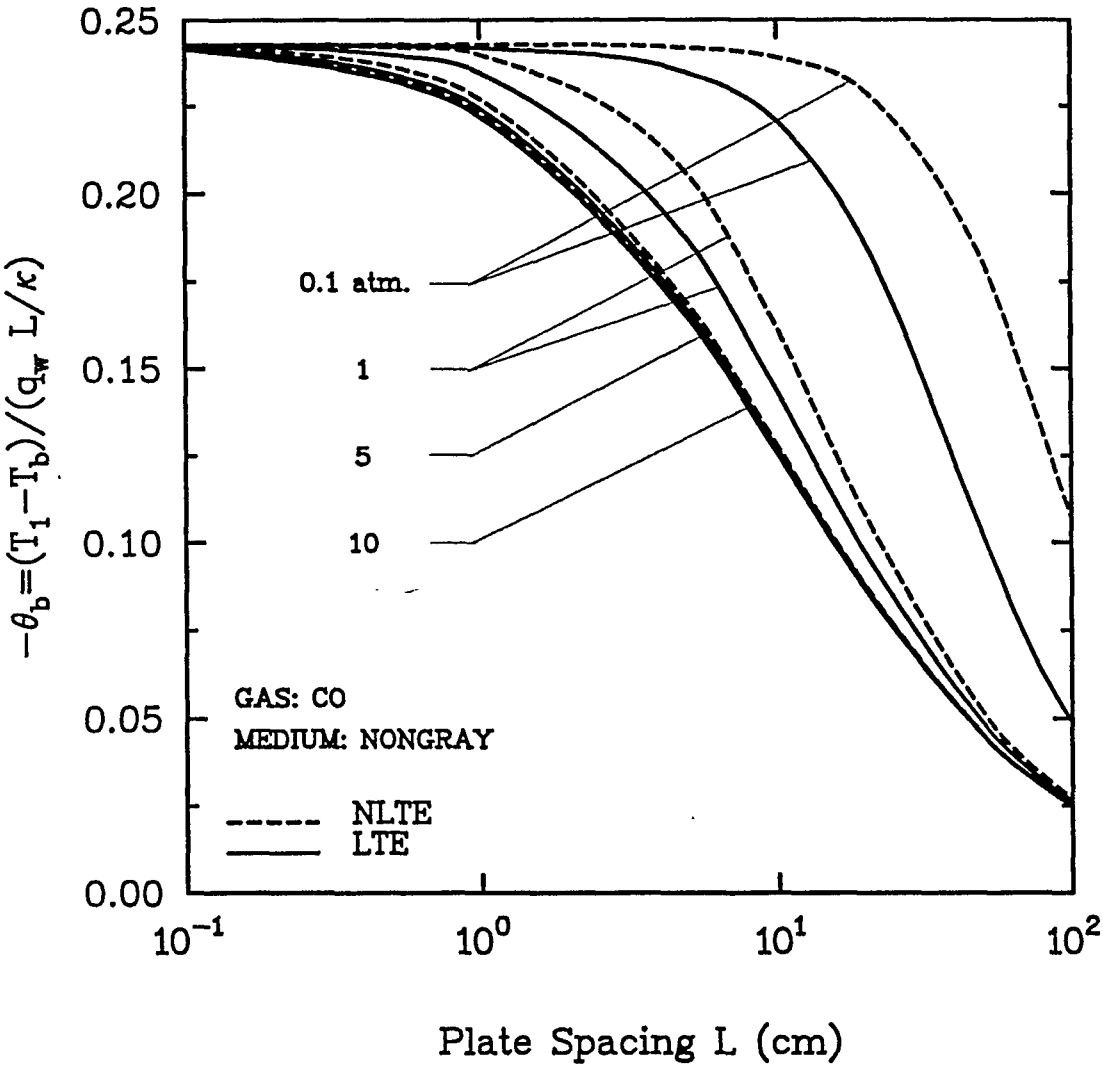

Fig. 6.9(d): LTE and NLTE results for CO, T_w=500 K, P=0.1–10 atm

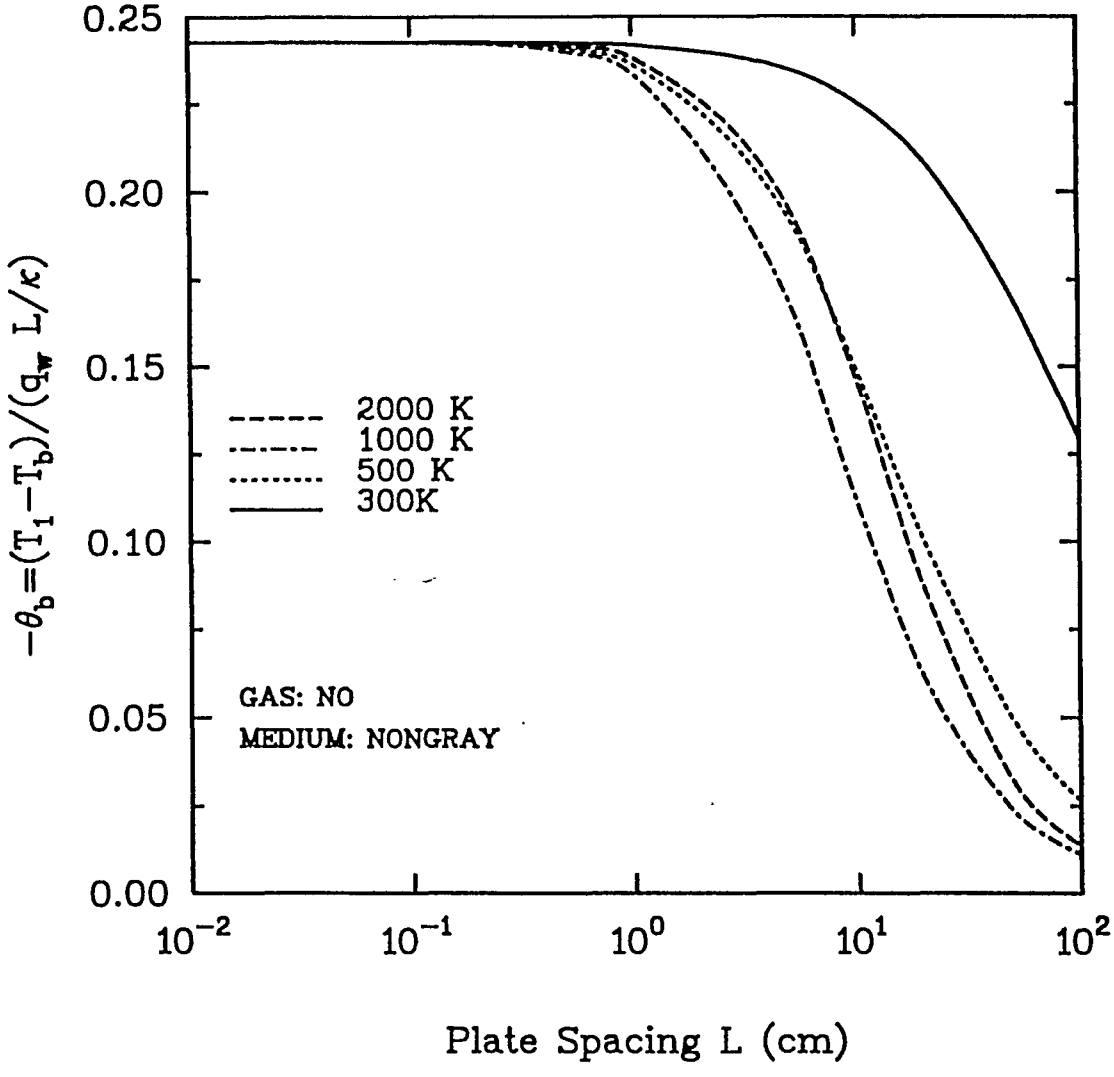

Fig. 6.10(a): LTE results for NO, P=1 atm, T_w=300–2000 K

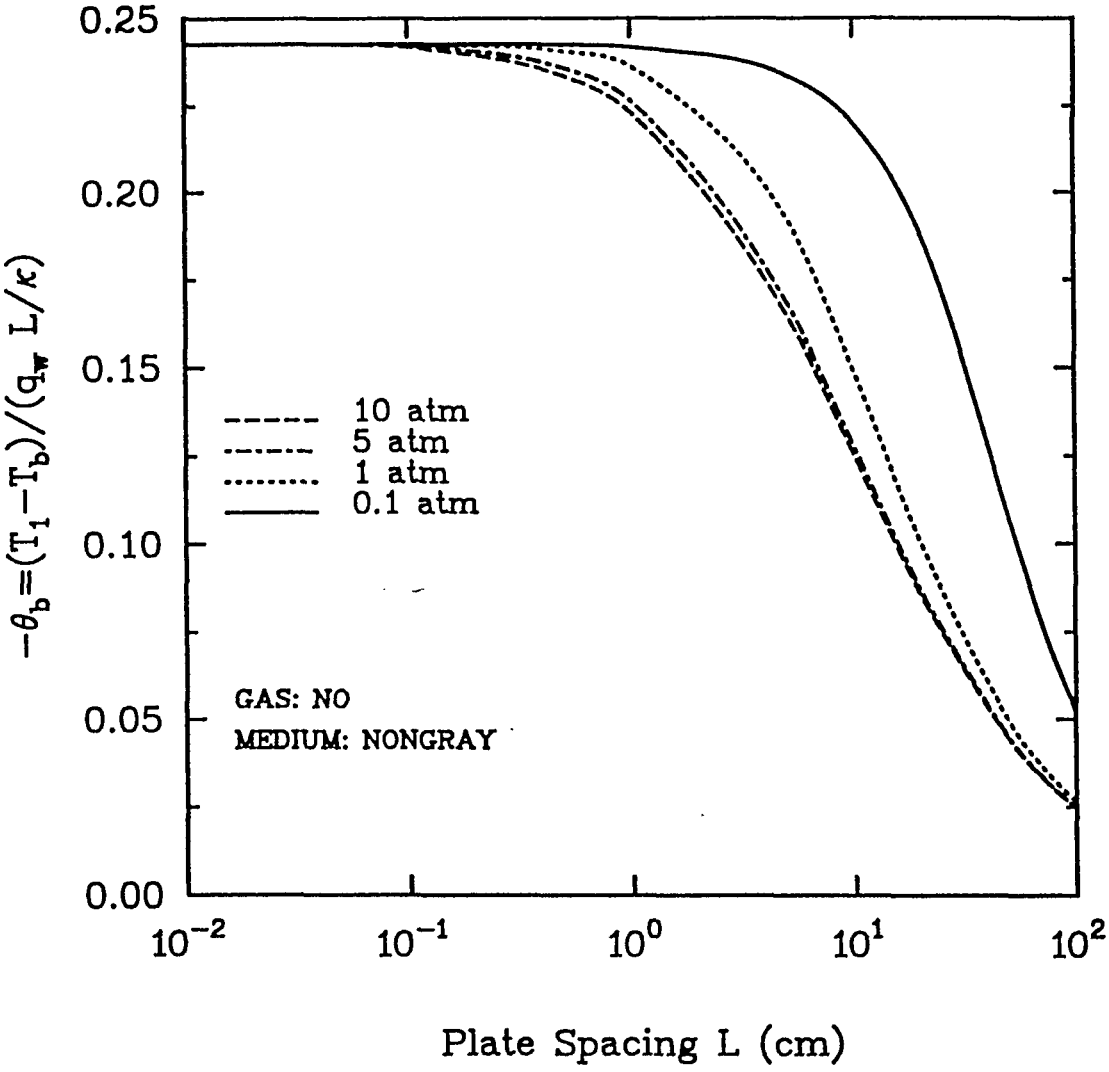

Fig. 6.10(b): LTE results for NO, T_w=500 K, P=0.1–10 atm

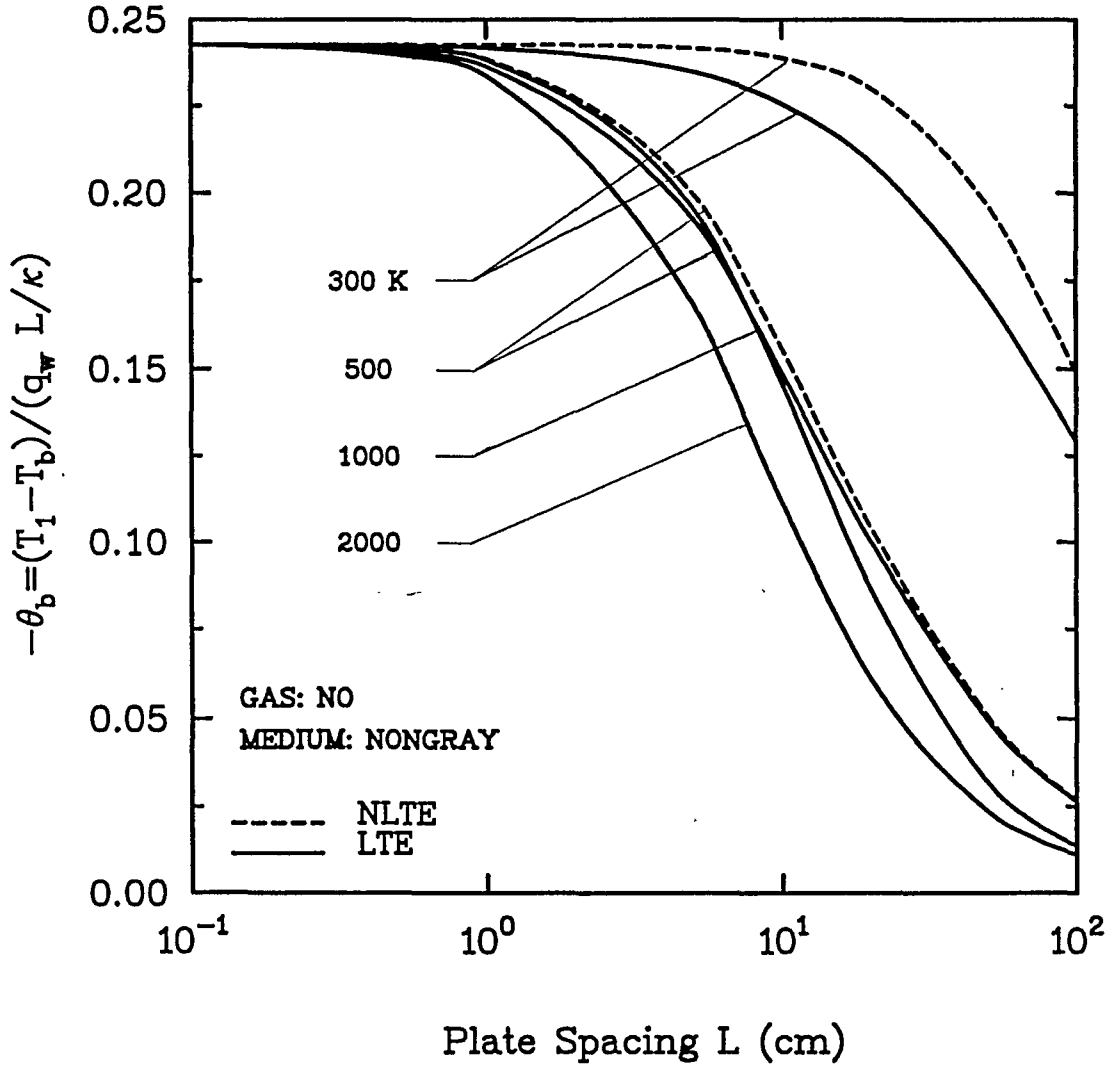

Fig. 6.10(c): LTE and NLTE results for NO, P=1 atm, T_w=300–2000 K

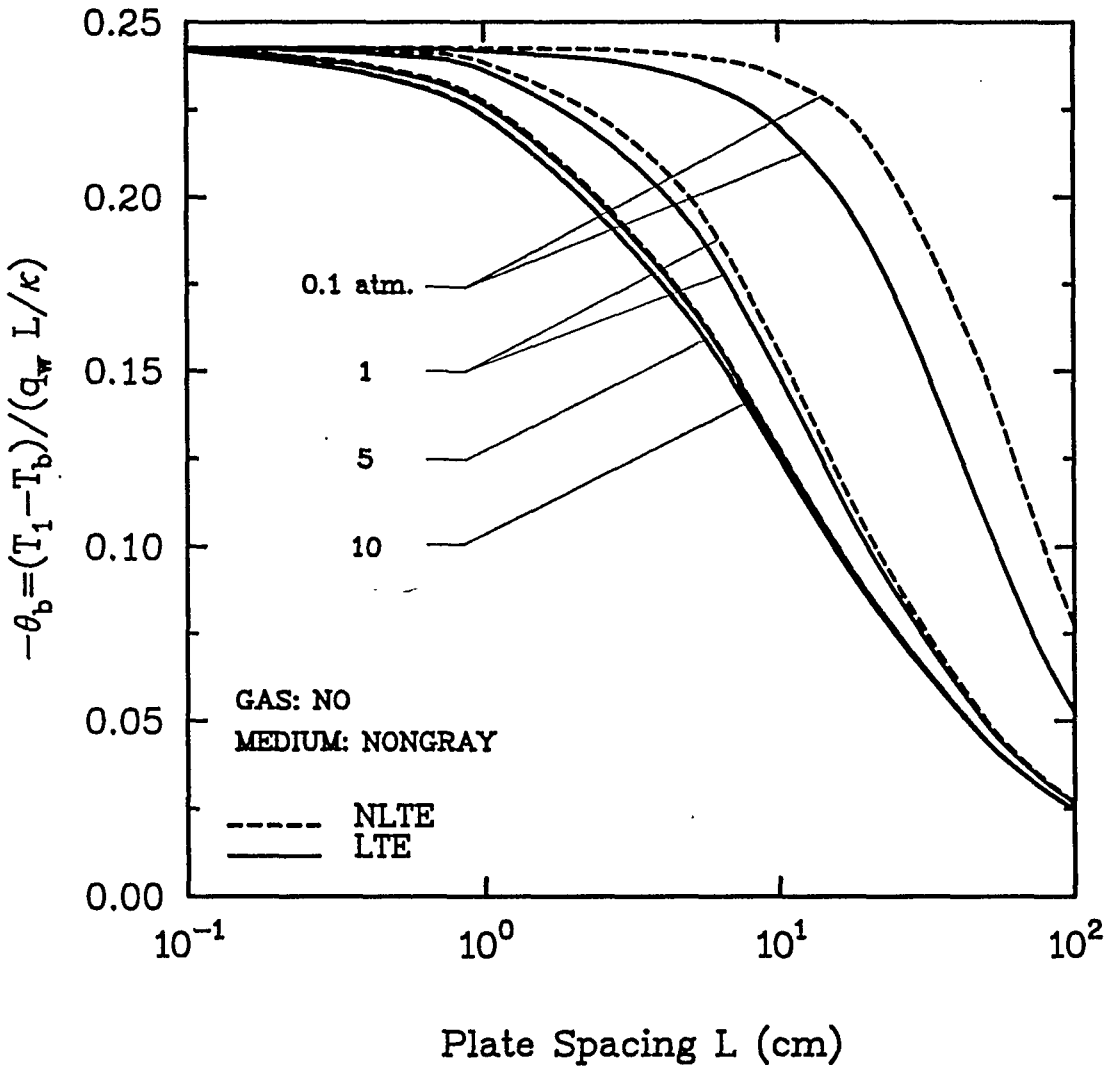

Fig. 6.10(d): LTE and NLTE results for NO, T_w=500 K, P=0.1–10 atm

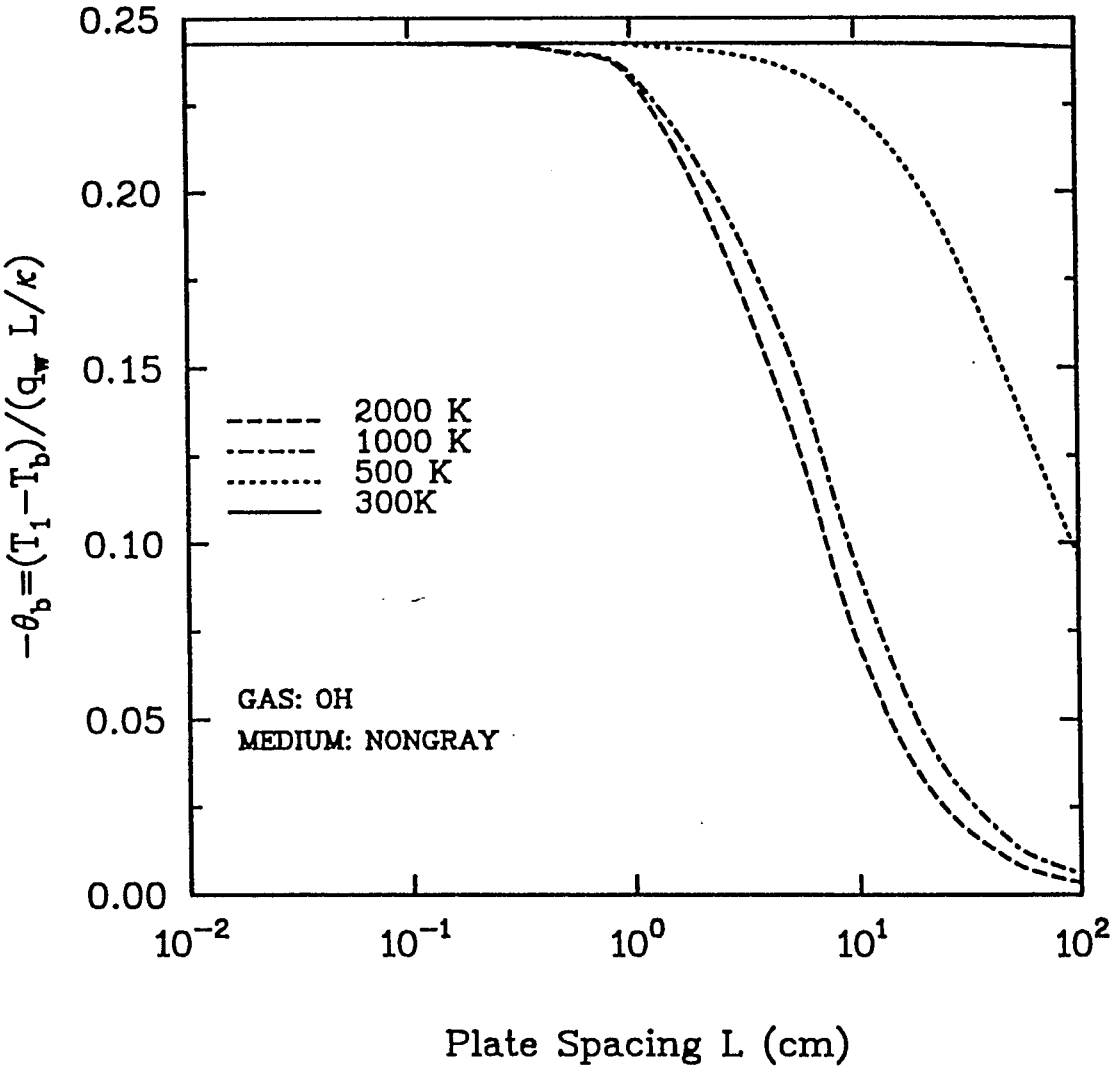

Fig. 6.11(a): LTE results for OH, P=1 atm, T_w=300–2000 K

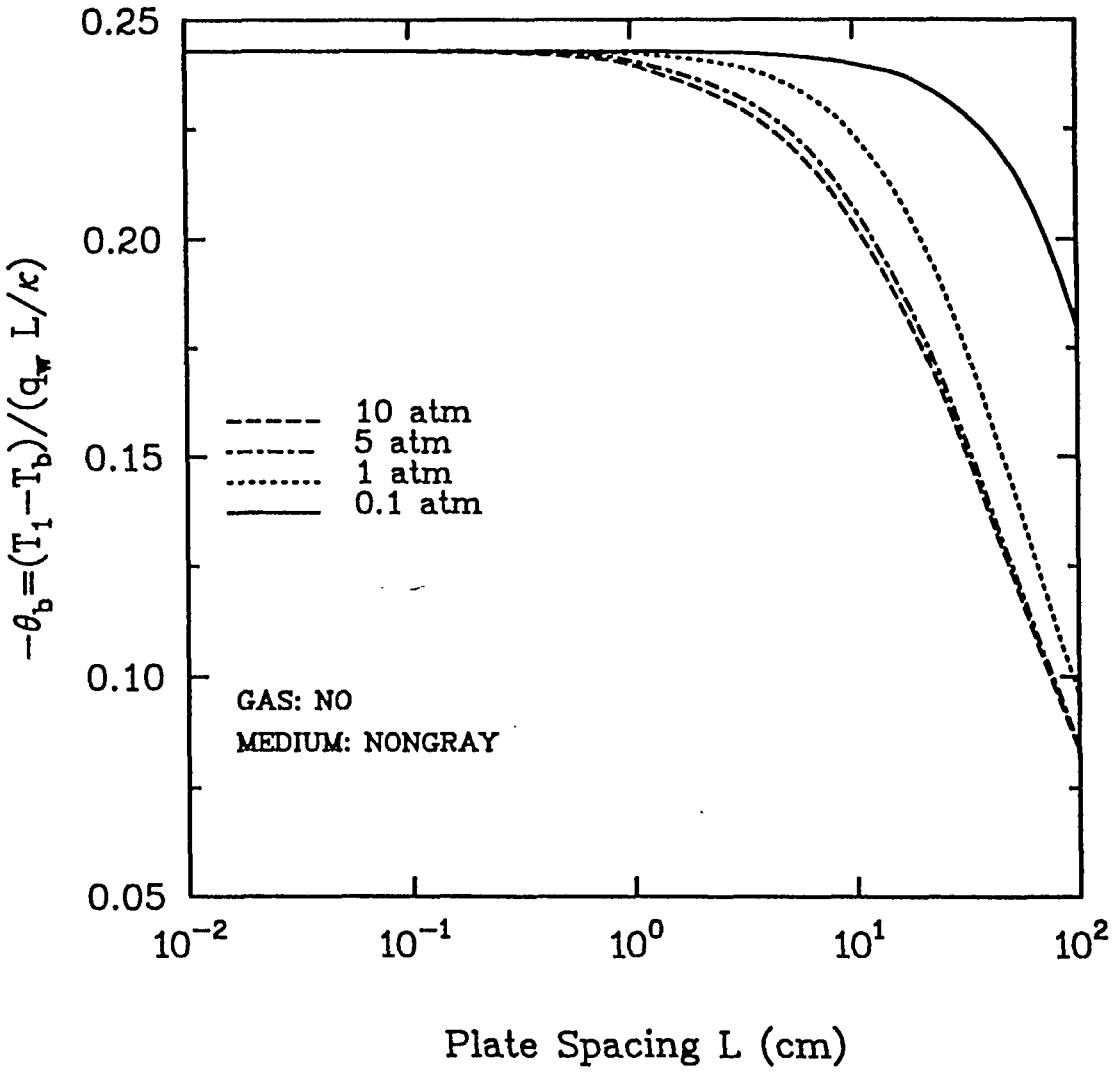

Fig. 6.11(b): LTE results for OH, T_w=500 K, P=0.1–10 atm

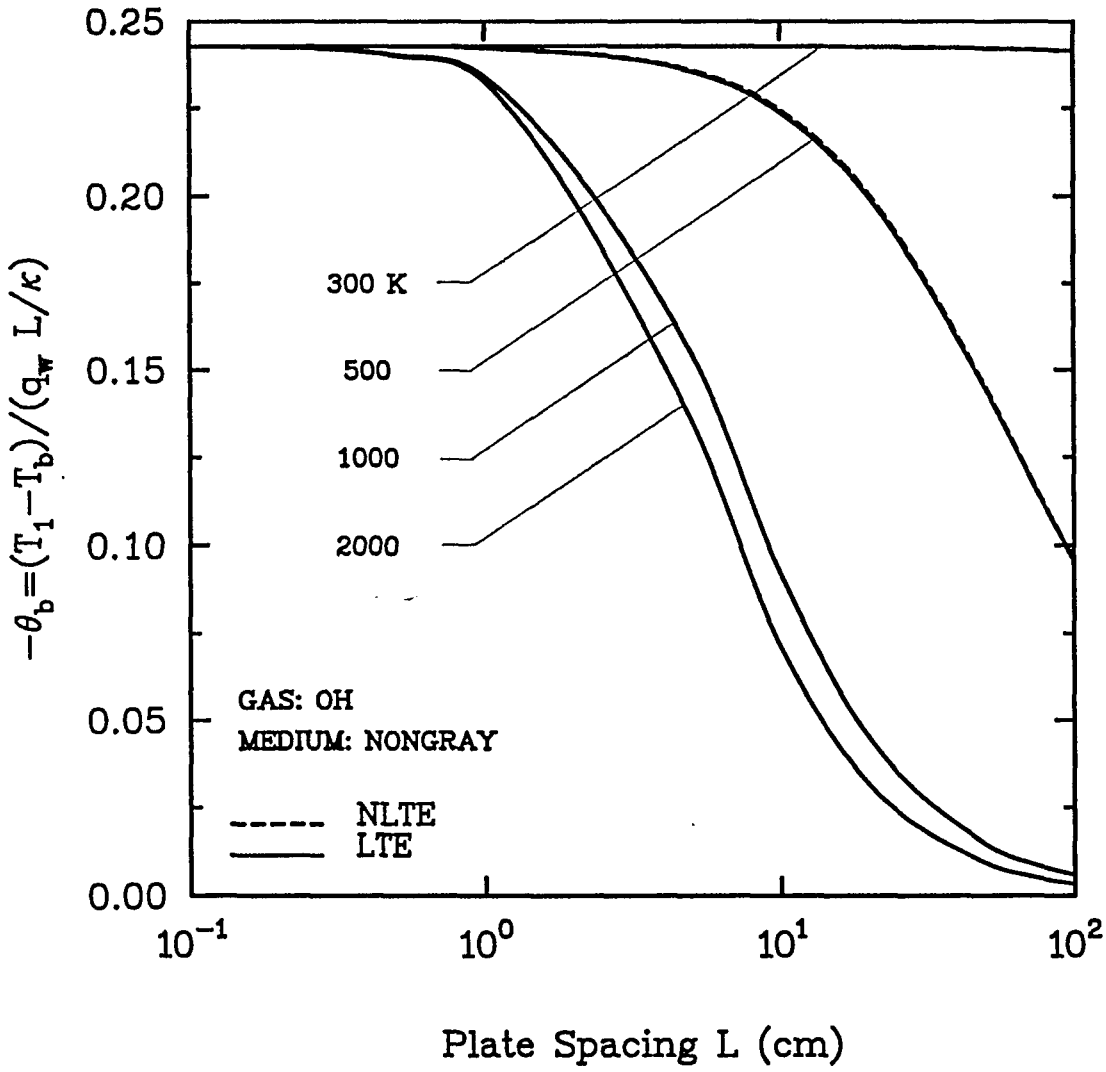

Fig. 6.11(c): LTE and NLTE results for OH, P=1 atm, T_w=300–2000 K

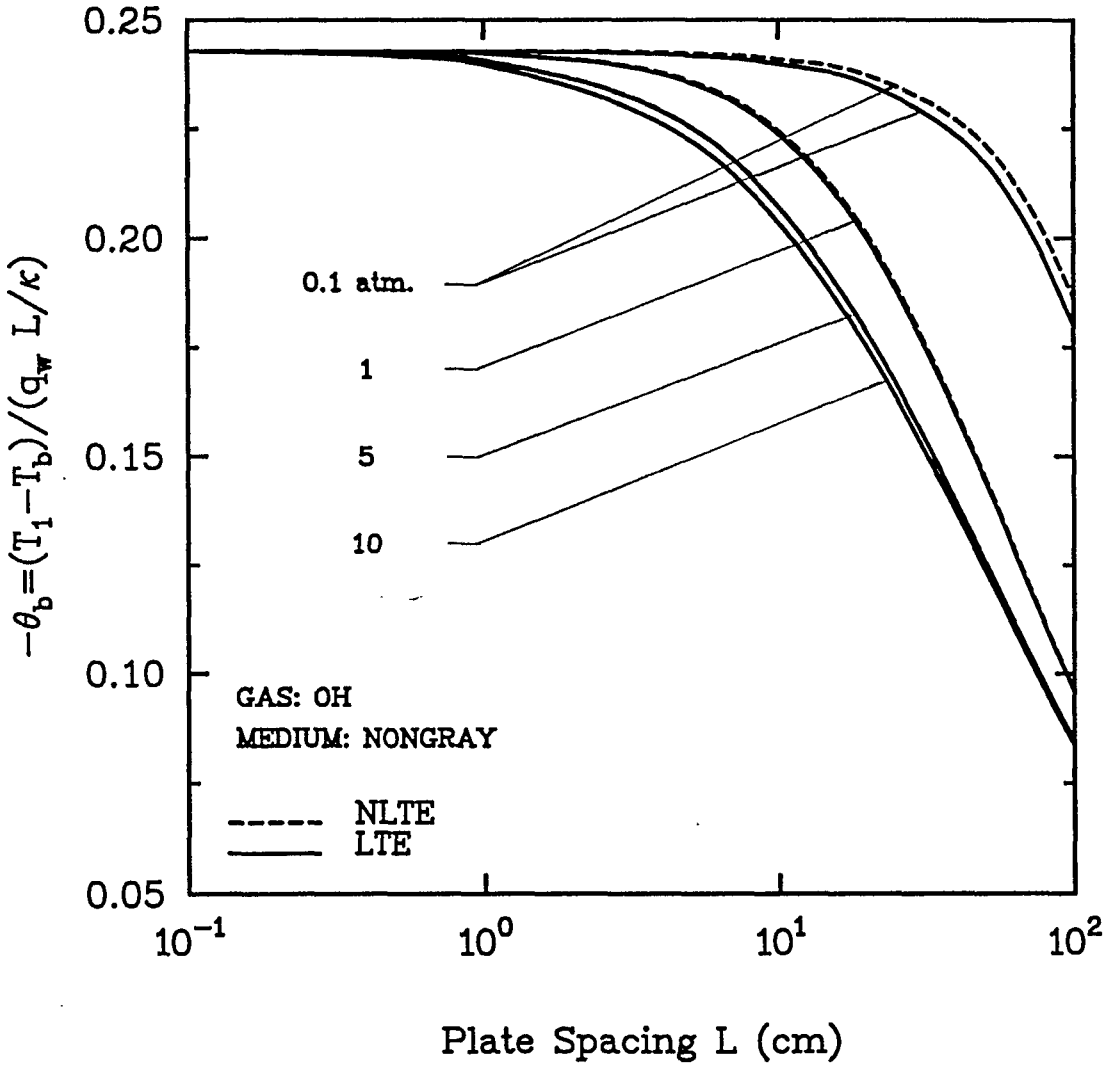

Fig. 6.11(d): LTE and NLTE results for OH, T_w=500 K, P=0.1–10 atm

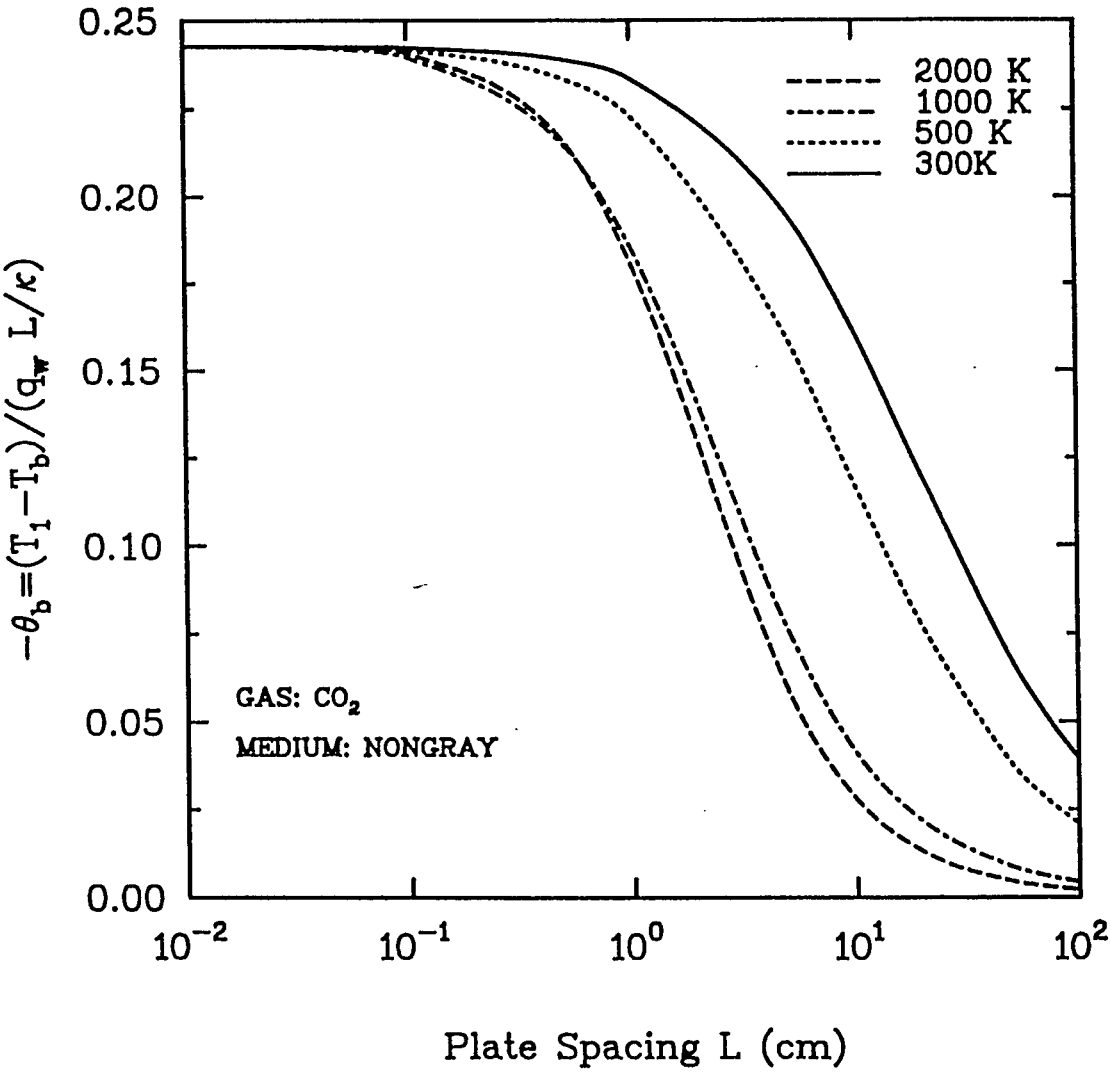

Fig. 6.12(a): LTE results for CO_2, P=1 atm, T_w=300–2000 K

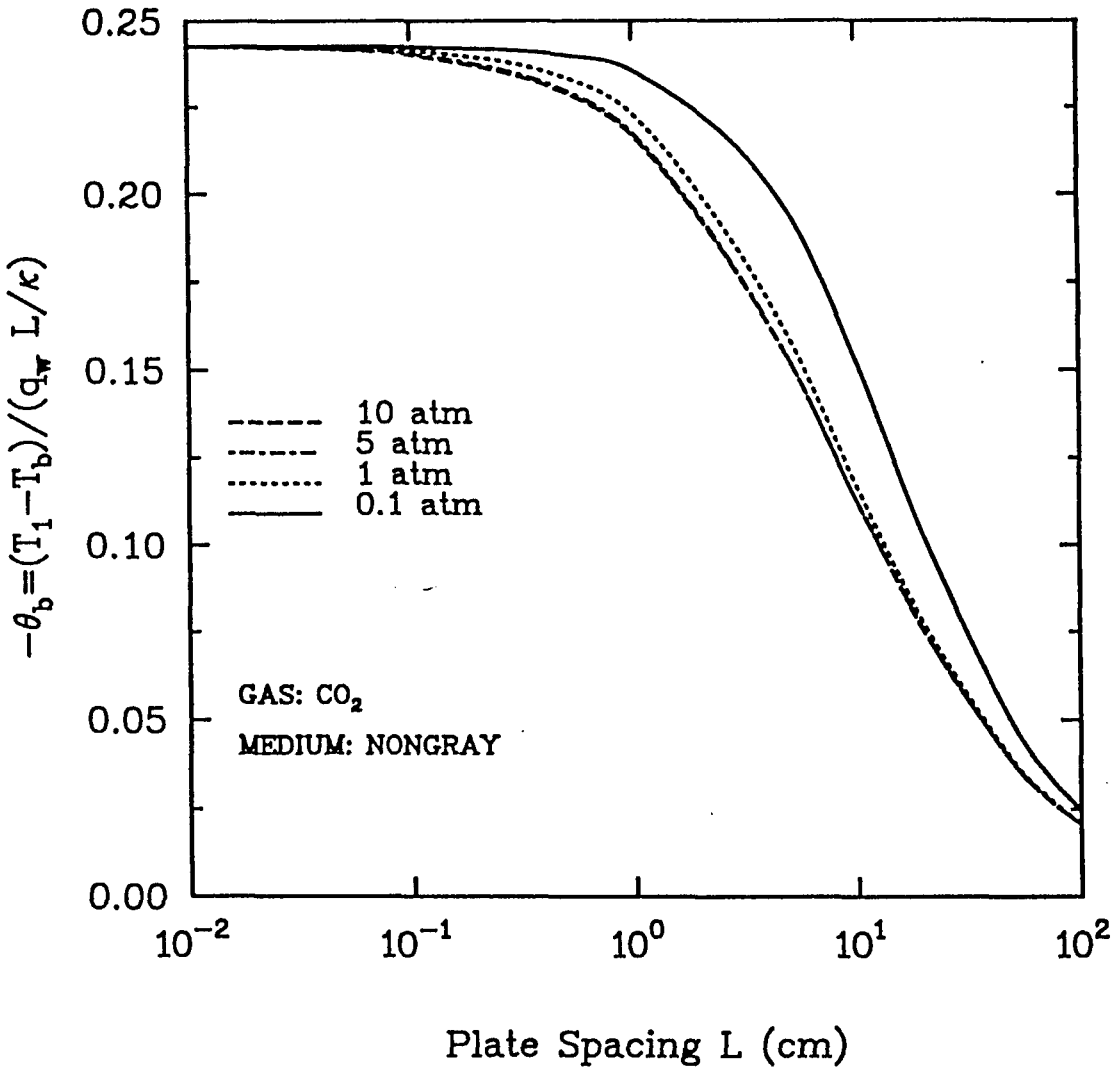

Fig. 6.12(b): LTE results for CO_2, T_w=500 K, P=0.1–10 atm

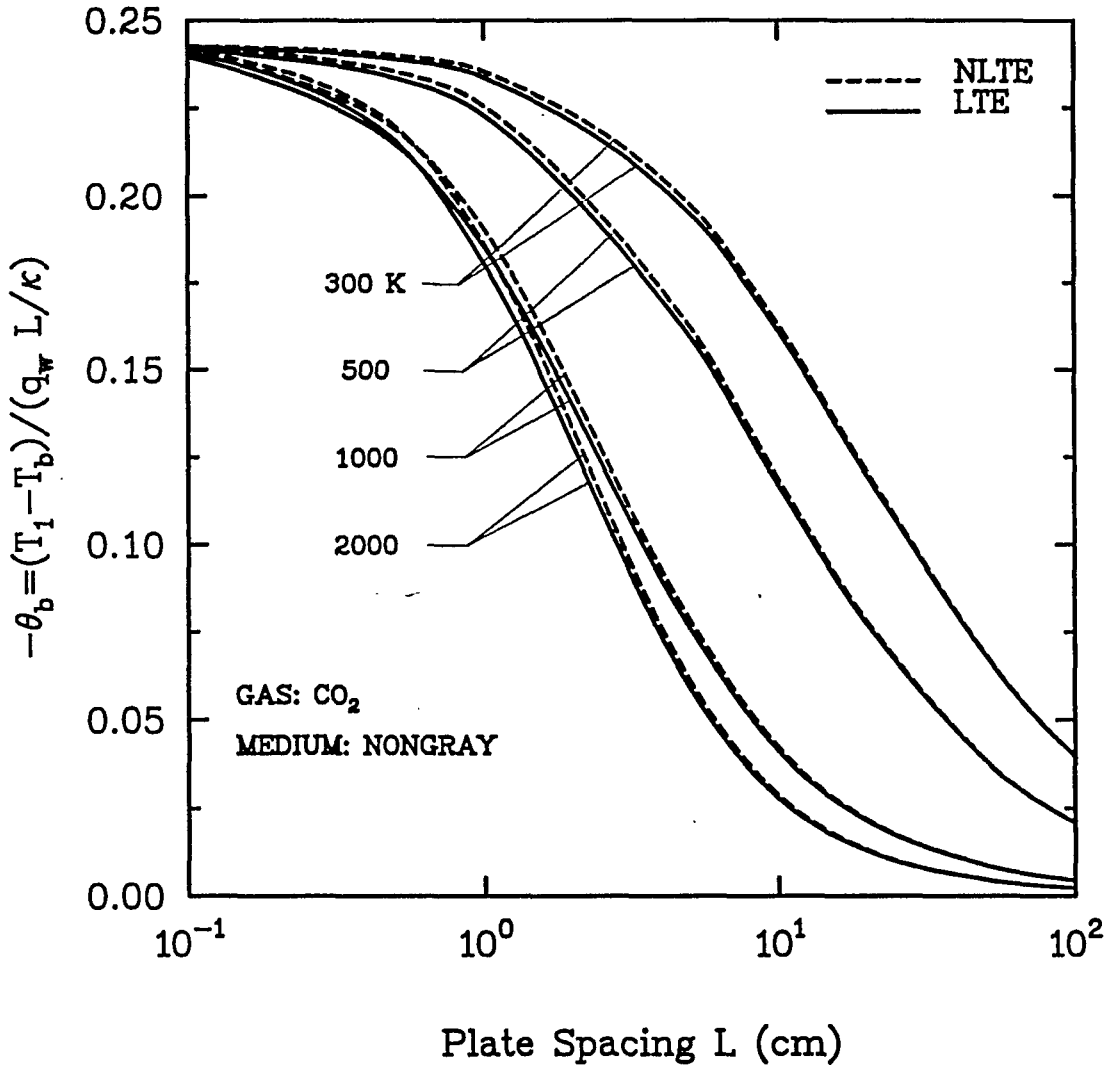

Fig. 6.12(c): LTE and NLTE results for CO_2, P=1 atm, T_w=300–2000 K

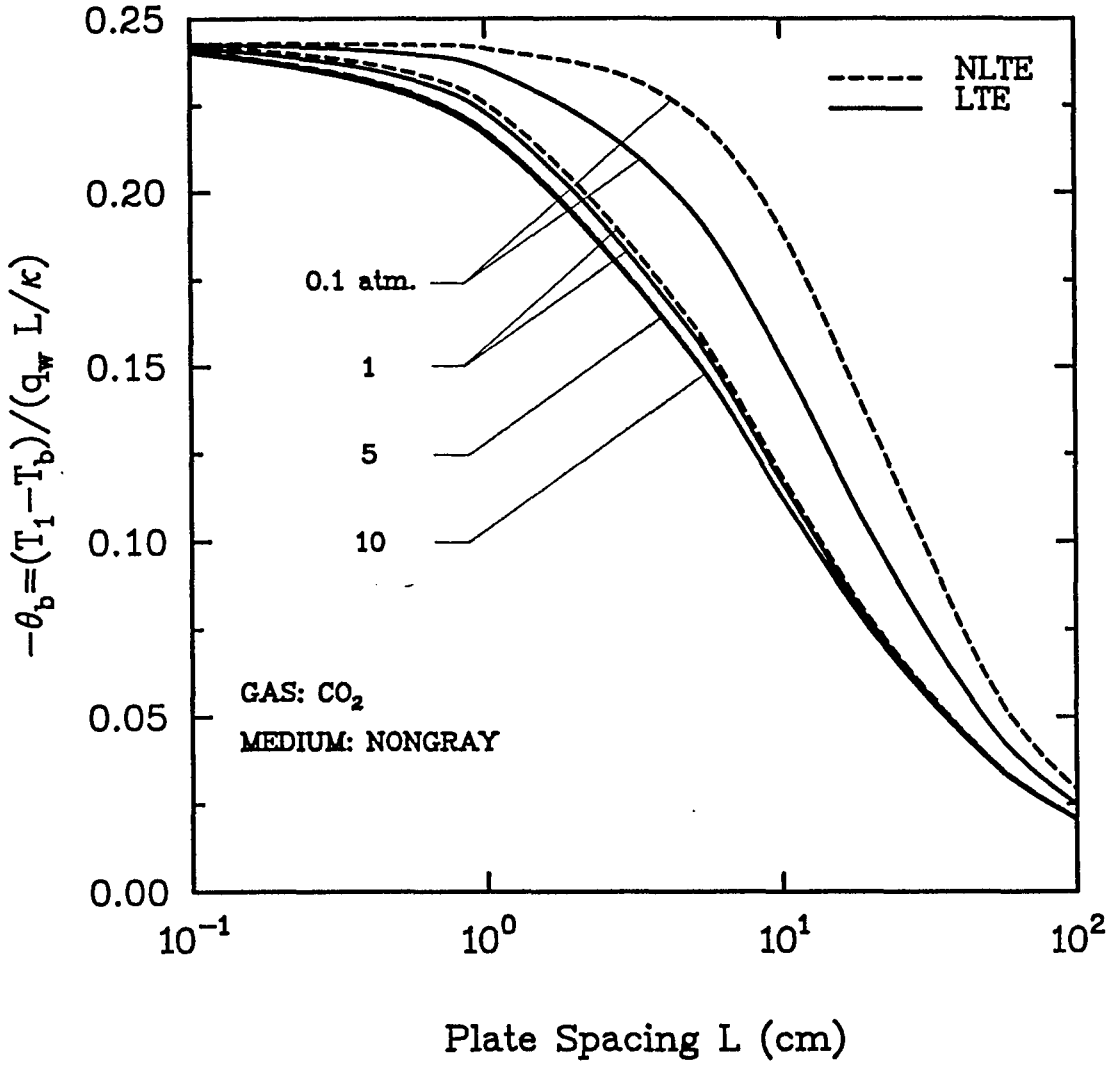

Fig. 6.12(d): LTE and NLTE results for CO_2, T_w=500 K, P=0.1–10 atm

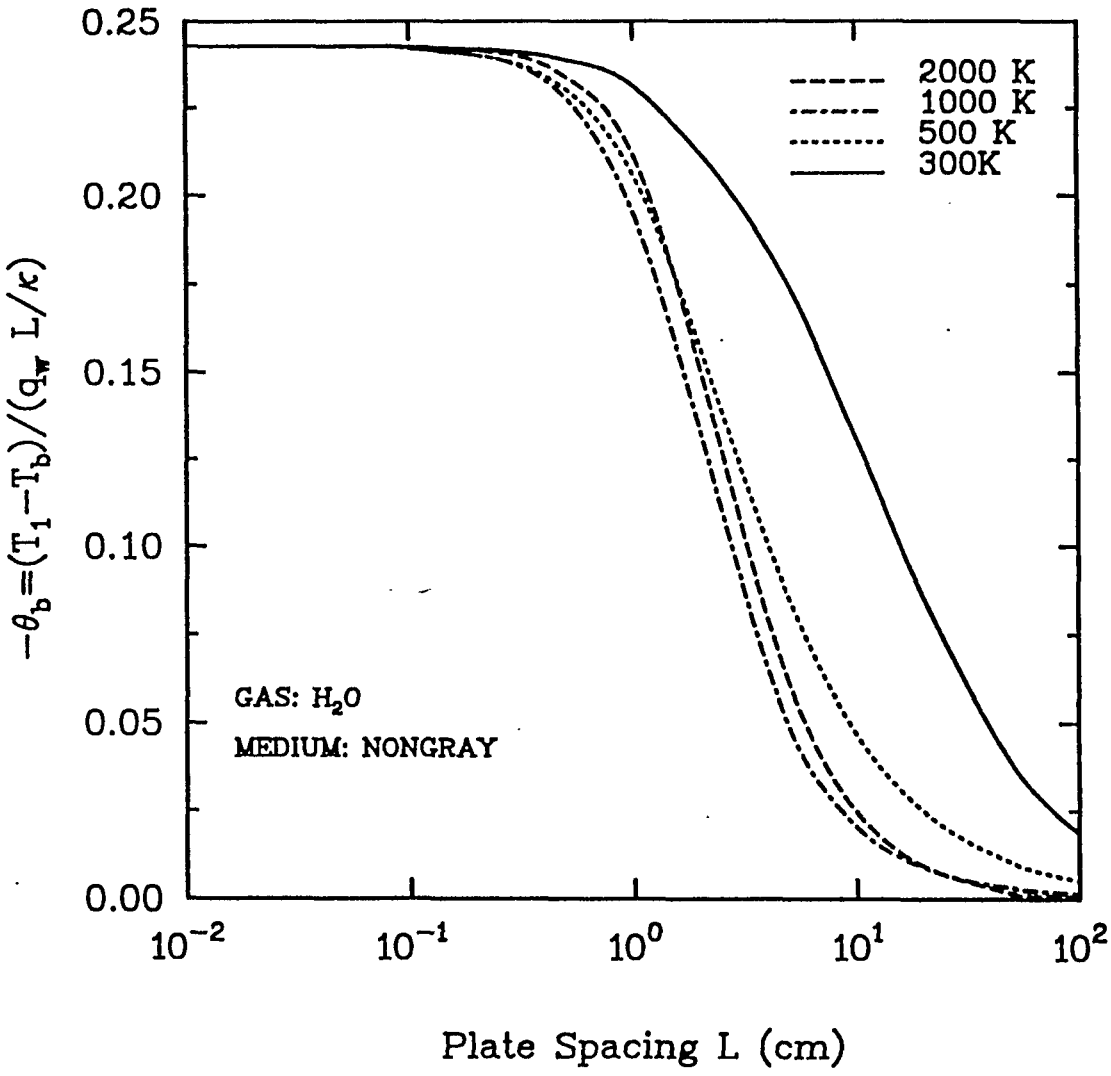

Fig. 6.13(a): LTE results for H_2O, P=1 atm, T_w=300–2000 K

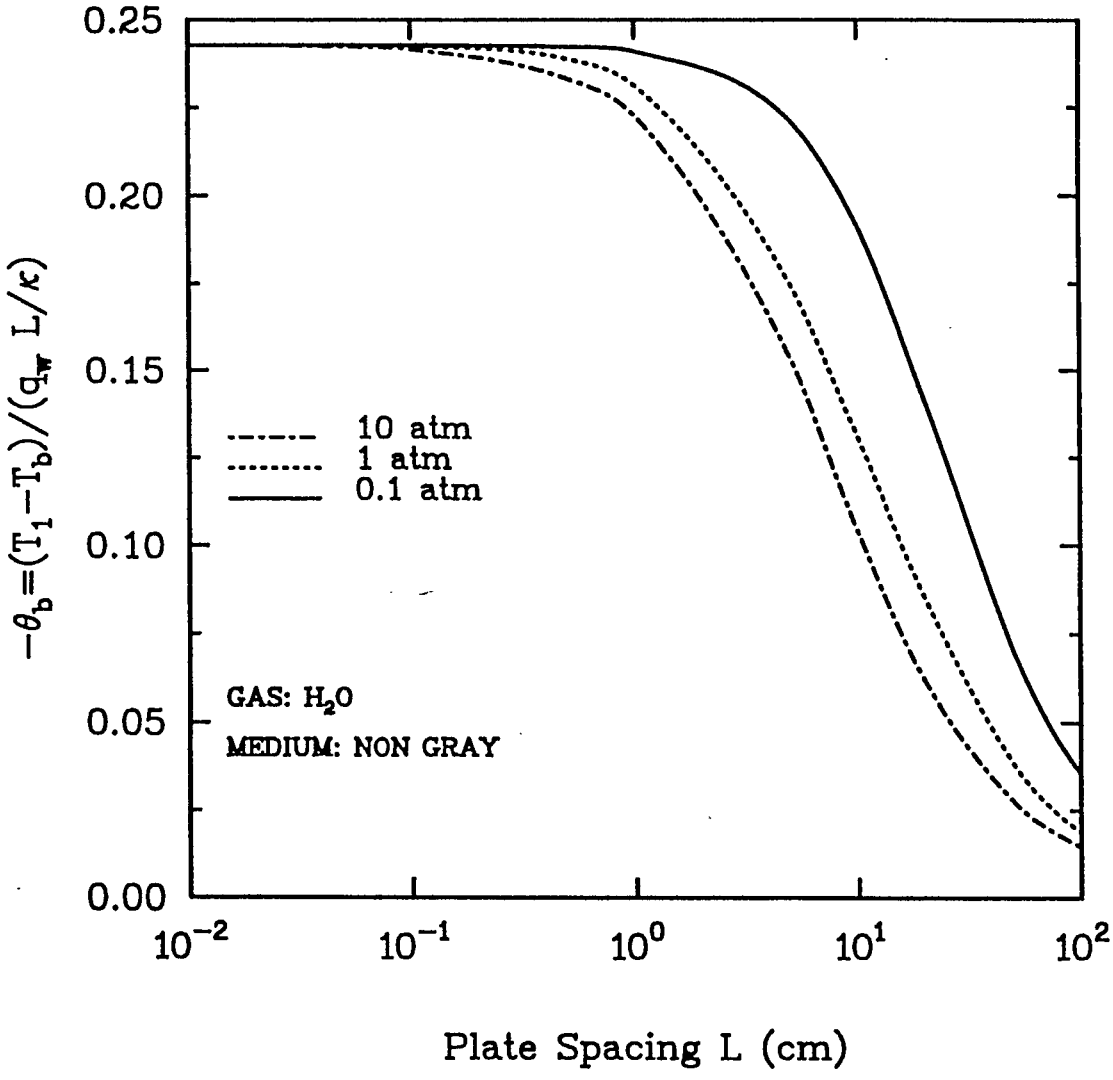

Fig.6.13(b): LTE results for H_2O, T_w=300 K, P=0.1–10 atm

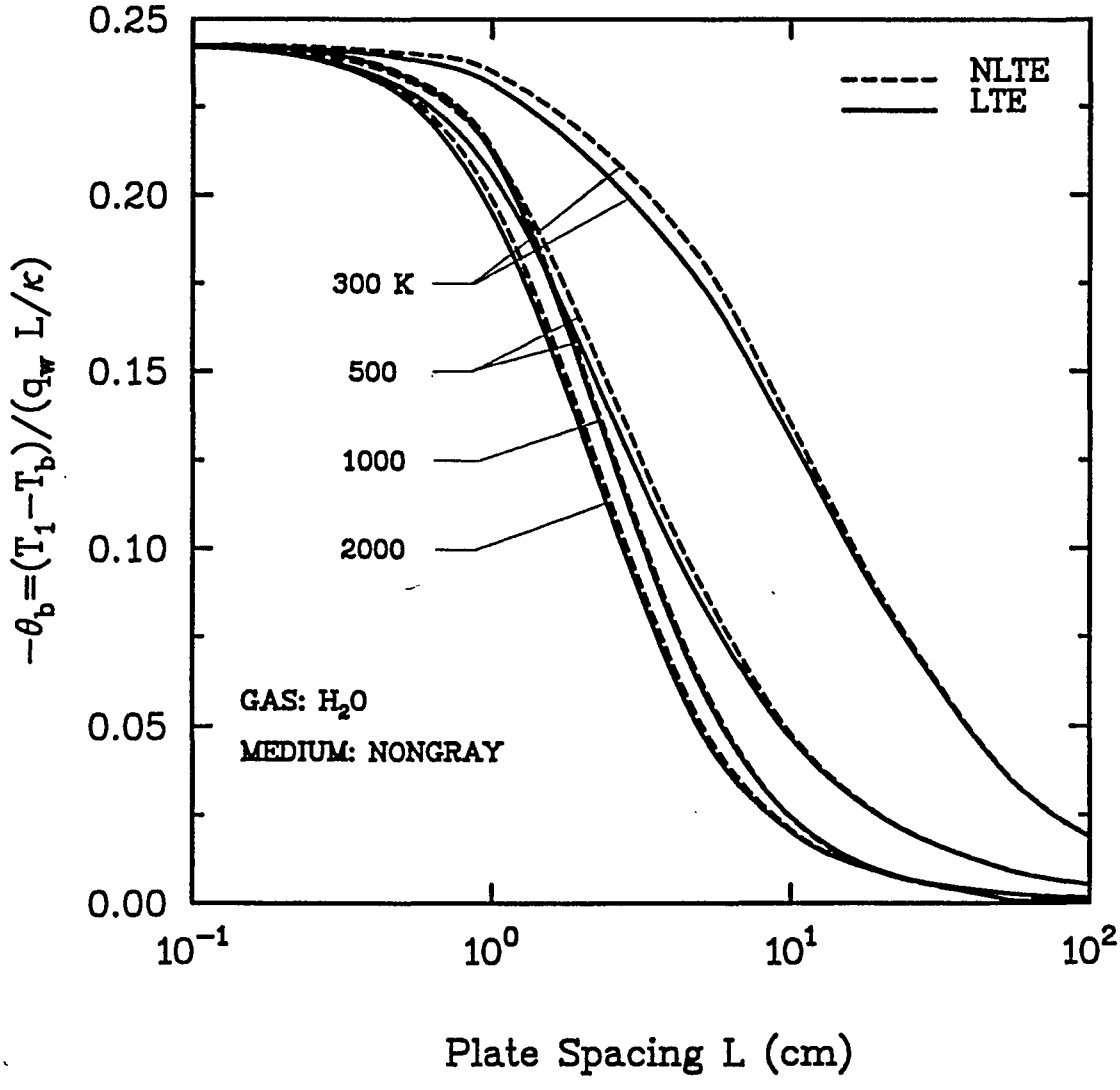

Fig. 6.13(c): LTE and NLTE results for H_2O, P=1 atm, T_w=300–2000 K

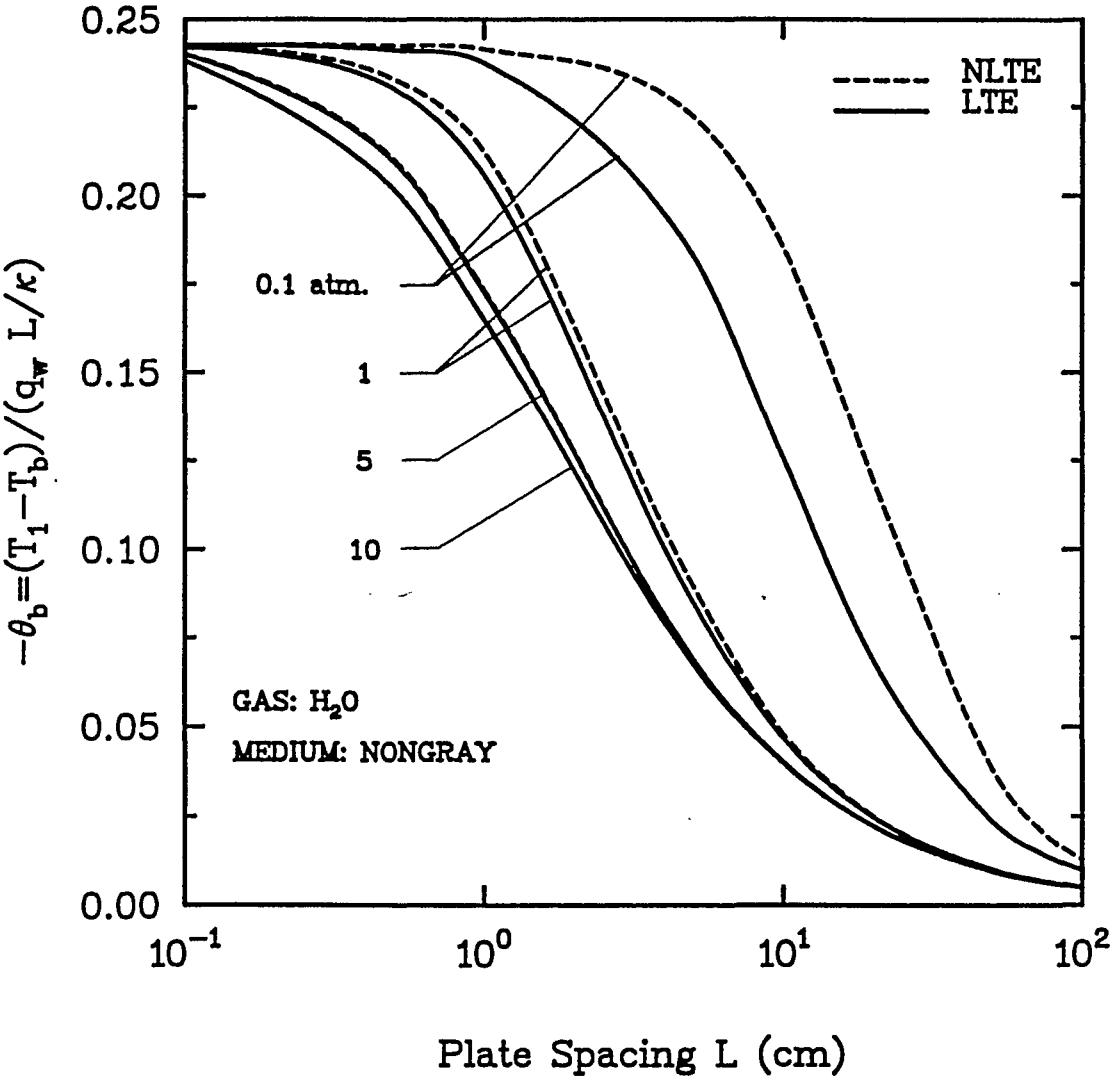

Fig. 6.13(d): LTE and NLTE results for H_2O, T_w=500 K, P=0.1–10 atm

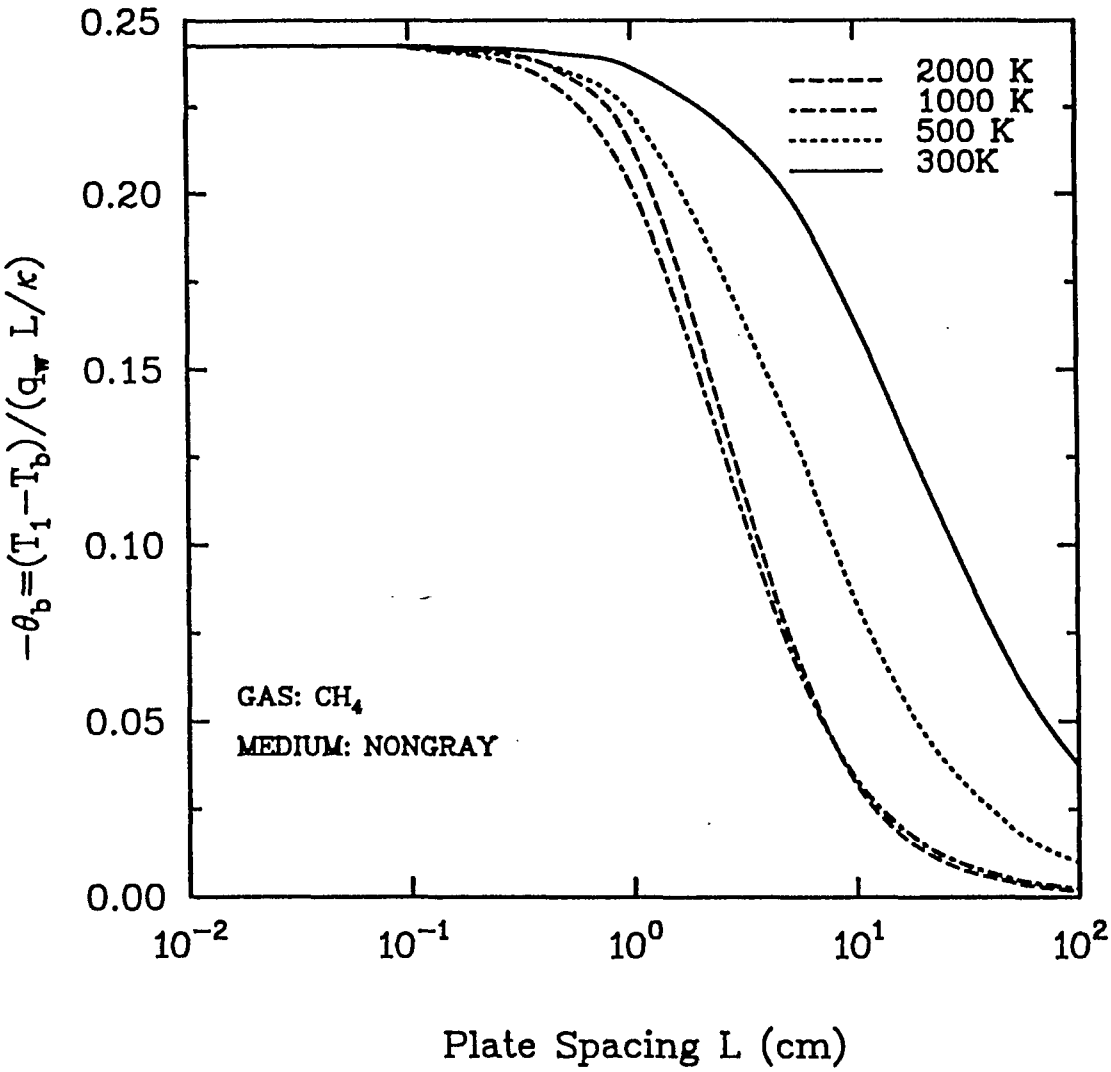

Fig. 6.14(a): LTE results for CH_4, P=1 atm, T_w=300–2000 K

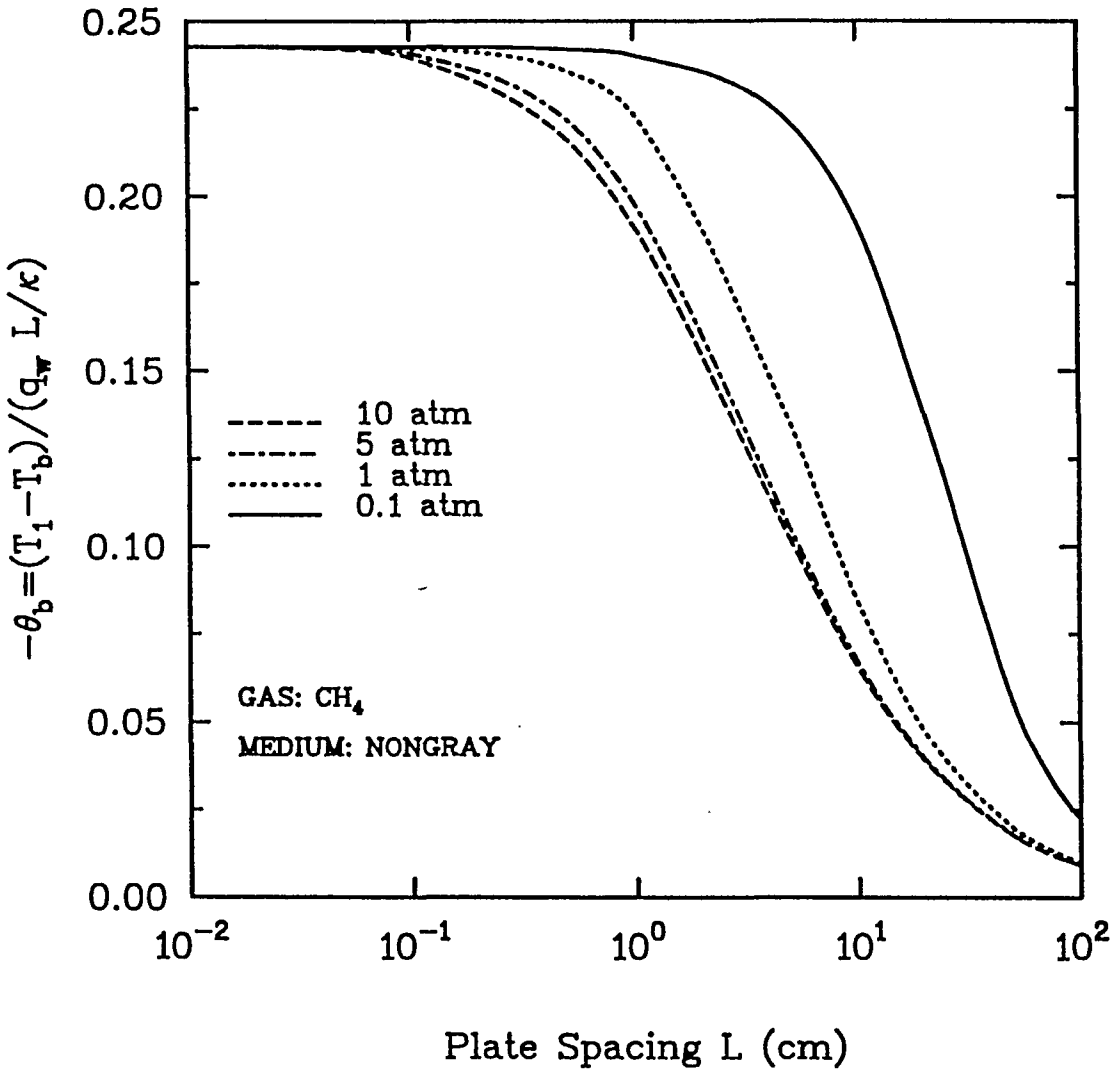

Fig. 6.14(b): LTE results for CH_4, T_w=500 K, P=0.1–10 atm

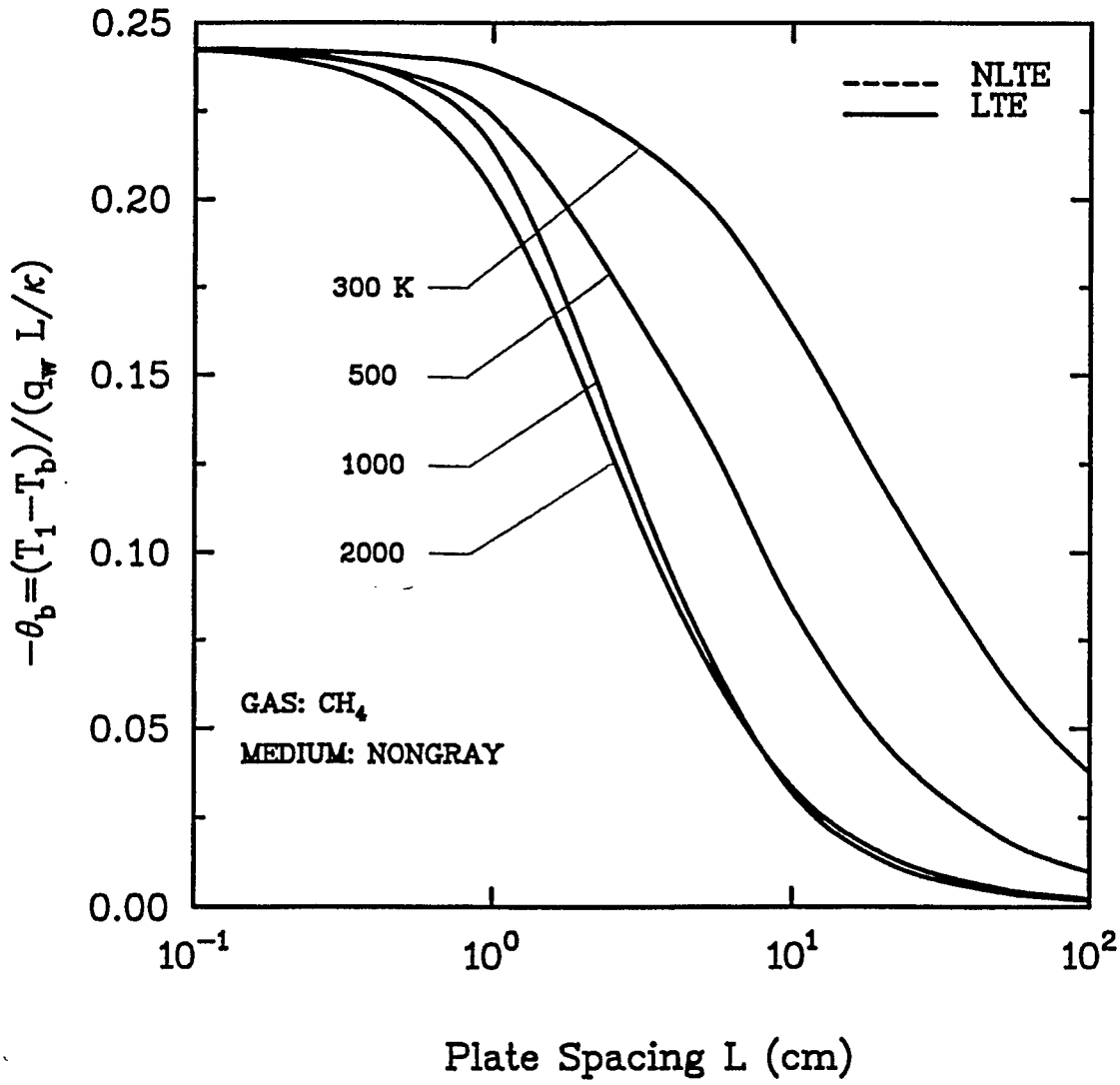

Fig. 6.14(c): LTE and NLTE results for CH_4, P=1 atm, T_w=300–2000 K

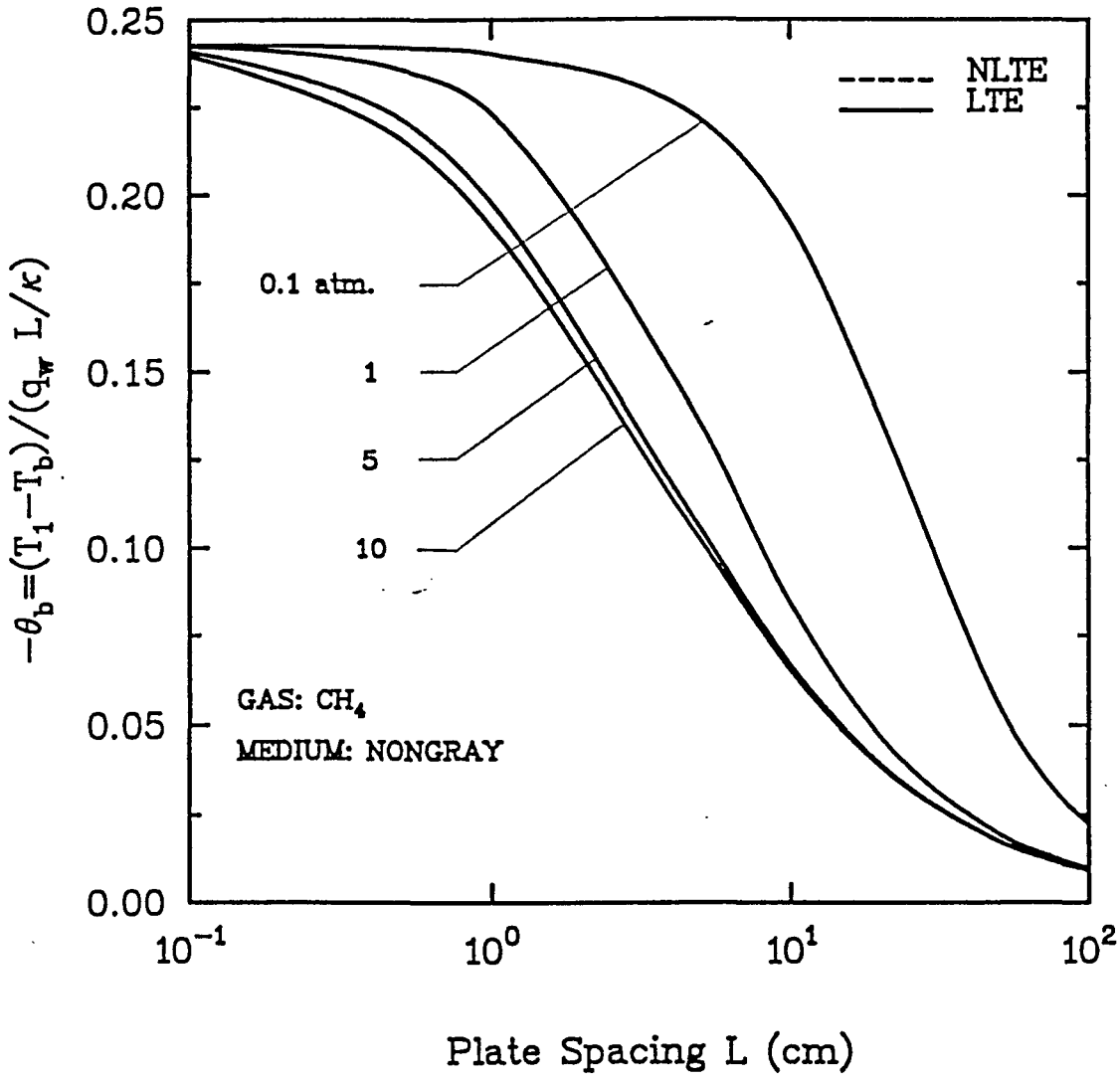

Fig. 6.14(d): LTE and NLTE results for CH_4, T_W=500 K, P=0.1–10 atm

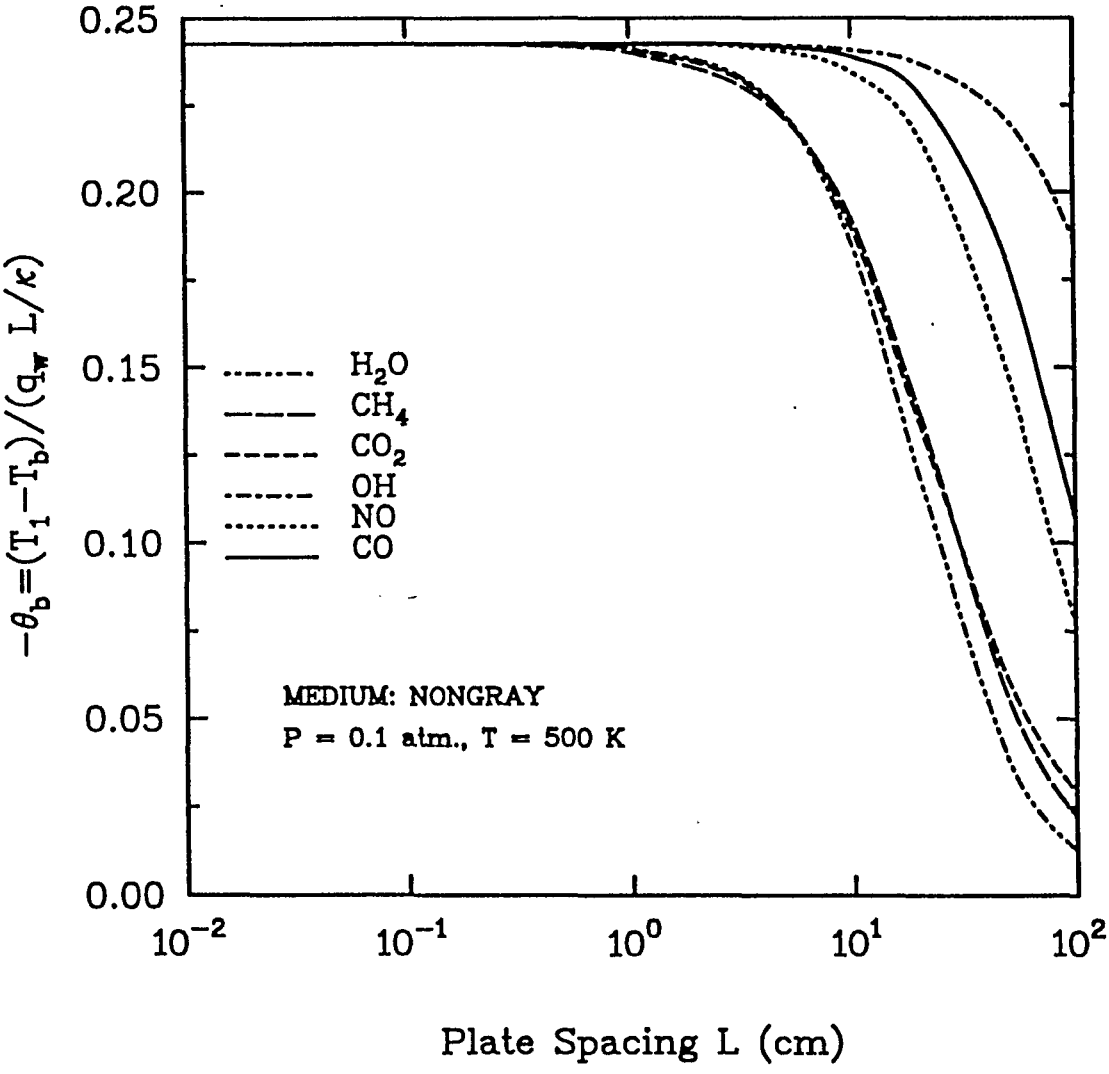

Fig. 6.15: Comparison of NLTE results for different gases

Figure 6.17(a) illustrates comparative results for gray and nongray for NO at four temperatures in the range of 300 to 2000 K and one atmospheric pressure. As seen in the case of CO, the difference between the two results is appreciable and decreases slowly with increasing temperature. Figure 6.17(b) provides the comparison at 500 K and 0.1,1, and 10 atm. It is seen that the difference between gray and nongray results increases with increasing pressure.

Figures 6.18 through 6.21 present results for OH, CO_2, H_2O, and CH_4, respectively. The results show the same behavior as shown by CO and NO. Thus, it is obvious that the difference between gray and nongray results is very significant at any temperature and pressure. The difference decreases slowly with increasing temperature and increases with increasing pressure. Another interesting observation is that the bulk temperature, under gray gas assumption at any pressure and temperature condition, is lower than that under nongray gas assumption. This means that radiating effect of the species under gray gas assumption is higher than that under nongray assumption, i.e., the gray gas approximation overpredicts the ability of a gas for radiative interaction.

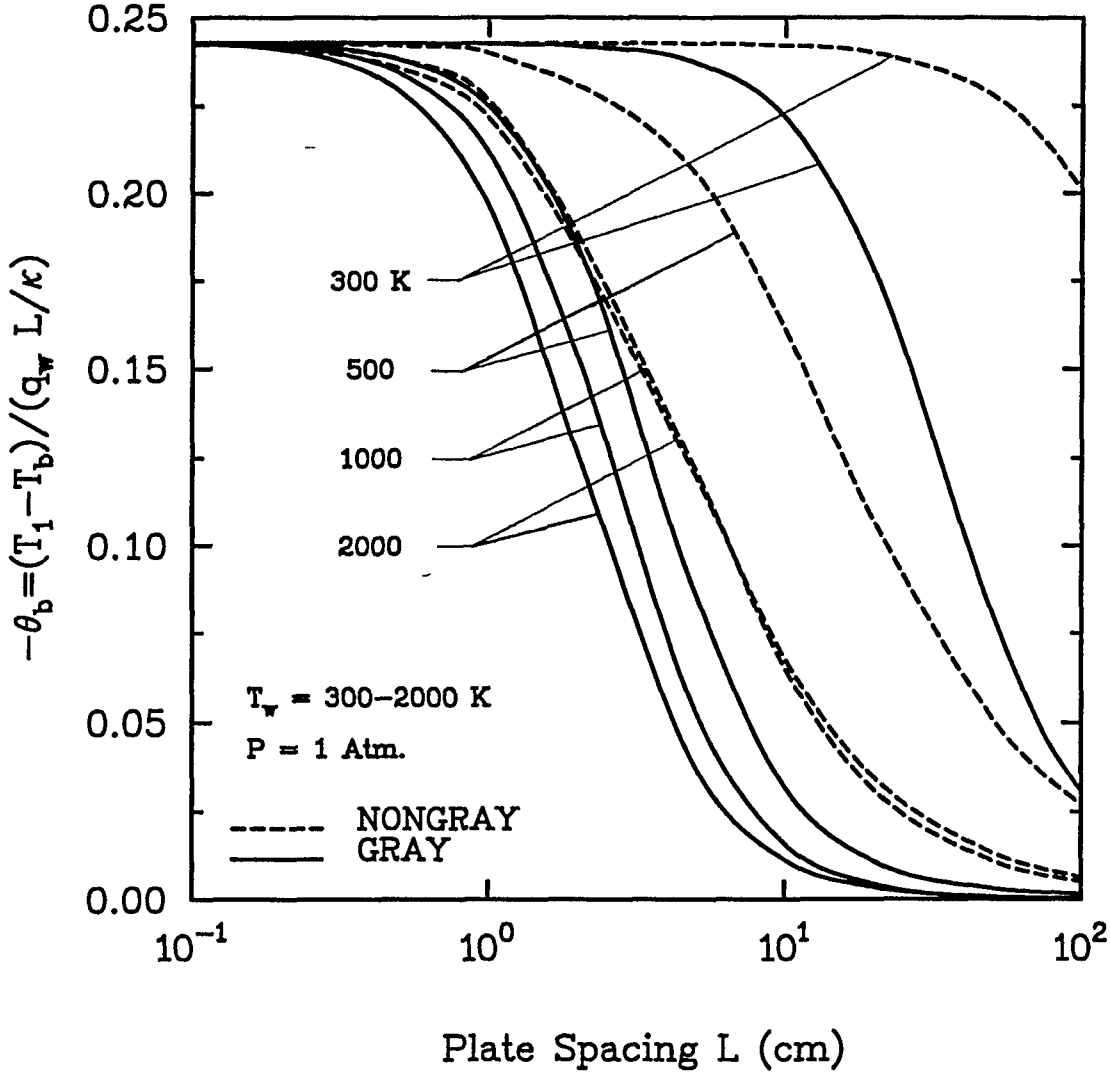

Fig. 6.16(a): Comparison of Gray and Nongray(NLTE) results for CO

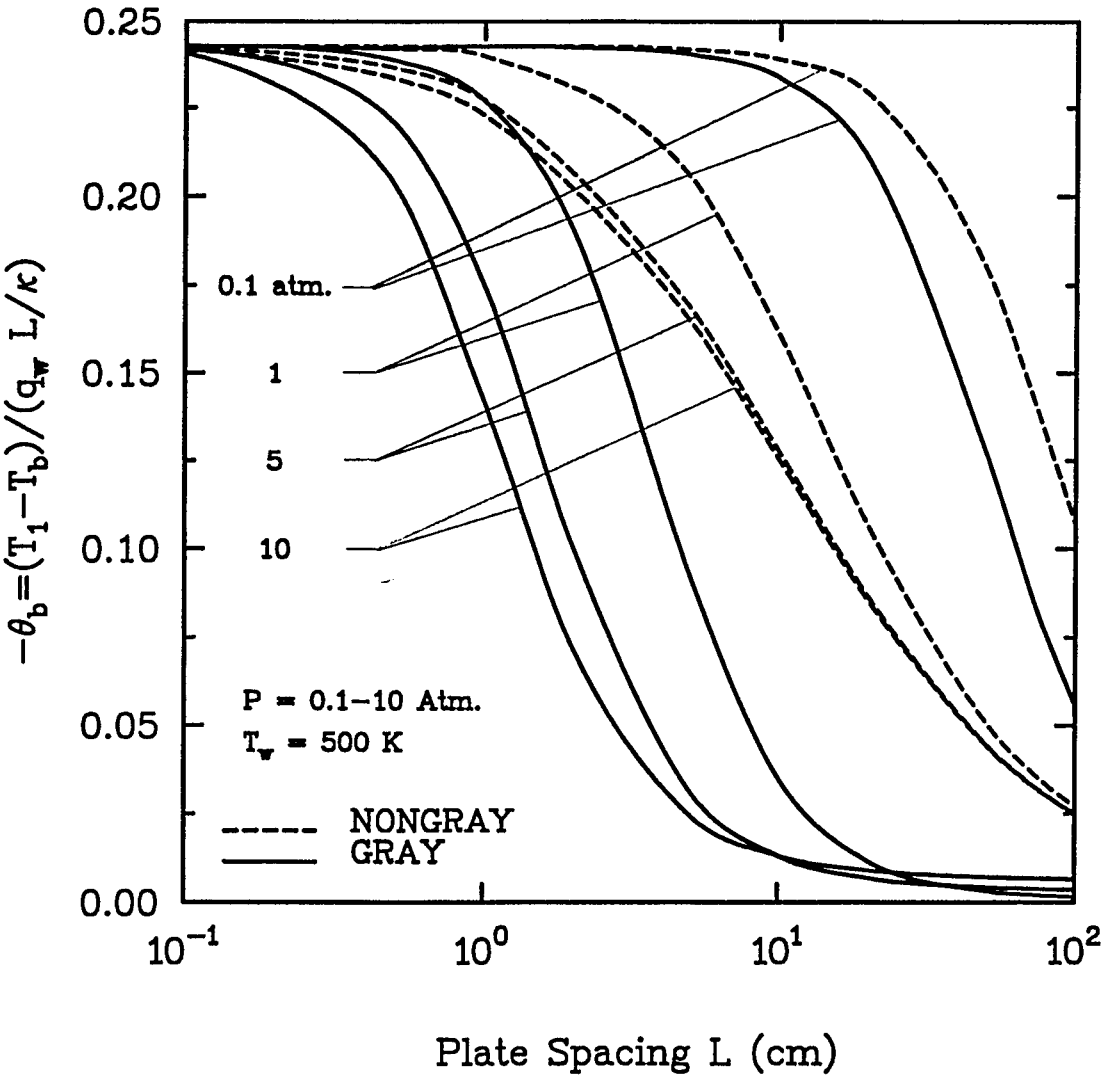

Fig. 6.16(b): Comparison of Gray and Nongray(NLTE) results for CO

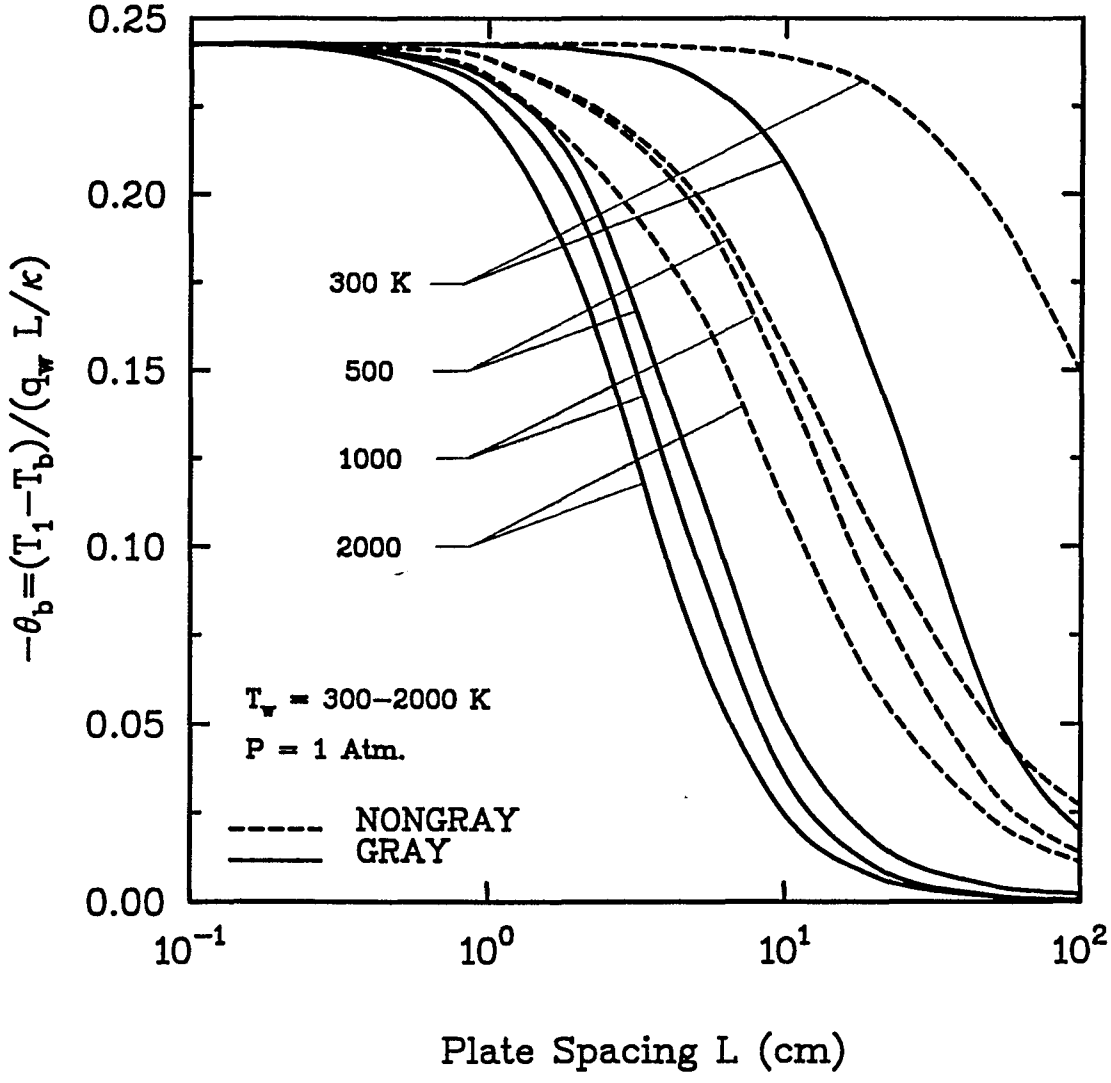

Fig. 6.17(a): Comparison of Gray and Nongray(NLTE) results for NO

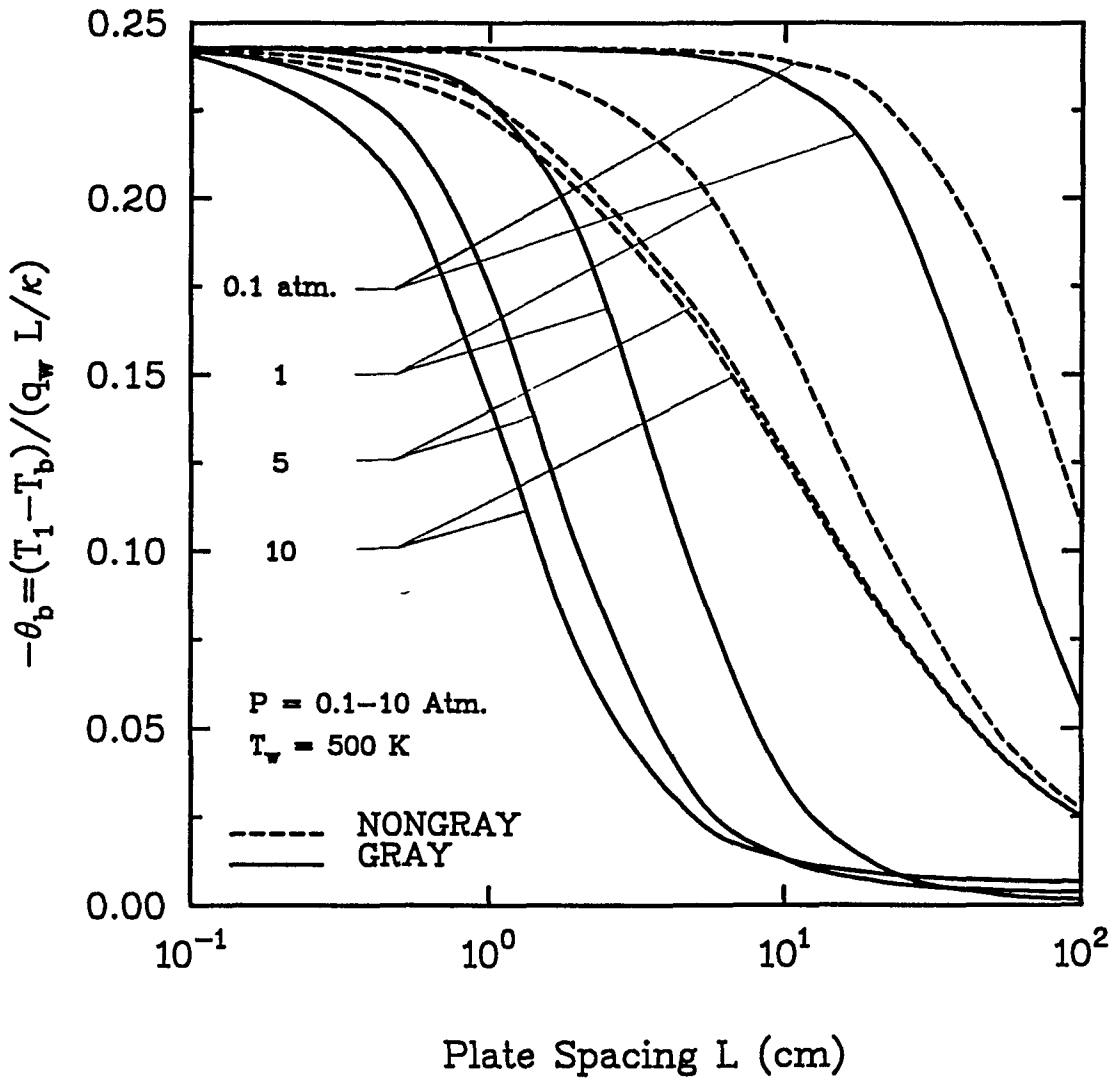

Fig. 6.17(b): Comparison of Gray and Nongray(NLTE) results for NO

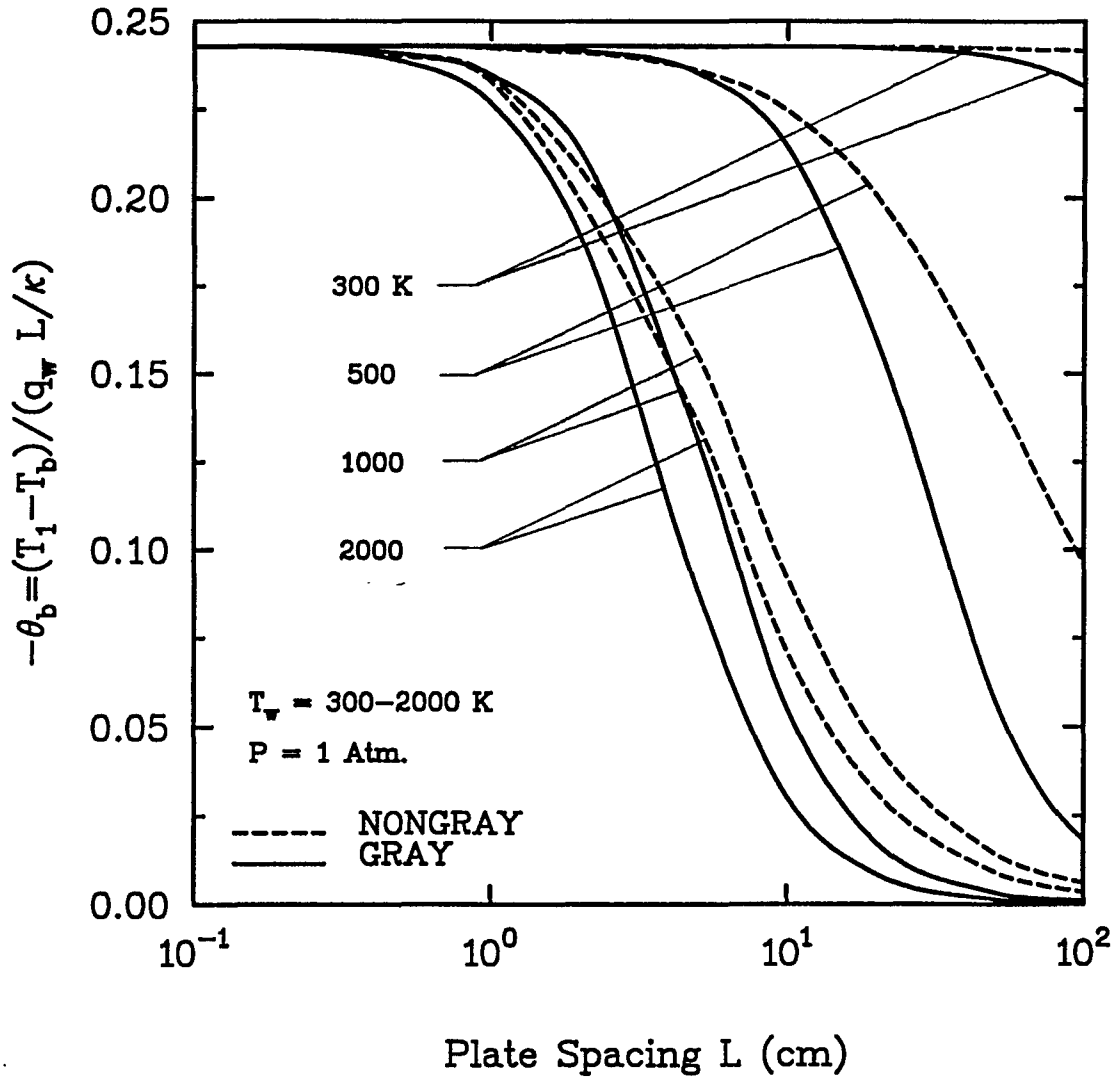

Fig. 6.18(a): Comparison of Gray and Nongray(NLTE) results for OH

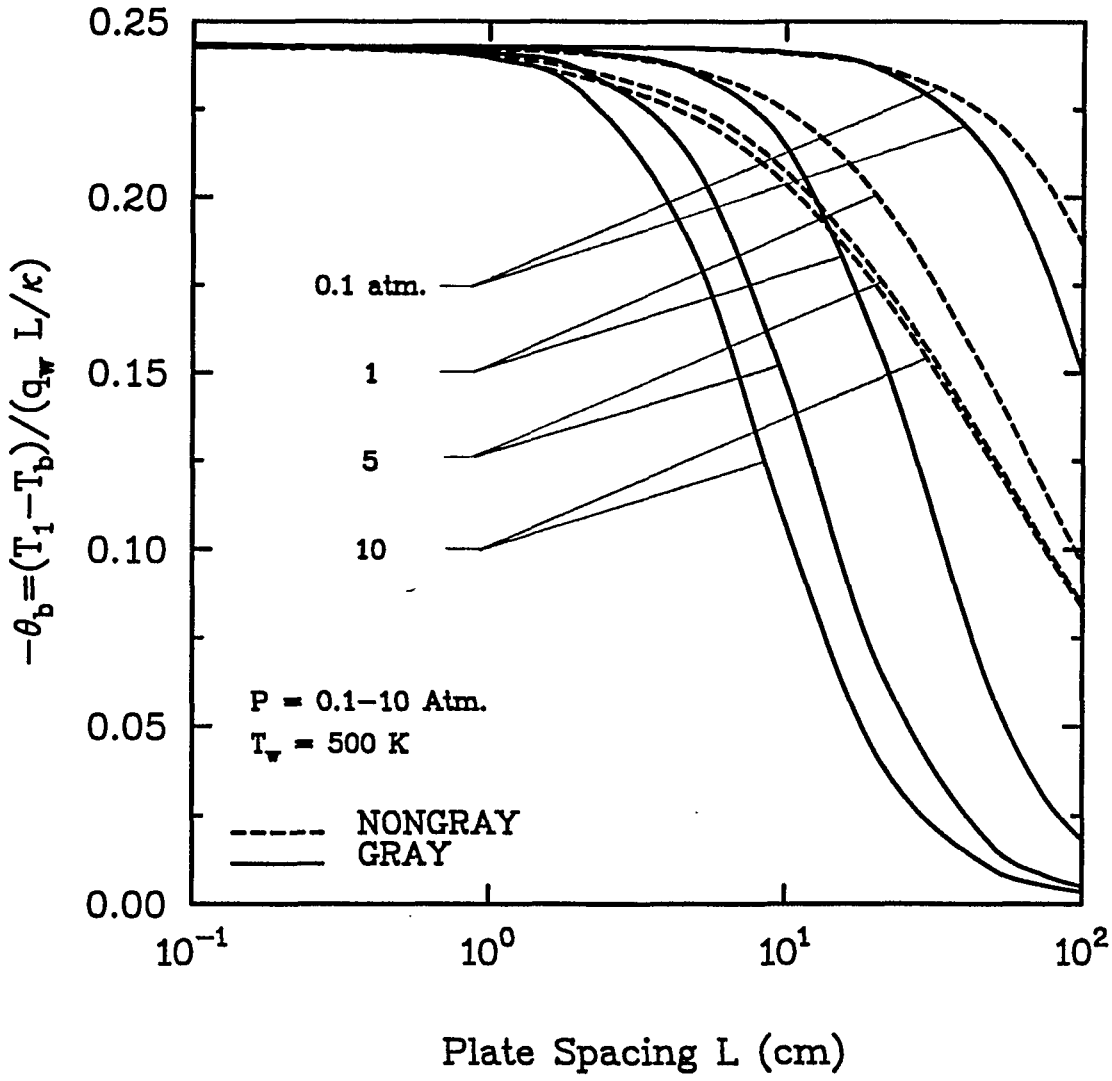

Fig. 6.18(b): Comparison of Gray and Nongray(NLTE) results for OH

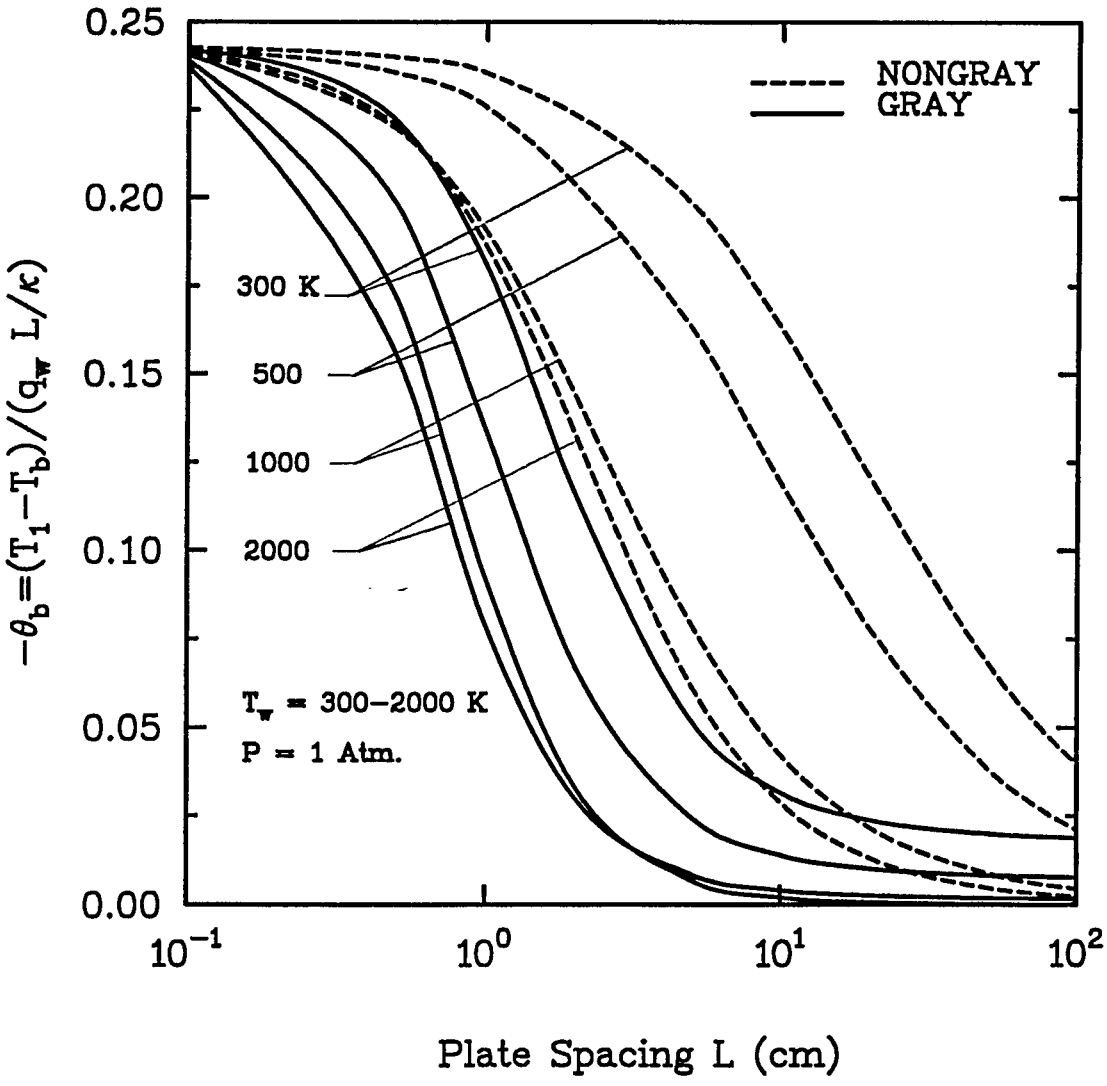

Fig. 6.19(a): Comparison of Gray and Nongray(NLTE) results for CO_2

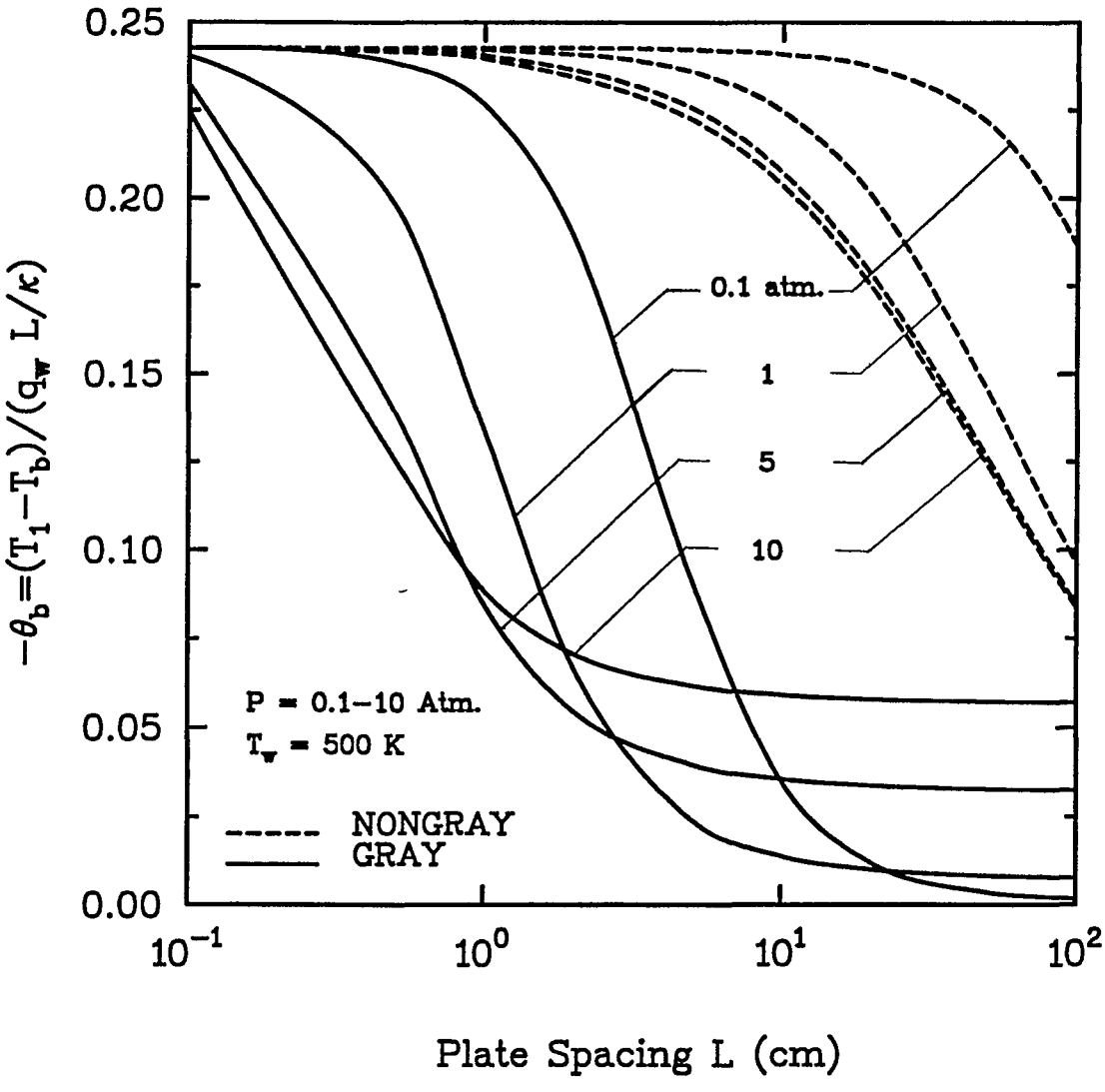

Fig. 6.19(b): Comparison of Gray and Nongray(NLTE) results for CO_2

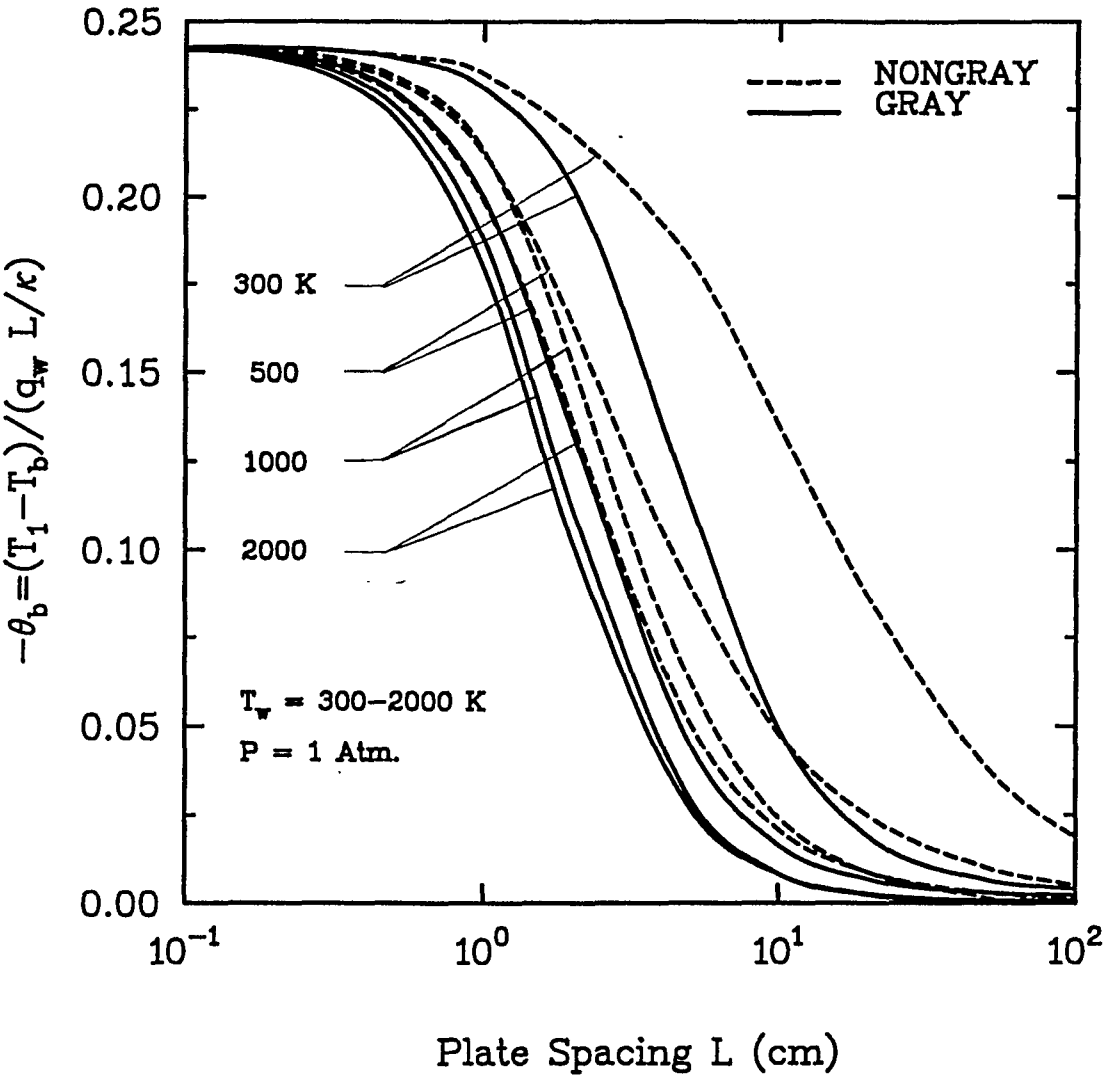

Fig. 6.20(a): Comparison of Gray and Nongray(NLTE) results for H_2O

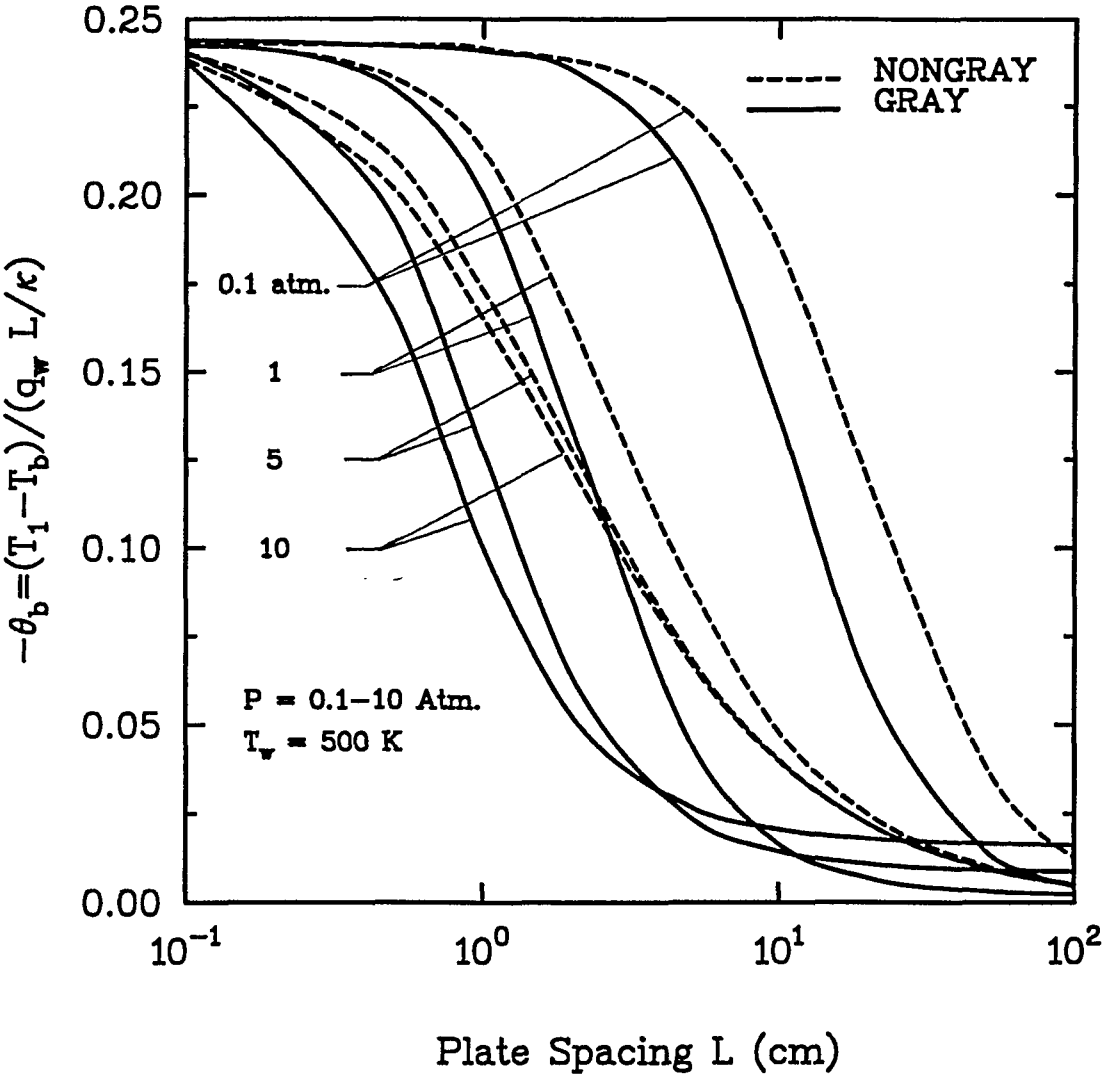

Fig. 6.20(b): Comparison of Gray and Nongray(NLTE) results for H_2O

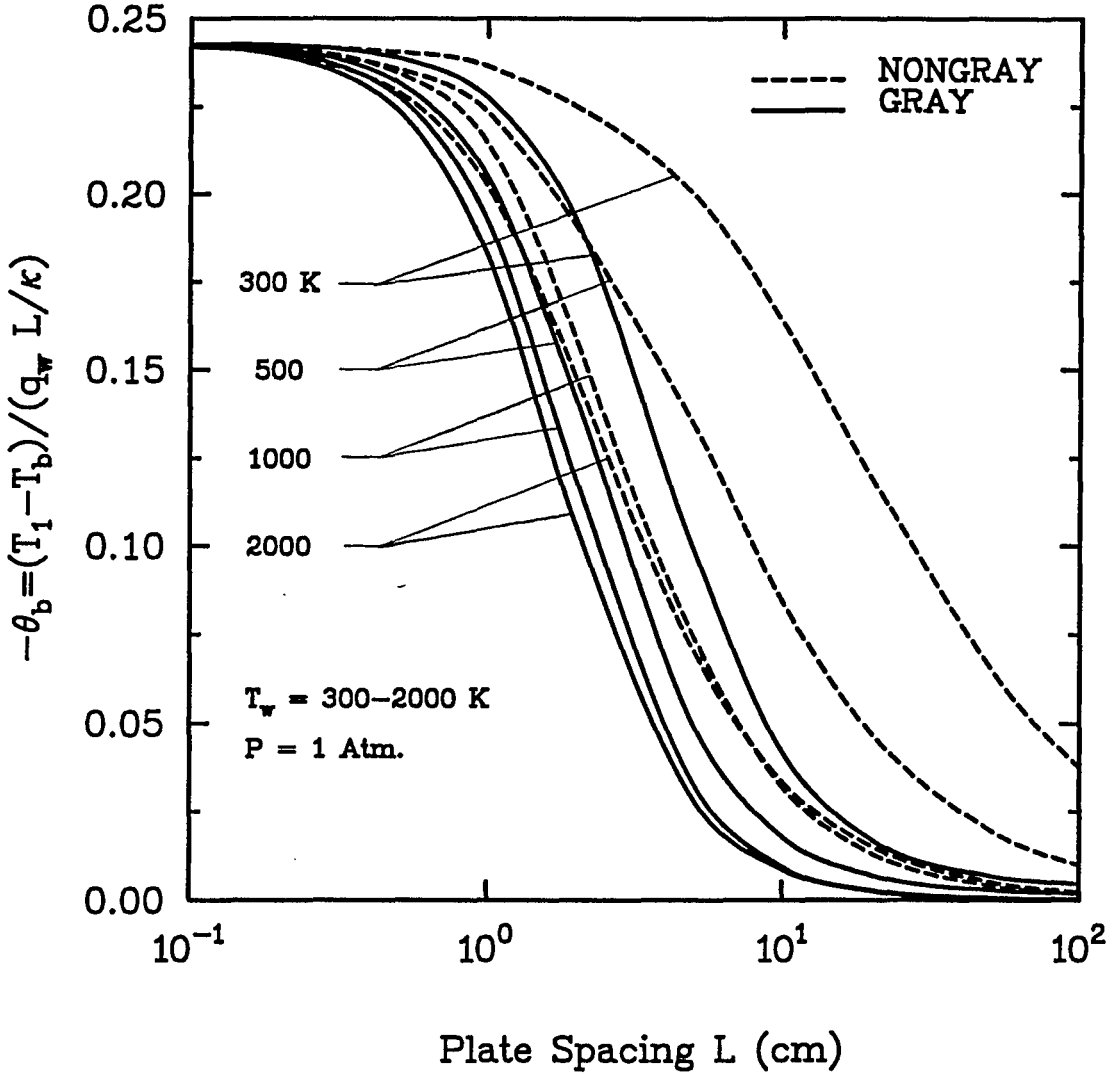

Fig. 6.21(a): Comparison of Gray and Nongray(NLTE) results for CH_4

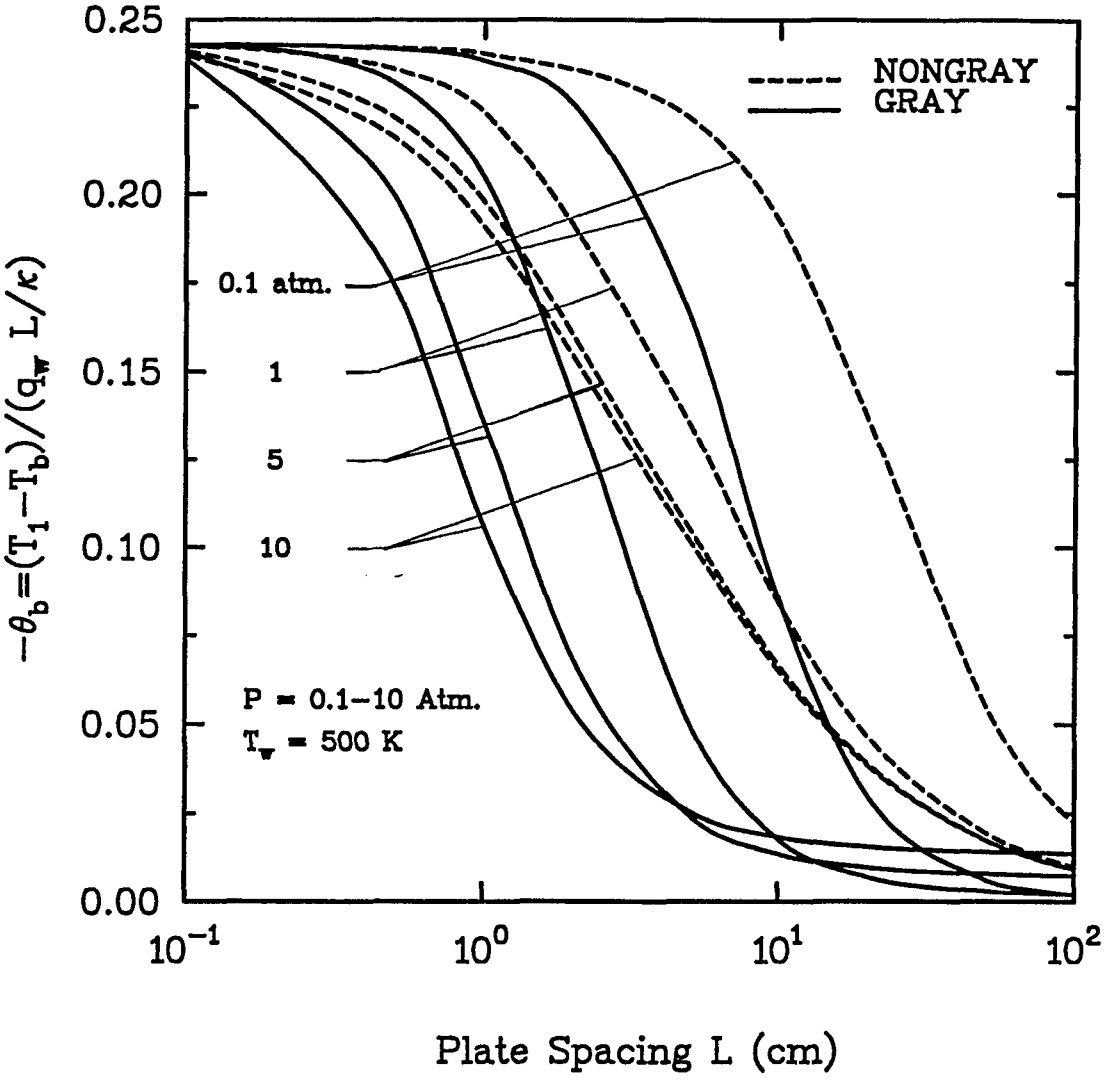

Fig. 6.21(b): Comparison of Gray and Nongray(NLTE) results for CH_4

Chapter 7

CONCLUDING REMARKS

Analytical and numerical procedures have been developed to treat a physical problem when local and nonlocal thermodynamic equilibrium conditions prevail. The NLTE effects have been investigated for some diatomic and polyatomic gases under gray and nongray gas assumptions. The NLTE results under gray and nongray assumption are compared at different temperatures and pressures. The NLTE condition is governed by the NLTE parameter η. For η = O(1), NLTE prevails and for η = 0, LTE prevails. The bulk temperature is expressed as a function of plate spacing at various temperatures and pressures. The limiting value of bulk temperature is 0.243 which corresponds to negligible radiation.

The results show that, in general, bulk temperature decreases with increasing temperatures, pressures, and plate spacings. This implies that the radiative ability of the gases increases with increasing temperatures, pressures, and plate spacings. The consideration of NLTE effect is important while dealing with diatomic gases. The NLTE effect becomes significant at lower temperatures and pressures. Therefore, it is necessary to take NLTE into account when working temperatures and pressures are moderate. Among the gases, OH shows least radiative effect and H_2O shows highest radiative effect under both gray and nongray assumption. Polyatomic gases, however, do not show much variation from LTE at any temperature

and pressure. Therefore, NLTE consideration is not important for polyatomic gases. The gray gas approximation overpredicts the ability of a gas for radiative interaction. The method developed can be applied to investigate NLTE effects in other diatomic and polyatomic gases, mixture of gases, and multidimensional problems using sophisticated spectral models for radiation absorption.

REFERENCES

1. Chandrasekhar, S., Radiative Transfer, Dover Publication, Inc., New York, 1960.

2. Kourganoff, V., Basic Methods in Transfer Problems, Dover Publications, Inc., New York, 1963.

3. Sobolev, V. V., A Treatise on Radiative Transfer, D. Van Nostrand Company, Inc., Princeton, New Jersey, 1963.

4. Goody, R. M., Atmospheric Radiation I: Theoretical Basis, Oxford University Press, London and New York, 1964.

5. Preisendorfer, R. W., Radiative Transfer on Discrete Spaces, Pergamon Press, London and New York, 1965.

6. Sparrow, E. M. and Cess, R. D., Radiation Heat Transfer, Brooks/Cole, Belmont, Calif., 1966 and 1970. New Augmented Edition, Hemisphere Publishing Corp., Washington, D. C., 1978.

7. Hottel, H. C. and Sarofim, A. F., Radiative Transfer, McGraw–Hill Book Co., New York,1967.

8. Love, T. J., Radiative Heat Transfer, Charles E. Merrill Publishing Co., Columbus, Ohio, 1968.

9. Siegel, R. and Howell, J. R., Thermal Radiation Heat Transfer, McGraw–Hill Book Co., New York, 1971; Second Edition, 1981.

10. Ozisik, M. N., Radiative Transfer and Interactions with Conduction and Convection, John Wiley and Sons, Inc., New York, 1973.

11. Liou, K. N., An Introduction to Atmospheric Radiation, Academic Press, 1980.

12. Schlichting, H., Boundary Layer Theory, McGraw–Hill Book Company, New York, 1950 (2nd ed.), 1960 (4th ed.), 1968 (6th ed.), and 1979 (7th ed.).

13. Batchelor, G. K., An Introduction to Fluid Dynamics, Cambridge University Press, London, 1967.

14. White, F. M., Viscous Fluid Flow, McGraw–Hill Book Company, New York, 1974.

15. Bird, R. B., Stewart, W. E., and Lightfoot, E. N., Transport Phenomena, John Wiley and Sons, Inc., New York, 1960.

16. Rohsenow, W. H. and Choi, H. Y., Heat, Mass, and Momentum Transfer, Prentice–Hall, Englewood Cliffs, New Jersey, 1961.

17. Eckert, E. R. G. and Drake, R. M., Analysis of Heat and Mass Transfer, McGraw–HillBook Company, New York, 1972.

18. Kays, W. M. and Crawford, M. E., Convection Heat and Mass Transfer, second edition, McGraw–Hill Book Company, New York 1980.

19. Anderson, D. A., Tannehill, J. C., and Pletcher, R. M., Computational Fluid Mechanics and Heat Transfer, Hemisphere Publishing Corporation, New York, 1984.

20. Usiskin, C. M. and Sparrow, E. M., "Thermal Radiation between Parallel Plates Separated by an Absorbing–Emitting Nonisothermal Gas," International Journal of Heat and Mass Transfer, Vol. 1, Number 1, 1960, pp. 28–36.

21. Viskanta, R. and Grosh, R. J., "Heat transfer in a Thermal Radiation Absorbing and Scattering Medium," Proceedings, International Heat Transfer Conference, Boulder, Colorado, 1961.

22. Lick, W., "Energy Transfer by Radiation and Conduction," Proceedings, 1963 Heat Transfer and Fluid Mechanics Institute, Palo Alto, Calif. : Stanford University Press, 1963, pp. 14–26.

23. Viskanta, R., "Radiation Transfer and Interaction of Convection with Radiation Heat Transfer," Advances in Heat Transfer, Vol. 3, Academic Press New York, 1966.

24. Cess, R. D. and Tiwari, S. N., "Heat Transfer to Laminar Flow of an Absorbing–Emitting Gas between Parallel Plates," Heat and Mass Transfer – USSR, Vol. 1, May 1968, pp. 229–283.25. Tiwari, S. N., "Radiative Interactions in Transient Energy Transfer in Gaseous Systems," NASA CR–17664 NAS 1.26:176644, December 1985.

25. Tiwari, S. N., "Radiative Interactions in Transient Energy Transfer in Gaseous Systems," NASA CR–176644, December 1985.

26. Tiwari, S. N. and Singh, D. J., "Interaction of Transient Radiation in Fully Developed Laminar Flows," AIAA Paper, 87–1521, also "Transient Radiative Energy Transfer in Incompressible Laminar Flows," NASA–CR–123456 NAS 1.26:123456, June 1987.

27. Gilles, S. E., "Flow with Coupled Radiative and Vibrational Nonequilibrium in a Diatomic Gas," Ph.D. Dissertation, stanford University, California, 1968; also, Gilles, S. E. and Vincenti, W. G., 1970, "Coupled Radiation and Vibrational Nonequilibrium in a Diatomic Gas with Application to Gas Dynamics," Journal of Quantitative Spectroscopy and Radiative Transfer, Vol. 10, Number 2, February 1970, pp. 71–97.

28. Mlynczak, M. G., "Nonlocal Thermodynamic Equilibrium Processes in Ozone: Implications for the Energy Budget of the Mesosphere and Lower Thermosphere," Journal of Geophysical Research, Vol. 96, Number D9, September 1992, pp. 17,217–17,228.

29. Tiwari, S. N. and Cess, R. D., "The Influence of Vibrational Nonequilibrium Upon Infrared Radiative Energy Transfer," Journal of Quantitative Spectroscopy and Radiative Transfer, Vol. 11, 1971, pp. 248–273.

30. Tiwari, S. N. and Manian, S. V., 1976, "Evaluation of Upwelling Infrared Radiance in a Nonhomogeneous and Nonequilibrium Atmosphere," NASA CR–149090, November 1976; also, MS Thesis by S. V. Manian, Old Dominion University, Norfolk, Virginia, December 1976.

31. Tiwari, S. N., "Elements of Radiative Interactions in Gaseous Systems," Department of Mechanical Engineering and Mechanics, College of Engineering and Technology, Old Dominion University, Norfolk, Virginia, TR/NAG–1–423, December 1991.

32. Tiwari, S. N., "Infrared Radiative Energy Transfer in Gaseous System," Institute of Computational and Applied Mechanics (ICAM), Old Dominion University, Norfolk, Virginia, ODU/ICAM Report 91–102, September 1991.

33. Tien, C. L., "Thermal Radiation Properties of Gases," Advances in Heat Transfer, Vol. 5, Academic Press, New York, 1968.

34. Cess, R. D. and Tiwari, S. N., "Infrared Radiative Energy Transfer in Gases,"Advances in Heat Transfer, Vol. 8, Academic Press, New York, 1972.

35. Edwards, D. K., "Molecular Gas Band Radiation," Advances in Heat Transfer, Vol. 12, Academic Press, New York, 1976; also Radiation Heat Transfer Notes, Hemisphere Publishing Corporation, Washington, D. C., 1981.

36. Millikan, R. C. and White, D. R., "Vibrational Energy Exchange Between N_2 and CO: The Vibrational Relaxation of Nitrogen," The Journal of Chemical Physics, Vol. 39, Number 1, July 1963, pp. 98–101.

37. Millikan, R. C. and White, D. R., "Systematics of Vibrational Relaxation," The Journal of Chemical Physics, Vol. 39, Number 12, December 1963, pp. 3209–3213.

APPENDICES

APPENDIX A

INFORMATION ON SPECTROSCOPIC PROPERTIES

To formulate radiative heat transfer problems, it is essential to know the various spectroscopic properties of the gases under consideration. Some relevant information for the gases into consideration is provided here. For a detailed understanding and information, one should refer to [31].

A correlation for the exponential wide band absorptance based on a set of mathematical properties of the total band absorptance was introduced by Tien and Lowder [33], and this is expressed as

$$A = A_0 \ln\left\{ uf(t)\left[\frac{u+2}{u+2f(t)}\right] + 1 \right\} \qquad (A.1a)$$

$$u = C_0^2 PY \; ; \; t = \left[\frac{C_2^2}{(4C_1C_3)}\right]P_e = B^2 P_e \qquad (A.1b)$$

$$f(t) = 2.94[1 - \exp(-2.60t)] \qquad (A.1c)$$

The quantities u, t, B^2, and P_e are all dimensionless. The band width parameter $A_0 = C_3$, and it is a function of temperature only. The correlation quantity C_0^2 is proportional to (C_1/C_3). It can be shown [33] that

$$A_0 C_0^2 = S(T) \qquad (A.2)$$

The quantity t is the line structure parameter, and P_e is the equivalent (effective) broadening pressure and is given by

$$P_e = [\frac{(P_B + bP_A)}{P_0}]^n, \; P_0 = 1atm \qquad (A.3)$$

where P_A is the partial pressure of the absorbing gas, P_B is the partial pressure of the broadening gas, and b is the self–broadening power of the molecule A with respect to molecule B (N_2 in all cases here). The pressure parameter,n, which is always less than or equal to unity, accounts for the partial overlapping of bands with different lower states [35]. The quantities b and n are obtained experimentally by using various gas compositions.

By using the information on C_1, C_2, and C_3, the quantities A_0, C_0^2, and B^2 were evaluated and expressed in the units employed here. These are given in Table A.1. The procedure for converting the correlation constants C_1, C_2, and C_3 from the data of Edwards et al. [35] into the relations and units of quantities A_0, C_0^2, and B^2 is discussed in [31].

Table A.1 Exponential Band Model Correlation Quantities *

Molecule	Band	Band Center cm^{-1}	Pressure Parameters		$A_0(T)$	$C_0^2(T)$	$B^2(T)$
	μ	ω_c	b	n	cm^{-1}	$atm^{-1}cm^{-1}$	dimensionless
CO	4.7	2143	1.1	0.8	38.1 $k_1(T)$	6.24 $k_2(T)$	0.314 $\delta_1(T)$
	2.35	4260	1.0	0.8	38.1 $k_1(T)$	0.024 $k_2(T)$	0.300 $\delta_1(T)$
NO	5.3	1876	1.0	0.65	36.0 $k_1(T)$	**	**
	2.7	3724	1.0	0.65	36.0 $k_1(T)$		
OH	2.8	3570	**	**	117 $k_1(T)$	**	**
	1.4	6974			117 $k_1(T)$		
CO_2	15	667	1.3	0.7	22.3 $k_1(T)$	15.2 $k_2(T)$	0.084 $k_1(T)$
	4.3	2350	1.3	0.8	19.9 $k_1(T)$	98.7 $k_2(T)$	0.329 $k_1(T)$
	2.7	3715	1.3	0.65	41.6 $k_1(T)$	1.72 $k_2(T)$ $\phi_2(T)$	0.111 $\delta_2(T)$
H_2O	I.R	500	5.0	1.0	49.4 $k_1(T)$	771 $k_2(T)$ $\phi_7(T)$	0.073/$k_1(T)$
	6.3	1600	5.0	1.0	90.1 $k_1(T)$	3.35 $k_2(T)$	0.130/$k_1(T)$
	2.7	3750	5.0	1.0	112.6 $k_1(T)$	1.52 $k_2(T)$	0.145/$k_1(T)$
	1.87	5350	5.0	1.0	79.7 $k_1(T)$	0.276 $k_2(T)$ $\phi_{011}(T)$	0.118/$k_1(T)$
	1.38	7250	5.0	1.0	79.7 $k_1(T)$	0.230 $k_2(T)$ $\phi_{101}(T)$	0.201/$k_1(T)$
CH_4	7.6	1310	1.3	0.8	39.8 $k_1(T)$	4.58 $k_2(T)$	0.067 $k_1(T)$
	3.3	3020	1.3	0.8	95.3 $k_1(T)$	3.15 $k_2(T)$	0.036 $k_1(T)$

* Notes on table A.1:

1. Notations: $k_1(T) = (T/300)^{1/2}$, $k_2(T) = (300/T)^{1/2}$, $\delta_1 = [\ \phi_1^2(T)/k_1(T)\ ] \times 10^{-3}$,

   $\delta_2 = \phi_3^2(T)/[\ \phi_2(T)\ k_1(T)\ ]$

   $h = 6.625 \times 10^{-27}$ erg–sec, $c = 2.998 \times 10^{10}$ cm/sec, $\kappa = 1.380 \times 10^{-16}$ erg/K,

   $hc/\kappa \simeq 1.44$ cm–K

2. For CO: $\omega = 2143\ cm^{-1}$, $\phi_1(T) = [\ 15.15 + 0.22\ (T/T_0)^{3/2}\ ]\ [\ 1 - \exp(-hc\omega/\kappa T)\ ]$,

   $T_0 = 100$ K, $S(T_{01}) = 289 \pm 30\ cm^{-2}\text{–}atm^{-1}$, $T_{01} = 300$ K, $\eta_r = 0.0297$ seconds.

3. For NO: $\omega = 1876\ cm^{-1}$, $S(T_{01}) = 132\ cm^{-2}\text{–}atm^{-1}$, $T_{01} = 300$ K, $\eta_r = 0.07$ secs.

4. For OH: $\omega = 3570\ cm^{-1}$, $S(T_{01}) = 110\ cm^{-2}\text{–}atm^{-1}$, $T_{01} = 300$ K, $\eta_r = 0.0232$ secs.

5. For CO_2: $\omega_1 = 1351\ cm^{-1}$, $\omega_2 = 667\ cm^{-1}$, $\omega_3 = 2396\ cm^{-1}$

$\phi_2(T) = \{\ 1 - \exp[\ (-hc/\kappa T)\ (\omega_1 + \omega_3)\ ]\ \} \times \{\ [\ 1 - \exp(-hc\,\omega_1/\kappa T)\ ]\ [\ 1 - \exp(-hc\,\omega_3/\kappa T)\ ]\ \}^{-1}$, $\phi_3(T) = 1 + 0.053\ (T/300)^{3/2}$, $S_1(T_{01}) = 362 \pm 90$, $S_2(T_{01}) = 2970$, $S_3(T_{01}) = 67\ cm^{-2}\text{–}atm^{-1}$, $T_{01} = 300$ K, $\eta_{1r} = 0.215$ secs., $\eta_{2r} = 0.0022$ secs., $\eta_{3r} = 0.0846$ secs.

6. For H_2O: $\omega_1 = 3652\ cm^{-1}$, $\omega_2 = 1595\ cm^{-1}$, $\omega_3 = 3756\ cm^{-1}$, $\phi_{v1v2v3}(T) = \{\ 1 - \exp[\ -hc\ (v_1\omega_1 + v_2\omega_2 + v_3\omega_3)/\kappa T\ ]\ \} \times \{\ [\ 1 - \exp(-hc\omega_2/\kappa T)\ ]\ [\ 1 - \exp(-hc\omega_3/\kappa T\ ]\ \}^{-1}$, $\phi_7(T) = \exp[\ -17.6\ (T/100)^{-1/2}\ ]$, $S_1(T_{01}) = 1840$, $S_2(T_{01}) = 300 \pm 60$, $S_3(T_{01}) = 200 \pm 20$ $cm^{-2}\text{–}atm^{-1}$, $T_{01} = 300$ K, $\eta_{2r} = 0.0468$ secs., $\eta_{3r} = 0.0127$ secs.

6. For CH_4: $\omega_1 = 1310\ cm^{-1}$, $\omega_2 = 3020\ cm^{-1}$, $S_1(T_{01}) = 185$, $S_2(T_{01}) = 320$, $cm^{-2}\text{–}atm^{-1}$, $T_{01} = 300$ K, $\eta_{1r} = 0.113$ secs., $\eta_{2r} = 0.0122$ secs.

** The information is not available in literature, and therefore suitable assumptions were made to calculate those quantities.

- For additional informations, one should refer to [31].

APPENDIX B

SOLUTION PROCEDURE FOR GRAY NLTE FORMULATION

In this appendix, solution procedure for gray gas analysis under NLTE assumption is provided.

The radiative flux equation for the present study is given by Eq. (3.44). Using the following relations

$$\int_0^\infty B_{1\omega} d\omega = B_1 = e_1 = \sigma T_1^4 \tag{B.1}$$

$$\int_0^\infty B_{2\omega} d\omega = B_2 = e_2 = \sigma T_2^4 \tag{B.2}$$

$$\int_0^\infty J_\omega(z) d\omega = J(z) = \frac{e(z)}{\pi} + \frac{1}{2}\eta \overline{H}(z) \tag{B.3}$$

where

$$\overline{H}(z) = \frac{-\frac{dq_R}{dz}}{2\pi PS(T)} \tag{B.4}$$

and substituting Eq. (3.40) in Eq. (3.44), one obtains

$$q_R = \sigma T_1^4 \exp(-b\tau) - \sigma T_2^4 \exp[(-b\tau_0 - \tau)]$$

$$+\frac{3}{2}\left\{\int_0^{\tau} e(t)\exp[-b(\tau-t)]dt-\int_{\tau}^{\tau_0} e(t)\exp[-b(t-\tau)]dt\right\}$$

$$-\frac{3}{8}\eta\left\{\int_0^{\tau}\frac{dq_R}{dt}\exp[-b(\tau-t)]dt-\int_{\tau}^{\tau_0}\frac{dq_R}{dt}\exp[-b(t-\tau)]dt\right\}\times\frac{1}{PS(T)} \qquad (B.5)$$

Equation (B.5) can be rewritten as

$$q_R(\tau) = q_{RL}(\tau) + q_{RN}(\tau) \qquad (B.6)$$

where $q_{RL}(\tau)$ and $q_{RN}(\tau)$ are defined as in Eqs. (3.49a) and (3.53a) respectively. Differentiating Eq. (B.6) twice using Leibnitz formula, one obtains

$$\frac{d^2q_R}{d\tau^2} = \frac{d^2F}{d\tau^2} + 2\Gamma\frac{dT^4}{d\tau} + \Gamma b^2(I) - 2KS\frac{d^2q_R}{d\tau^2} - KSb^2(II) \qquad (B.7a)$$

where $$I = \int_0^{\tau} T^4(t)\exp[-b(\tau-t)]dt - \int_{\tau}^{\tau_0} T^4(t)\exp[-b(t-\tau]dt \qquad (B.7b)$$

$$II = \int_0^{\tau}\frac{dq_R}{dt}\exp[-b(\tau-t)]dt - \int_{\tau}^{\tau_0}\frac{dq_R}{dt}\exp[-b(t-\tau)]dt \qquad (B.7c)$$

and $F(\tau)$, b, Γ, and KS are defined as in Eqs. (3.49b), (3.49c), and (3.53b) respectively. the quantity I can be obtained from Eq. (3.49a) as

$$I = \frac{q_{RL}(\tau) - F(\tau)}{\Gamma} \qquad (B.8a)$$

Similarly, the quantity II can be obtained from Eq. (3.53a) as

$$II = -\frac{q_{RN}}{KS} \qquad (B.8b)$$

Substituting Eqs. (B.8a) and (B.8b) in Eq. (B.7a), there is obtained

$$M_2 \frac{d^2 q_R}{d\tau^2} - \frac{9}{4} q_R = 3\sigma \frac{dT^4}{d\tau} \qquad (B.9)$$

which is Eq. (3.55a), and M_2 is defined as in Eq. (3.55b).

APPENDIX C

SOLUTION PROCEDURE FOR NONGRAY NLTE FORMULATION

In this appendix, some important steps to solve the nongray NLTE equation, Eq. (5.13), are given.

Substituting Eq. (5.10) in 5.(13), one obtains

$$a_1(1 - 6\xi^2 + 4\xi^3) + a_2(2\xi - 6\xi^2 + 4\xi^3) - 2(3\xi^2 \_ 2\xi^2 - 2\xi^3) + 1 =$$

$$\frac{3}{2}\left(\frac{L}{\varkappa}\right)Hu_0\left\{\int_0^{\xi}\theta(\xi')\overline{A}'(I)d\xi' - \int_{\xi}^{1}\theta(\xi')\overline{A}'(II)d\xi'\right\}$$

$$-\frac{3}{8}\eta\left[\int_0^{\xi}\left(1 + \frac{d^2\theta}{d\xi'^2}\right)\overline{A}'(I)d\xi' - \int_{\xi}^{1}\left(1 + \frac{d^2\theta}{d\xi'^2}\right)\overline{A}'(II)d\xi'\right] \qquad (C1)$$

where $\overline{A}'(I)$ and $\overline{A}'(II)$ are defined as Eq. (5.3b).

Solving Eq. (B1) at $\xi = 0$, and assuming a multiband species, there is obtained

$$a_1\alpha_1 + a_2\alpha_2 = \alpha_0 \qquad (C2)$$

where

$$a_0 = (\frac{3}{8}\eta c R_0 - 1) \tag{C3}$$

$$a_1 = 1 + [(\frac{L}{\varkappa})H_1(cR_1 - 2c^3R_3 + c^4R_4)] - [(\frac{9}{2})\eta(c^3R_2 - c^2R_1)] \tag{C4}$$

$$a_2 = [(\frac{L}{\varkappa})H_1(c^2R_2 - 2c^3R_3 + c^4R_4)] - [(\frac{3}{4})\eta(cR_0 - 6c^2R_1 + 6c^3R_2)] \tag{C5}$$

where $c = 2/(3\ u_0)$, $b = 1/u$, and R_i's are integral functions defined as

$$R_0 = \int_o^b \overline{A}'(u)du \tag{C6}$$

$$R_1 = \int_0^b u\overline{A}'(u)du \tag{C7}$$

$$R_2 = \int_0^b u^2\overline{A}'(u)du \tag{C8}$$

$$R_3 = \int_0^b u^3\overline{A}'(u)du \tag{C9}$$

$$R_4 = \int_0^b u^4\overline{A}'(u)du \tag{C10}$$

In a similar manner, solving at $\xi = 1/4$, one obtains

$$a_1a_3 + a_2a_4 = a_5 \tag{C11}$$

where

$$a_3 = \left\{(\frac{L}{\varkappa})H_1[(\frac{57}{256})S_1 + (\frac{11}{16})c(S_2 + S_3) - (\frac{9}{8})c^2S_4 - c^3(S_5 + S_6) + c^4S_7]\right\} +$$

$$\left\{\left(\frac{3}{8}\right)\eta\left[\left(\frac{9}{4}\right)cS_1 + 6c^2(S_2 + S_3) - 12c^3S_4\right]\right\} + \frac{11}{16} \qquad (C12)$$

$$a_4 = \left\{\left(\frac{L}{\varkappa}\right)H_1\left[\left(\frac{9}{256}\right)S_1 + \left(\frac{3}{16}\right)c(S_2 + S_3) - \left(\frac{1}{8}\right)c^2S_4 - c^3(S_5 + S_6) + c^4S_7\right]\right\} +$$

$$\left\{\left(\frac{3}{8}\right)\eta\left[\left(\frac{1}{4}\right)cS_1 + 6c^2(S_2 + S_3) - 12c^3S_4\right]\right\} + \frac{3}{16} \qquad (C13)$$

$$a_5 = \left\{\left(\frac{3}{8}\right)\eta c\right\}S_1 - \frac{11}{16} \qquad (C14)$$

and S_i's are integral functions defined as

$$S_1 = \int_{b/4}^{3b/4} \overline{A}'(u)du \qquad (C15)$$

$$S_2 = \int_{0}^{b/4} u\,\overline{A}'(u)du \qquad (C16)$$

$$S_3 = \int_{0}^{3b/4} u\,\overline{A}'(u)du \qquad (C17)$$

$$S_4 = \int_{b/4}^{3b/4} u^3\,\overline{A}'(u)du \qquad (C18)$$

$$S_5 = \int_{0}^{b/4} u^3\,\overline{A}'(u)du \qquad (C19)$$

$$S_6 = \int_0^{3b/4} u^3 \, \overline{A}'(u) du \qquad (C20)$$

$$S_7 = \int_{b/4}^{3b/4} u^4 \, \overline{A}'(u) du \qquad (C21)$$

Thus, the constants a_1 and a_2 can be evaluated by solving Eqs. (C2) and (C11)

$$a_1 = \frac{\alpha_0 \alpha_4 - \alpha_2 \alpha_5}{DEN} \qquad (C22a)$$

$$a_2 = \frac{\alpha_0 \alpha_3 - \alpha_2 \alpha_5}{-DEN} \qquad (C22b)$$

where $$DEN = \alpha_4 \alpha_1 - \alpha_2 \alpha_3 \qquad (C22c)$$

Once a_1 and a_2 are evaluated, the solution for bulk temperature, θ_{bp} is given by Eq. (5.11). For additional information, one should refer to [32].

APPENDIX D

SELECTED COMPUTER PROGRAMS AND RESULTS

In this appendix, computer programs for CO_2 are presented which were used to obtain the results. Two general programs are provided which can solve LTE and NLTE problems under gray as well as nongray assumption. After every program, results are presented in tabulated form. The programs can be used to obtain results for other gases simply by changing the spectroscopic properties.

```
c     This program solves for bulk temperature for CO_2
c     under gray gas assumption. The program calculates bulk
c     temperature under both LTE and NLTE condition.
c*************************************************************
      implicit double precision (a-h,o-z)
      real l,kfb
      dimension u(10),press(4),temp(4)
      data u/0.1,0.5,1.0,2.0,5.0,10.0,20.0,50.0,75.,100.0/
      data press/0.1,1.,5.,10.0/
      data temp/500.0,300.,1000.0,2000.0/
      open(unit=12,file='out12.dat')
      open(unit=11,file='nlp')
      open(10,file='lp')
      write(11,13)
     write(11,*) 10,1
 13   format('3',/,'x',/,'t',/, 't1',/,i4,x,'1')
      write(12,111)
      write(10,14)
      write(10,*) 10,1
 14   format('2',/,'x',/,'t',/, /,i4,x,'1')
      do 10 it=1,1
      Tw=temp(it)
      do 20 kk=1,4
      P=press(kk)
      do 30 i=1,10
      L=u(i)
c*************************************************************
c     Calculation of Plank's function and it's derivative
c     wnb  Band Center
c     hck  Constant
c     ccc=c1*c2
c     pfbi  Plank's Function for the ith band
c     pfdbi  Derivative of Plank's Function for ith band
c*************************************************************
      tk1=tw**2
      tk2=tw**0.5
      tk3=tw/273.0
      hck=1.439257246
      ts=300.0/tw
c*************************************************************
c     Now we will consider the spectroscopic properties of co2
c     We have considered only three bands(15,4.3&2.7 microns)
c*************************************************************
      wnb1=667.0
      wnb2=2347.0
      wnb3=3716.0
      c2b1=hck*wnb1
```

```
      c2b2=hck*wnb2
      c2b3=hck*wnb3
      ccc=0.000053847734
      ccb1=ccc*(wnb1**4)
      ccb2=ccc*(wnb2**4)
      ccb3=ccc*(wnb3**4)
      tb1=c2b1/tw
      tb2=c2b2/tw
      tb3=c2b3/tw
      teb1=exp(tb1)
      teb2=exp(tb2)
      teb3=exp(tb3)
      c1b1=ccb1/c2b1
      c1b2=ccb2/c2b2
      c1b3=ccb3/c2b3
      pfb1=c1b1/(teb1-1.0)
      pfb2=c1b2/(teb2-1.0)
      pfb3=c1b3/(teb3-1.0)
      dev1=tk1*((teb1-1.0)**2.0)
      dev2=tk1*((teb2-1.0)**2.0)
      dev3=tk1*((teb3-1.0)**2.0)
      pfdb1=(ccb1*teb1)/dev1
      pfdb2=(ccb2*teb2)/dev2
      pfdb3=(ccb3*teb3)/dev3
c**********************************************************************
c     Band Model Correlations(Tien & Lowder wide band model)
c     azi  aoi is band width parameter
c     czsi=coi**2 coi is correlation parameter
c     bsi=b**2 is non dimensional quantity
c     omegi is wave number
c     si is integrated band intensity
c**********************************************************************

      ak1=(tw/300.0)**0.5
      ak2=(300.0/tw)**1.5
      az1=1.29*tk2
      az2=1.15*tk2
      az3=2.4*tk2
      kfb=(1488.365171)*(tk3**1.23)
      omeg1=1351.0
      omeg2=667.0
      omeg3=2396.0
      tx=-(hck/tw)
      tx1=tx*omeg1
      tx2=tx*omeg2
      tx3=tx*omeg3
      etx1=exp(tx1)
```

```
etx2=exp(tx2)
etx3=exp(tx3)
c1=1.0–etx1
c2=1.0–etx2
c3=1.0–etx3
brkt=tx*(omeg1+omeg3)
phi2=(1.0–exp(brkt))/(c1*c3)
ts=300.0/tw
s1=339.685*ts
s2=2702.7*ts
s3=71.497*ts*phi2
ETC1=((36.5*(TW**(–1/3.)))+3.9)
ETC2=EXP(ETC1)*(1.E–6)
ETAC=ETC2/P
ETR11=8.*3.14*(667.**(2.))*4.08*(1.E–12)*300.*339.685
ETAR1=1./ETR11
ETR12=8.*3.14*(2347.**(2.))*4.08*(1.E–12)*300.*2702.7
ETAR2=1./ETR12
ETR13=8.*3.14*(3716.**(2.))*4.08*(1.E–12)*300.*71.497*PHI2
ETAR3=1./ETR13
ETA11=ETAC/ETAR1
ETA12=ETAC/ETAR2
ETA13=ETAC/ETAR3
aap1=eta11/s1
aap2=eta12/s2
aap3=eta13/s3
aapx1=(3./4.)*(aap1)/p
aapx2=(3./4.)*(aap2)/p
aapx3=(3./4.)*(aap3)/p
am2=1.+(aapx1+aapx2+aapx3)
 tin=p*l**2.0/kfb*(s1*pfdb1+s2*pfdb2+s3*pfdb3)
 tn=exp(–(3.0*tin)**0.5)
 anexp=(1.0–tn)/(1.0+tn)
 tcm=l/kfb*(pfdb1*az1+pfdb2*az2+pfdb3*az3)
 ala=0.00005668
 akp=p/(ala*tw**4.0)*(s1*pfb1+s2*pfb2+s3*pfb3)
 tao=akp*l
 anba=kfb*akp/(4.0*ala*tw**3.0)
 r=3.0*tao**2.0/anba
 aim=3.0*tao**2.0*(0.75+1.0/anba)
 am=sqrt(aim)
 em=exp(–am)
 ad=3.0*tao*(1.0–em)+2.0*am*(1.0+em)
 ac=r/am**8.0*(48.0–3.0*tao*am**2.0+36.0*tao)/ad
 pa1=24.0–12.0*am+am**3.0+(am**3.0–12.0*am–24.0)*em
 pa2=–12.0*r/(5.0*am**4.0)+17.0*r/(70.0*am**2.0)
 ambar=am/(sqrt(am2))
```

```
      rbar=r/am2
      embar=exp(-ambar)
      adbar=3.0*tao*(1.0-embar)+2.0*ambar*(1.0+embar)
      acbar=(rbar/(ambar**8.))*(48.-3.*tao*(ambar**
     *  2.0)+36.0*tao)/adbar
      pa1bar=24.0-12.0*ambar+ambar**3.0
     *  +(ambar**3.0-12.0*ambar-24.0)*embar
      pa2bar=-12.0*rbar/(5.0*ambar**4.0)+
     *  17.0*rbar/(70.0*ambar**2.0)
      tbulk=ac*pa1+pa2-17.0/70.0
      tbulkn=acbar*pa1bar+pa2bar-17.0/70.0
      write(12,200)tw,p,l,tbulk,tbulkn
      write(11,202)l,-tbulk,-tbulkn
      write(10,203)l,-tbulkn
  111   format(4x,'tw',8x,'p',6x,'l',9x,'tbulk',9x,'tbulkn')
   30   continue
   20   continue
   10   continue
  202    format(1x,f9.2,2(3x,e10.4))
  203    format(1x,f9.2,3x,e10.4)
  200   format(8x,f7.2,3x,f6.2,3x,f6.2,3x,e10.4,3x,e10.4)
      stop
      end
```

GRAY LTE AND NLTE RESULTS FOR CO_2

T_w	P	L	T_b (LTE)	T_b (NLTE)
500.00	0.10	0.10	–.2426E+00	–.2427E+00
500.00	0.10	0.50	–.2369E+00	–.2385E+00
500.00	0.10	1.00	–.2210E+00	–.2265E+00
500.00	0.10	2.00	–.1751E+00	–.1894E+00
500.00	0.10	5.00	–.7442E–01	–.9157E–01
500.00	0.10	10.00	–.2671E–01	–.3500E–01
500.00	0.10	20.00	–.9026E–02	–.1195E–01
500.00	0.10	50.00	–.2722E–02	–.3442E–02
500.00	0.10	75.00	–.1854E–02	–.2260E–02
500.00	0.10	100.00	–.1497E–02	–.1773E–02
500.00	1.00	0.10	–.2405E+00	–.2405E+00
500.00	1.00	0.50	–.1980E+00	–.1981E+00
500.00	1.00	1.00	–.1340E+00	–.1342E+00
500.00	1.00	2.00	–.6695E–01	–.6711E–01
500.00	1.00	5.00	–.2407E–01	–.2413E–01
500.00	1.00	10.00	–.1378E–01	–.1380E–01
500.00	1.00	20.00	–.9968E–02	–.9978E–02
500.00	1.00	50.00	–.8174E–02	–.8178E–02
500.00	1.00	75.00	–.7828E–02	–.7831E–02
500.00	1.00	100.00	–.7663E–02	–.7665E–02
500.00	5.00	0.10	–.2323E+00	–.2323E+00
500.00	5.00	0.50	–.1391E+00	–.1391E+00
500.00	5.00	1.00	–.8487E–01	–.8487E–01
500.00	5.00	2.00	–.5473E–01	–.5474E–01
500.00	5.00	5.00	–.3961E–01	–.3961E–01
500.00	5.00	10.00	–.3557E–01	–.3557E–01
500.00	5.00	20.00	–.3378E–01	–.3378E–01
500.00	5.00	50.00	–.3279E–01	–.3279E–01
500.00	5.00	75.00	–.3258E–01	–.3258E–01
500.00	5.00	100.00	–.3248E–01	–.3248E–01
500.00	10.00	0.10	–.2246E+00	–.2246E+00
500.00	10.00	0.50	–.1254E+00	–.1254E+00
500.00	10.00	1.00	–.8858E–01	–.8858E–01
500.00	10.00	2.00	–.7075E–01	–.7075E–01
500.00	10.00	5.00	–.6172E–01	–.6172E–01
500.00	10.00	10.00	–.5914E–01	–.5914E–01
500.00	10.00	20.00	–.5794E–01	–.5794E–01
500.00	10.00	50.00	–.5726E–01	–.5726E–01
500.00	10.00	75.00	–.5711E–01	–.5711E–01
500.00	10.00	100.00	–.5703E–01	–.5703E–01

```
C   THIS PROGRAM SOLVES FOR BULK TEMPERATURE FOR CO_2
C   UNDER NONGRAY ASSUMPTION. THE PROGRAM CAN CALCULATE BULK
C   TEMPERATURE UNDER BOTH LTE AND NLTE CONDITIONS.
c   IMPLICIT DOUBLE PRECISION (A-H,O-Z)
    DOUBLE PRECISION IERR
    REAL L,KFB
    EXTERNAL F101,F102,F103,F111,F112,F113,F121,F122,F123,F131,F132,
   *F133,F141,F142,F143
    DIMENSION U(9),PRES(4),TEMP(4),EPS(3)
    COMMON F1,F2,F3
    OPEN(6,file='output1')
    open(7,file='nlp')
    open(8,file='lp')
    DATA U/0.1,0.5,1.0,5.0,10.0,20.0,50.0,75.,100.0/
    DATA PRES/0.1,1.,5.,10.0/
    DATA TEMP/500.,300.,1000.0,2000.0/
    WRITE(6,111)
    write(7,13)
    write(7,*) 11,1
 13  format('3',/,'x',/,'t',/, 't1',/,i4,x,'1')
      write(8,14)
     write(8,*) 11,1
 14  format('2',/,'x',/,'t',/, /,i4,x,'1')
    DO 44 IT = 1,1
    TW = TEMP(IT)
    DO 55 KK = 1,4
    P = PRES(KK)
    DO 66 I = 1, 9
     L= U(I)
C-------------------------------------------------------------
C   CALCULATION OF PLANK'S FUNCTION IT'S DERIVATIVES
C
C   WNB  BAND CENTER (1/CM)
C   HCK  CONSTANT (K CM)
C   CCC  C1*C2 (ERG-K-CM**3?SEC)
C   PFDBI  PLANCK FUNCTION DERIVATIVE FOR I BAND
C-------------------------------------------------------------
    CESS = TW**2
    STU = TW**0.5
    SNT = TW/273.
    HCK = 1.439257246
    AK1 = (TW/300.)**0.5
    TS = 300./TW
C-------------------------------------------------------------
C   SPECTROSCOPIC PROPERTIES OF CO2
C   HERE WE HAVE CONSIDERED ONLY THREE BANDS(15,4.3 & 2.7 MICRONS)
C   WNBI BAND CENTER (1/CM)
```

```
C-------------------------------------------------------------------
      WNB1 = 667.
      WNB2 = 2347.
      WNB3 = 3716.
      C2B1 = HCK*WNB1
      C2B2 = HCK*WNB2
      C2B3 = HCK*WNB3
      CCC  = 0.000053847734
      CCB1 = CCC*(WNB1**4)
      CCB2 = CCC*(WNB2**4)
      CCB3 = CCC*(WNB3**4)
      TB1 = C2B1/TW
      TB2 = C2B2/TW
      TB3 = C2B3/TW
      TEB1 = EXP(TB1)
      TEB2 = EXP(TB2)
      TEB3 = EXP(TB3)
      SNTB1 = CESS*((TEB1-1.)**2.)
      SNTB2 = CESS*((TEB2-1.)**2.)
      SNTB3 = CESS*((TEB3-1.)**2.)
      PFDB1 = (CCB1*TEB1)/SNTB1
      PFDB2 = (CCB2*TEB2)/SNTB2
      PFDB3 = (CCB3*TEB3)/SNTB3
C-------------------------------------------------------------------
C     BAND MODEL CORRELATIONS (TIEN & LOWDER WIDE BAND MODEL)
C     AZI  AOI (1/CM)
C     CZSI  COI**2 (1/(ATM-CM))
C     BSI  B**2 (NON DIMENSIONAL)
C     OMGI  WAVE NUMBER (1/CM)
C     SI   INTEGRATED BAND TNTENSITY (1/(ATM CM**2))
C-------------------------------------------------------------------
      AK1 = (TW/300.)**0.5
      AK2 = (300./TW)**1.5
      AZ1 = 1.29*STU
      AZ2 = 1.15*STU
      AZ3 = 2.4*STU
C-----------------------------------------------------
C     DKF THERMAL CONDUCTIVITY (ERG/CM-SEC-K)
C-----------------------------------------------------
      KFB = (1488.365171)*(SNT**1.23)
      AMB = H/KFB
      OMG1 = 1351.0
      OMG2 = 667.0
      OMG3 = 2396.0
      TX  =-(HCK/TW)
      TX1 = TX*OMG1
      TX2 = TX*OMG2
```

```
      TX3 = TX*OMG3
      ETX1 = EXP(TX1)
      ETX2 = EXP(TX2)
      ETX3 = EXP(TX3)
      C1 = 1.0-ETX1
      C2 = 1.0-ETX2
      C3 = 1.0-ETX3
      BRKT = TX*(OMG1+OMG3)
      PHI2 = (1.0- EXP(BRKT))/(C1*C3)
      TS = 300.0/TW
      S1 = 339.685*TS
      S2 = 2702.7*TS
      S3 = 71.497*TS*PHI2
      CZS1 = S1/AZ1
      CZS2 = S2/AZ2
      CZS3 = S3/AZ3
C-----------------------------------------
C     PL  PRESSURE PATH LENGTH (ATM-CM)
C-----------------------------------------
      PL = P* L
      UZ1 = CZS1*PL
      UZ2 = CZS2*PL
      UZ3 = CZS3*PL
      BS1 = 0.0841*AK1
      BS2 = 0.32895*AK1
      PHI3 = 1.0+0.053*((TW/100.0)**1.5)
      DEL2 = (PHI3**2.0)/(PHI2  *AK1)
      BS3 = 0.1112*DEL2
C-----------------------------------------------------------
C     PEI  EFFECTIVE PRESSURE FOR EACH BAND (NON DIMENSIONAL)
C-----------------------------------------------------------
      PE1 = (1.3*P)**0.7
      PE2 = (1.3*P)**0.8
      PE3 = (1.3*P)**0.65
C-------------------------------
C     BETAI  LINE STRUCTURE PARAMETR
C-------------------------------
      BETA1 = BS1*PE1
      BETA2 = BS2*PE2
      BETA3 = BS3*PE3
C-----------------------------
C     CORRELATION FOR EACH BAND
C-----------------------------
      F1 = 2.94*(1.0- EXP(-(2.6*BETA1)))
      F2 = 2.94*(1.0- EXP(-(2.6*BETA2)))
      F3 = 2.94*(1.0- EXP(-(2.6*BETA3)))
C-------------------------
```

```
C   NUMERICAL INTEGRATION
C-------------------------
      EPS(2) = 1E-04
      EPS(1) = 1E-04
      EP = 1.E-5
      X1 = 0.0
      X21 = (3./8.)*UZ1
      X22 = (3./8.)*UZ2
      X23 = (3./8.)*UZ3
      Y11 = 1.5*UZ1
      Y12 = 1.5*UZ2
      Y13 = 1.5*UZ3
      Y21 = 3.0*X21
      Y22 = 3.0*X22
      Y23 = 3.0*X23
      CALL QDAGS (F101,X1,Y11,EPS(2),EPS(1),R01,IERR)
      CALL QDAGS (F102,X1,Y12,EPS(2),EPS(1),R02,IERR)
      CALL QDAGS (F103,X1,Y13,EPS(2),EPS(1),R03,IERR)
      CALL  QDAGS(F111,X1,Y11,EPS(2),EPS(1),R11,IERR)
      CALL  QDAGS(F112,X1,Y12,EPS(2),EPS(1),R12,IERR)
      CALL  QDAGS(F113,X1,Y13,EPS(2),EPS(1),R13,IERR)
      CALL  QDAGS(F121,X1,Y11,EPS(2),EPS(1),R21,IERR)
      CALL  QDAGS(F122,X1,Y12,EPS(2),EPS(1),R22,IERR)
      CALL  QDAGS(F123,X1,Y13,EPS(2),EPS(1),R23,IERR)
      CALL  QDAGS(F131,X1,Y11,EPS(2),EPS(1),R31,IERR)
      CALL  QDAGS(F132,X1,Y12,EPS(2),EPS(1),R32,IERR)
      CALL  QDAGS(F133,X1,Y13,EPS(2),EPS(1),R33,IERR)
      CALL  QDAGS(F141,X1,Y11,EPS(2),EPS(1),R41,IERR)
      CALL  QDAGS(F142,X1,Y12,EPS(2),EPS(1),R42,IERR)
      CALL  QDAGS(F143,X1,Y13,EPS(2),EPS(1),R43,IERR)
      CALL  QDAGS(F101,X21,Y21,EPS(2),EPS(1),S11,IERR)
      CALL  QDAGS(F102,X22,Y22,EPS(2),EPS(1),S12,IERR)
      CALL  QDAGS(F103,X23,Y23,EPS(2),EPS(1),S13,IERR)
      CALL  QDAGS(F111,X1,X21,EPS(2),EPS(1),S21,IERR)
      CALL  QDAGS(F112,X1,X22,EPS(2),EPS(1),S22,IERR)
      CALL  QDAGS(F113,X1,X23,EPS(2),EPS(1),S23,IERR)
      CALL  QDAGS(F111,X1,Y21,EPS(2),EPS(1),S31,IERR)
      CALL  QDAGS(F112,X1,Y22,EPS(2),EPS(1),S32,IERR)
      CALL  QDAGS(F113,X1,Y23,EPS(2),EPS(1),S33,IERR)
      CALL  QDAGS(F121,X21,Y21,EPS(2),EPS(1),S41,IERR)
      CALL  QDAGS(F122,X22,Y22,EPS(2),EPS(1),S42,IERR)
      CALL  QDAGS(F123,X23,Y23,EPS(2),EPS(1),S43,IERR)
      CALL  QDAGS(F131,X1,X21,EPS(2),EPS(1),S51,IERR)
      CALL  QDAGS(F132,X1,X22,EPS(2),EPS(1),S52,IERR)
      CALL  QDAGS(F133,X1,X23,EPS(2),EPS(1),S53,IERR)
      CALL  QDAGS(F131,X1,Y21,EPS(2),EPS(1),S61,IERR)
      CALL  QDAGS(F132,X1,Y22,EPS(2),EPS(1),S62,IERR)
```

```
CALL QDAGS(F133,X1,Y23,EPS(2),EPS(1),S63,IERR)
CALL QDAGS(F141,X21,Y21,EPS(2),EPS(1),S71,IERR)
CALL QDAGS(F142,X22,Y22,EPS(2),EPS(1),S72,IERR)
CALL QDAGS(F143,X23,Y23,EPS(2),EPS(1),S73,IERR)
H1=AZ1*PFDB1
H2=AZ2*PFDB2
H3=AZ3*PFDB3
H=H1+H2+H3
AM=(H*L)/KFB
CU1 = 2./(3.*UZ1)
CU2 = 2./(3.*UZ2)
CU3 = 2./(3.*UZ3)
BR1A1 = (CU1*R11)-2.*(CU1**3.)*R31+(CU1**4.)*R41
BR1A2 = (CU2*R12)-2.*(CU2**3.)*R32+(CU2**4.)*R42
BR1A3 = (CU3*R13)-2.*(CU3**3.)*R33+(CU3**4.)*R43
BR1B1=((CU1**2.)*R21)-(CU1*R11)
BR1B2=((CU2**2.)*R22)-(CU2*R12)
BR1B3=((CU3**2.)*R23)-(CU3*R13)
ETC1=((36.5*(TW**(-1/3.)))+3.9)
ETC2=EXP(ETC1)*(1.E-6)
ETAC=ETC2/P
ETR11=8.*3.14*(667.**(2.))*4.08*(1.E-12)*300.*339.685
ETAR1=1./ETR11
ETR12=8.*3.14*(2347.**(2.))*4.08*(1.E-12)*300.*2702.7
ETAR2=1./ETR12
ETR13=8.*3.14*(3716.**(2.))*4.08*(1.E-12)*300.*71.497*PHI2
ETAR3=1./ETR13
ETA11=ETAC/ETAR1
ETA12=ETAC/ETAR2
ETA13=ETAC/ETAR3
SUMA1 = H1*BR1A1
SUMA2 = H2*BR1A2
SUMA3 = H3*BR1A3
SUMAL=SUMA1+SUMA2+SUMA3
AL1L = 1.+(L/KFB)*SUMAL
SUMAN1=ETA11*CU1*BR1B1
SUMAN2=ETA12*CU2*BR1B2
SUMAN3=ETA13*CU3*BR1B3
SUMAN=(9./2.)*(SUMAN1+SUMAN2+SUMAN3)
ALPH1=AL1L-SUMAN
BR2A1 = (CU1**2.)*R21-2.*(CU1**3.)*R31+(CU1**4.)*R41
BR2A2 = (CU2**2.)*R22-2.*(CU2**3.)*R32+(CU2**4.)*R42
BR2A3 = (CU3**2.)*R23-2.*(CU3**3.)*R33+(CU3**4.)*R43
BR2B1=R01-(6.*CU1*R11)+(6.*(CU1**2.)*R21)
BR2B2=R02-(6.*CU2*R12)+(6.*(CU2**2.)*R22)
BR2B3=R03-(6.*CU3*R13)+(6.*(CU3**2.)*R23)
SUMB1 = H1*BR2A1
```

```
SUMB2 = H2*BR2A2
SUMB3 = H3*BR2A3
SUMBL=SUMB1+SUMB2+SUMB3
SUMBN1=ETA11*CU1*BR2B1
SUMBN2=ETA12*CU2*BR2B2
SUMBN3=ETA13*CU3*BR2B3
SUMBN=(3./4.)*(SUMBN1+SUMBN2+SUMBN3)
AL2L = (L/KFB)*SUMBL
ALPH2=AL2L-SUMBN
ALPH01=ETA11*(CU1**2.)*(CU1*R21-R11)
ALPH02=ETA12*(CU2**2.)*(CU2*R22-R12)
ALPH03=ETA13*(CU3**2.)*(CU3*R23-R13)
ALPH0=(9./2.)*(ALPH01+ALPH02+ALPH03)-1.
BR3A1 = (57./256.)*S11+(11./16.)*CU1*(S21+S31)
*-(9./8.)*(CU1**2.)*S41-(CU1**3.)*(S51+S61)+(CU1**4.)*S71
BR3A2 = (57./256.)*S12+(11./16.)*CU2*(S22+S32)
*-(9./8.)*(CU2**2.)*S42-(CU2**3.)*(S52+S62)+(CU2**4.)*S72
BR3A3 = (57./256.)*S13+(11./16.)*CU3*(S23+S33)
*-(9./8.)*(CU3**2.)*S43-(CU3**3.)*(S53+S63)+(CU3**4.)*S73
BR3B1=((9./4.)*CU1*S11)+(6.*(CU1**2.)*(S21+S31))
*-(12*(CU1**3.)*S41)
BR3B2=((9./4.)*CU2*S12)+(6.*(CU2**2.)*(S22+S32))
*-(12*(CU2**3.)*S42)
BR3B3=((9./4.)*CU3*S13)+(6.*(CU3**2.)*(S23+S33))
*-(12*(CU3**3.)*S43)
SUMC1 = H1*BR3A1
SUMC2 = H2*BR3A2
SUMC3 = H3*BR3A3
SUMCL=SUMC1+SUMC2+SUMC3
SUMCN1=ETA11*BR3B1
SUMCN2=ETA12*BR3B2
SUMCN3=ETA13*BR3B3
SUMCN=(3./8.)*(SUMCN1+SUMCN2+SUMCN3)
AL3L =(11./16.)+( L/KFB)*SUMCL
ALPH3=AL3L+SUMCN
BR4A1 = (9.0/256.)*S11+(3.0/16.)*CU1*(S21+S31)
*-(1./8.)*(CU1**2.)*S41-(CU1**3.)*(S51+S61)+(CU1**4.)*S71
BR4A2 = (9.0/256.)*S12+(3.0/16.)*CU2*(S22+S32)
*-(1./8.)*(CU2**2.)*S42-(CU2**3.)*(S52+S62)+(CU2**4.)*S72
BR4A3 = (9.0/256.)*S13+(3.0/16.)*CU3*(S23+S33)
*-(1./8.)*(CU3**2.)*S43-(CU3**3.)*(S53+S63)+(CU3**4.)*S73
BR4B1=((1./4.)*CU1*S11)+(6.*(CU1**2.)*(S21+S31))-
*(12.*(CU1**3.)*S41)
BR4B2=((1./4.)*CU2*S12)+(6.*(CU2**2.)*(S22+S32))-
*(12.*(CU2**3.)*S42)
BR4B3=((1./4.)*CU3*S13)+(6.*(CU3**2.)*(S23+S33))-
*(12.*(CU3**3.)*S43)
```

```
      SUMD1 = H1*BR4A1
      SUMD2 = H2*BR4A2
      SUMD3 = H3*BR4A3
      SUMDL=SUMD1+SUMD2+SUMD3
      SUMDN1=ETA11*BR4B1
      SUMDN2=ETA12*BR4B2
      SUMDN3=ETA13*BR4B3
      SUMDN=(3./8.)*(SUMDN1+SUMDN2+SUMDN3)
      AL4L = (3.0/16.)+(L/KFB)*SUMDL
      ALPH4=AL4L+SUMDN
      BR5B1=(3./16.)*(CU1*S11)+(1./2.)*(CU1**2.)*(S21+S31)-(CU1**3.)*S41
      BR5B2=(3./16.)*(CU2*S12)+(1./2.)*(CU2**2.)*(S22+S32)-(CU2**3.)*S42
      BR5B3=(3./16.)*(CU3*S13)+(1./2.)*(CU3**2.)*(S23+S33)-(CU3**3.)*S43
      SUMEN1=ETA11*BR5B1
      SUMEN2=ETA12*BR5B2
      SUMEN3=ETA13*BR5B3
      SUMEN=SUMEN1+SUMEN2+SUMEN3
      ALPH5=-((9./2.)*SUMEN+(11./16.))
      DENA = (ALPH1*ALPH4)-(ALPH2*ALPH3)
      A1=((ALPH0*ALPH4)-(ALPH2*ALPH5))/DENA
      A2=((ALPH1*ALPH5)-(ALPH0*ALPH3))/DENA
      TBULK = (1./70.)*((17.*A1)+(3.*A2))
      CONST=1./(16.*(AL1L*AL4L-AL2L*AL3L))
      a1l=(11.*al2l-16.*al4l)*CONST
      A2L=(16.*AL3L-11.*AL1L)*CONST
      TBULKL=(1/70.)*(17.*A1L+3.*A2L)
      WRITE(6,200) TW,P,L,-TBULK,-TBULKL
      write(7,202)l,-tbulkl,-tbulk
      write(8,201)l,-tbulk
   66 CONTINUE
   55 CONTINUE
   44 CONTINUE
  200  FORMAT(8X,F7.2, 3X,F6.2, 3X,F6.2, 2(3X,E10.4))
  111  FORMAT(8X,'TW',8X,'P',6X,'L',9X,'TBULK',7X,'TBULKL')
  201  format (1x,f9.2,3x,e10.4)
  202  format (1x,f9.2,2(3x,e10.4))
      STOP
      END
C-------------------------------------------------------------------
      FUNCTION F101(U1)
      COMMON F1,F2,F3
      DEN1 = (F1*((U1**2.)+(2.*U1)+2.)+U1)*(U1+(2.*F1))
      AUD1 = (F1*((U1**2.)+(4.*U1*F1)+(4.*F1)))/DEN1
      F101 = AUD1
      RETURN
      END
      FUNCTION F102(U2)
```

```
COMMON F1,F2,F3
DEN2 =  (F2*((U2**2.)+(2.*U2)+2.)+U2)*(U2+(2.*F2))
AUD2 =  F2*((U2**2.)+(4.*U2*F2)+(4.*F2))/DEN2
F102 = AUD2
RETURN
END
FUNCTION F103(U3)
COMMON F1,F2,F3
DEN3 =((F3*((U3**2.)+2.*U3)+2.)+U3)*(U3+(2.*F3))
AUD3 = (F3*((U3*2.)+(4.*U3*F3)+(4.*F3)))/DEN3
F103 = AUD3
RETURN
END
FUNCTION F111(U1)
COMMON F1,F2,F3
DEN1 = (F1*((U1**2.)+(2.*U1)+2.)+U1)*(U1+(2.*F1))
AUD1 = (F1*((U1**2.)+(4.*U1*F1)+(4.*F1)))/DEN1
F111 = AUD1*U1
RETURN
END
FUNCTION F112(U2)
COMMON F1,F2,F3
DEN2 = (F2*((U2*U2 )+(2.*U2)+2.)+U2)*(U2+(2.*F2))
AUD2 = (F2*((U2*U2 )+(4.*U2*F2)+(4.*F2)))/DEN2
F112 = AUD2*U2
RETURN
END
FUNCTION F113(U3)
COMMON F1,F2,F3
DEN3 = (F3*((U3**2.)+(2.*U3)+2.)+U3)* (U3+(2.*F3))
AUD3 = (F3*((U3**2.)+(4.*U3*F3)+(4.*F3)))/DEN3
F113 = AUD3*U3
RETURN
END
FUNCTION F121(U1)
COMMON F1,F2,F3
DEN1 = (F1*((U1**2.)+(2.*U1)+2.)+U1)*(U1+(2.*F1))
AUD1 = (F1*((U1**2.)+(4.*U1*F1)+(4.*F1)))/DEN1
F121 = AUD1*U1*U1
RETURN
END
FUNCTION F122(U2)
COMMON F1,F2,F3
DEN2 = (F2*((U2**2.)+(2.*U2)+2.)+U2)*(U2+(2.*F2))
AUD2 = (F2*((U2**2.)+(4.*U2*F2)+(4.*F2)))/DEN2
F122 = AUD2*U2**2.
RETURN
```

```
END
FUNCTION F123(U3)
COMMON F1,F2,F3
DEN3 = (F3*((U3**2.)+(2.*U3)+2.)+U3)*(U3+(2.*F3))
AUD3 = (F3*((U3**2.)+(4.*U3*F3)+(4.*F3)))/DEN3
F123 = AUD3*U3*U3
RETURN
END
FUNCTION F131(U1)
COMMON F1,F2,F3
DEN1 = (F1*((U1**2.)+(2.*U1)+2.)+U1)*(U1+(2.*F1))
AUD1 = (F1*((U1**2.)+(4.*U1*F1)+(4.*F1)))/DEN1
F131 = AUD1*U1**3.
RETURN
END
FUNCTION F132(U2)
COMMON F1,F2,F3
DEN2 = (F2*((U2**2.)+(2.*U2)+2.)+U2)*(U2+(2.*F2))
AUD2 = (F2*((U2**2.)+(4.*U2*F2)+(4.*F2)))/DEN2
F132 = AUD2*U2**3.
RETURN
END
FUNCTION F133(U3)
COMMON F1,F2,F3
DEN3 = (F3*((U3**2.)+(2.*U3)+2.)+U3)*(U3+(2.*F3))
AUD3 = (F3*((U3**2.)+(4.*U3*F3)+(4.*F3)))/DEN3
F133 = AUD3*U3**3.
RETURN
END
FUNCTION F141(U1)
COMMON F1,F2,F3
DEN1 = (F1*((U1**2.)+(2.*U1)+2.)+U1)*(U1+(2.*F1))
AUD1 = (F1*((U1**2.)+(4.*U1*F1)+(4.*F1)))/DEN1
F141 = AUD1*U1**4.
RETURN
END
FUNCTION F142(U2)
COMMON F1,F2,F3
DEN2 = (F2*((U2**2.)+(2.*U2)+2.)+U2)*(U2+(2.*F2))
AUD2 = (F2*((U2**2.)+(4.*U2*F2)+(4.*F2)))/DEN2
F142 = AUD2*U2*U2*U2*U2
RETURN
END
FUNCTION F143(U3)
COMMON F1,F2,F3
DEN3 = (F3*((U3**2.)+(2.*U3)+2.)+U3)*(U3+(2.*F3))
AUD3 = (F3*((U3**2.)+(4.*U3*F3)+(4.*F3)))/DEN3
```

```
F143 = AUD3*U3**4.
RETURN
END
```

NONGRAY LTE AND NLTE RESULTS FOR CO_2

T_w	P	L	T_b (LTE)	T_b (NLTE)
500.00	0.10	0.10	0.2428E+00	0.2426E+00
500.00	0.10	0.50	0.2425E+00	0.2402E+00
500.00	0.10	1.00	0.2415E+00	0.2359E+00
500.00	0.10	5.00	0.2227E+00	0.1949E+00
500.00	0.10	10.00	0.1899E+00	0.1528E+00
500.00	0.10	20.00	0.1338E+00	0.1020E+00
500.00	0.10	50.00	0.6055E–01	0.4815E–01
500.00	0.10	75.00	0.3971E–01	0.3290E–01
500.00	0.10	100.00	0.2915E–01	0.2486E–01
500.00	1.00	0.10	0.2421E+00	0.2417E+00
500.00	1.00	0.50	0.2355E+00	0.2337E+00
500.00	1.00	1.00	0.2258E+00	0.2232E+00
500.00	1.00	5.00	0.1625E+00	0.1596E+00
500.00	1.00	10.00	0.1189E+00	0.1171E+00
500.00	1.00	20.00	0.7753E–01	0.7672E–01
500.00	1.00	50.00	0.3832E–01	0.3813E–01
500.00	1.00	75.00	0.2705E–01	0.2696E–01
500.00	1.00	100.00	0.2092E–01	0.2087E–01
500.00	5.00	0.10	0.2408E+00	0.2407E+00
500.00	5.00	0.50	0.2302E+00	0.2299E+00
500.00	5.00	1.00	0.2178E+00	0.2176E+00
500.00	5.00	5.00	0.1535E+00	0.1533E+00
500.00	5.00	10.00	0.1131E+00	0.1130E+00
500.00	5.00	20.00	0.7470E–01	0.7467E–01
500.00	5.00	50.00	0.3752E–01	0.3751E–01
500.00	5.00	75.00	0.2662E–01	0.2662E–01
500.00	5.00	100.00	0.2065E–01	0.2065E–01
500.00	10.00	0.10	0.2404E+00	0.2403E+00
500.00	10.00	0.50	0.2293E+00	0.2292E+00
500.00	10.00	1.00	0.2168E+00	0.2168E+00
500.00	10.00	5.00	0.1532E+00	0.1531E+00
500.00	10.00	10.00	0.1130E+00	0.1130E+00
500.00	10.00	20.00	0.7474E–01	0.7473E–01
500.00	10.00	50.00	0.3754E–01	0.3754E–01
500.00	10.00	75.00	0.2664E–01	0.2664E–01
500.00	10.00	100.00	0.2066E–01	0.2066E–01